

**UNIVERSITY OF NAPLES “FEDERICO II”**



**DOCTORATE SCHOOL IN BIOLOGY**

Cycle XXXIV

Eco-physiological and structural strategies of microbial biofilm: their evolutionary implications and roles in biodeterioration

**Supervisor**  
Prof. Antonino Pollio

**Ph.D. student**  
Mariagioia Petraretti

Academic Year 2020 – 2021

*Dedicate to Emmanuel,*

So that you can always pursue your dreams, just like I did.

Never stop believing in yourself and your dreams, continuing to maintain the humility and purity of soul that distinguish you.

## Index

Abbreviations.....	5
List of Figures .....	8
List of Tables.....	12
Abstract .....	13
Riassunto .....	15
CHAPTER 1 .....	17
GENERAL INTRODUCTION .....	17
1.1. Subaerial biofilms.....	18
1.1.1. <i>Ecology of subaerial biofilms</i> .....	19
1.1.2. <i>Development of subaerial biofilm on lithic surfaces</i> .....	20
1.2. Biological weathering of lithic surfaces .....	21
1.2.1. <i>Biodeterioration</i> .....	22
1.2.2. <i>Bioreceptivity</i> .....	24
1.3. In vitro experiments for the understanding of biofilm ecology.....	26
1.4. Traditional and modern methods to control or prevent biological development on cultural heritage .....	27
1.4.1. <i>Traditional methods</i> .....	27
1.4.2. Recent methods .....	29
1.5. Landscape ecology applied to microbial communities.....	31
CHAPTER 2 .....	33
AIMS OF THE WORK .....	33
CHAPTER 3 .....	36
MICROBIAL BIOFILM COMMUNITY STRUCTURE AND COMPOSITION ON THE LITHIC SUBSTRATES OF HERCOLANEUM SUBURBAN BATHS .....	36
CHAPTER 4 .....	66
COMMUNITY COMPOSITION AND EX SITU CULTIVATION OF FUNGI ASSOCIATED WITH UNESCO HERITAGE MONUMENTS IN THE BAY OF NAPLES.....	66
CHAPTER 5 .....	87
FUNGAL METABOLITES WITH ANTAGONISTIC ACTIVITY AGAINST FUNGI OF LITHIC SUBSTRATA.....	87
CHAPTER 6 .....	110
A BIOLOGICAL AND QUANTITATIVE STUDY ON IN VITRO COLONISATION OF NEAPOLITAN YELLOW TUFF BY	

<b><i>BRACTEACOCCLUS MINOR, FUSARIUM OXYSPORUM AND NOSTOC COMMUNE</i></b> .....	<b>110</b>
<b>CHAPTER 7</b> .....	<b>136</b>
<b>AN ECOTOXICOLOGICAL EVALUATION OF FOUR FUNGAL METABOLITES WITH POTENTIAL</b> .....	<b>136</b>
<b>ANTIFOULING PROPERTIES FOR STONE-BUILT CULTURAL HERITAGE</b> .....	<b>136</b>
<b>CHAPTER 8</b> .....	<b>160</b>
<b>GENERAL CONCLUSIONS</b> .....	<b>160</b>
<b>BIBLIOGRAPHY</b> .....	<b>163</b>
<b>AKNOWLEDGEMENTS</b> .....	<b>175</b>

## **Abbreviations**

---

**ACUF:** Algal Collection University of Naples Federico II

**AD:** After Christ, anno domini

**AIC:** Akaike's information criterion

**ANOVA:** Analysis of Variance

**AUC:** area under the curve

**BBM:** Bold's Basal Medium

**BLAST:** Basic Local Alignment Search Tool

**BLASTn:** nucleotide–Basic Local Alignment Search Tool

**BYE:** Bacto Yeast Extract

**BPR:** Biocidal Products Regulation

**CABI:** Centre for Agriculture and Biosciences International

**CBS:** Centraalbureau voor Schimmelcultures

**CC:** Column chromatography

**CFU:** Colony forming unit

**CLSM:** Confocal Laser Scanning Microscopy

**CTCF:** Corrected Total Cell Fluorescence

**CTRL:** control

**Da:** average density

**DGGE:** Denaturing Gradient Gel Electrophoresis

**DNA:** DeoxyriboNucleic Acid

**dNTP:** DeoxyribonNucleotide TriPhosphate

**EC10:** Effective concentration required to induce a 10% effect

**EC20:** Effective concentration required to induce a 10% effect

**EC5:** Effective concentration required to induce a 5% effect

**EC50:** Effective Concentration required to induce a 50% effect

**EPS:** extracellular polymeric substances

**ESI MS:** Electrospray ionization mass spectrometry

**EtOAc:** Ethyl acetate solution

**FR:** Fruchterman-Reingold

**Fw:** forward

**GI, %:** growth inhibition

**HPLC:** high-performance liquid chromatography

**HSTs:** Heat Shock Treatments

**I, %:** immobility test

**ID:** identification

**ISO:** International Organization for Standardization

**ITS:** Internal transcribed spacer

**IUPAC:** International Union of Pure and Applied Chemistry

**LC/MS:** liquid chromatography/mass spectrometry

**LI, %:** luminescence inhibition

**lme4:** Linear Mixed-Effects Models using 'Eigen' and S4

**LMMs:** linear mixed models

**LOD:** limit of detection

**LOQ:** limit of quantitation

**M, %:** mobility test

**MEA:** Malt-Yeast Extract Agar

**MIPs:** Maximum Intensity Projections

**MuMIn:** Multi-Model Inference

**MUT:** Mycotheca Universitatis Taurinensis

**NCBI:** National Center for Biotechnology Information

**nMDS:** nonmetric dimensional scaling

**NMR:** nuclear magnetic resonance

**NYT:** Neapolitan Yellow Tuff

**PBS:** Phosphate buffered saline

**PCNB:** Pentachloronitrobenzene

**PCR:** polymerase chain reaction

**PDA:** Potato Dextrose Agar

**Ra:** average roughness

**RbcL:** Ribulose 1,5-biphosphate carboxylase large subunit

**RH:** relative humidity

**RNA:** RiboNucleic Acid

**Rq:** root mean square surface roughness

**rRNA:** ribosomal RNA

**Rt:** maximum roughness

**Rv:** reverse

**Rz:** mean roughness depth

**SAB:** subaerial biofilm

**SD:** Standard Deviation

**SP:** scatter plot

**SSRs:** Simple Sequence Repeats

**TLC:** thin-layer chromatography

**UNESCO:** United Nations Educational, Scientific and Cultural Organization

**WAC:** water absorption coefficient

## List of Figures

---

### Chapter 3

**Figure 1.** (a) Map of the Suburban Baths, with details of the *Vestibulum* (b), the *Tepidarium* (c), and of the room with a large heated swimming pool (d). Light blue highlights sampled rooms, with numbers marking the biofilm sampling sites. In following panels (e, f, g) are matched CLS-M microphotographs of sampled biofilms Scale bar 20  $\mu\text{m}$ .

**Figure 2.** Scatter Plot (SP) of environmental parameters, i.e., of temperature, RH, and irradiance for all the samples of the baths.

**Figure 3.** List of the species identified in Herculaneum Suburban Baths samplings. The list is ordered first by classification and then by name. Different square colors stand for different classification, while the dots at the side of species names indicates the ID method used for that species.

**Figure 4. Characterization of microbial community.** a) nonmetric dimensional scaling (stress = 0.03) of the communities found at the nine sampling points with respect to the relative taxa count within the different functional groups. Weighted average scores of the four functional groups are displayed as colored dots to ease the interpretation of the ordination, as well as sampling sites and substrates, following the color code presented in Fig 3. The ellipsoids visually cluster sites belonging to the same substrate, while the isolines represent irradiance values ( $\mu\text{E m}^{-2}\text{s}^{-1}$ ); b) Bar plots of relative (%) richness and abundance for all the sampling sites.

**Figure 5.** Network display of the communities found in the sampled points of the Herculaneum Suburban Baths using the Fruchterman-Reingold layout (see text). Each circle represents the community found in a single sample. Node diameter is proportional to the number of sites the species is found in, while edge color is red if the species pair is found more than once in any site, and cyan if the species pair is only

found in that specific site. The substrates are color-coded as per the other figures.

## Chapter 4

**Figure 1.** Location of the sampling site of UNESCO heritage monuments in the bay of Naples, Campania, Italy.

**Figure 2.** Archeological sites: Sibyl Caves in Cuma (**a**), Suburban Baths in Ercolano (**d**), the Roman Amphitheater in Nola (**g**), the House of Poppea in Oplonti (**j**), and the House of Fauno (**m**) and the House of Castricio (**p**) in Pompei; the visible alteration at the same sites (**b,e,h,k,n,q**); the recorded adhesive tape samples observed on the CLSM (**c,f,i,l,o,r**; scale bar, 50  $\mu\text{m}$ ).

**Figure 3.** The relative abundance of fungal isolated according to (A) classes, (B) orders, and (C) families.

**Figure 4.** The relative prevalence of fungal genera found in: Sibyl Caves in Cuma (A), Suburban Baths in Ercolano (B), the Roman Amphitheater in Nola (C), the House of Poppea in Oplonti (D), and the House of Fauno (E) and the House of Castricio (F) in Pompei.

## Chapter 5

**Figure 1.** Structures of cavoxin, cyclopaldic acid and *epi*-epoformin (1–3).

**Figure 2.** Percentage of inhibition, normalized to the positive control (PCNB) (black bar), of cavoxin (grey bar) and *epi*-epoformin (white bar), against *A. niger* (A) and *F. oxysporum* (B).

**Figure 3.** Development of fungal growth on tuff tiles at 20 days after inoculation of *A. niger* and *F. oxysporum* coupled with the respective metallurgical microscopy images.

**Figure 4.** Percentage of surface occupied by *F. oxysporum* on central region (A), median region (B), and distal region (C) of the tuff tile. Untreated (black bar), treated with cavoxin (grey bar), treated with *epi*-epoformin (white bar). Data shown are means  $\pm$  SD of three independent experiments. \*\* indicates  $p < 0.005$ , and \*\*\*\* indicates  $p < 0.0001$ .

**Figure 5.** Percentage of surface occupied by *A. niger* on central region (A), median region (B), and distal region (C) of the tuff tile. Untreated (black bar), treated with cavoxin (grey bar), treated with *epi*-epoformin (white bar). Data shown are means  $\pm$  SD of three independent experiments. \* Indicates  $p < 0.05$ , \*\* indicates  $p < 0.005$ , and \*\*\*\* indicates  $p < 0.0001$ .

**Figure 6.** Thickness of *F. oxysporum* on central region (A), median region (B), and distal region (C) of the tuff tile. Untreated (black bar), treated with cavoxin (grey bar), treated with *epi*-epoformin (white bar). Data shown are means  $\pm$  SD of three independent experiments. \*\*\*\* indicates  $p < 0.0001$ .

**Figure 7.** Thickness of *A. niger* on central region (A), median region (B), and distal region (C) of the tuff tile. Untreated (black bar), treated with cavoxin (grey bar), treated with *epi*-epoformin (white bar). Data shown are means  $\pm$  SD of three independent experiments. \* Indicates  $p < 0.05$ , \*\*\*\* indicates  $p < 0.0001$ .

## Chapter 6

**Figure 1** - Experimental strategy

**Fig. 2** - Sampling points on NYT tile

**Figure 3.** Percentage of surface occupied by *F. oxysporum* (A), *N.commune* (B), and *B.minor* (C) of the tuff tile.

**Figure 4.** Thickness of *B.minor*, *F.oxysporum* and *N.commune* in control experiments (A), *F.oxysporum* and *B.minor* in interaction experiments (B), and *F.oxysporum* and *N.commune* in interaction experiments (C) of the tuff tile.

**Figure 5.** The relationship between landscape metrics (logged values) and time fitted by LMMs, plotted for interaction fungus + cyanobacteria.

**Figure 6.** The relationship between landscape metrics (logged values) and time fitted by LMMs, plotted for interaction fungus + algae.

## Chapter 7

**Figure 1.** Chemical structures of compounds 1-4.

**Figure 2.** Chromatographic profiles of tested compounds.

**Figure 3.** Concentration-response relationship of Cavoxin (A), *epi*-Epoformin (B), Seiridin (C) and Sphaeropsidone (D) exposed to *R. subcapitata*.

**Figure 4.** Concentration-response relationship of Cavoxin (A), *epi*-Epoformin (B), Seiridin (C) and Sphaeropsidone (D) exposed to *A. fischeri*.

**Figure 5.** Concentration-response relationship of Cavoxin (A), *epi*-Epoformin (B), Seiridin (C) and Sphaeropsidone (D) exposed to *D. magna*.

**Figure 6.** Concentration-response relationship of Cavoxin (A), *epi*-Epoformin (B), Seiridin (C) and Sphaeropsidone (D) exposed to *C. elegans*.

## List of Tables

---

### Chapter 3

**Table 1.** Fluorescence microscopy information. Red has no labeller because pigments are observed by autofluorescence.

**Table 2.** Mean temperature, relative humidity and light irradiance at the nine sample points.

**Table 3.** Selected CLSM structural parameters of sampled biofilms

### Chapter 4

**Table 1.** Values of environmental parameters (light, pH, relative humidity, and temperature) at each sampling site.

**Table 2.** Identification of the fungal species complex level based on ITS sequences with the description of their sampling site and lithic substrate. ACUF Collection Codes and Gene Bank Accession numbers are given for each strain.

### Chapter 6

**Table 1** – Petrographic features of Neapolitan yellow tuff (NYT).

### Chapter 7

**Table 1.** Classes, Sources, and Biological Activities of Fungal Metabolites (1-4) Used in this Study.

**Table 2.** Analytical characteristics of the calibration curves and quantification of compounds 1-4 culture medium (BBM) after 72 h.

**Table 3.** EC5, EC10, EC20 and EC50 values for the tested compounds after exposure of *R. subcapitata*, *A. fischeri*, *D. magna* and *C. elegans*.

## Abstract

Stone worldwide artworks represents cultural heritage as precious as fragile. Sculptures, buildings materials, statues, caves, mosaics, catacombs, archeological remains are elements that make stone unique works of art but exposed to microbial colonisation that can lead to slowly, but irreversible, stone disappear. To ensure the transmission of this legacy to future generations, the preservation of this material is a matter of the utmost importance. Biofilms living at rock-atmosphere interface are heterologous, both in terms of the microbiome's structure and composition whose ability to alter properties of the substratum is defined biodeterioration. In consequence to biological activity of microorganisms together with weathering, many cultural heritages made of stone may lose some of their cultural and monetary value. The present work contributes to a deeper understanding on eco-physiological and structural strategies of microbial biofilm involved in deterioration of stone surfaces aimed to develop safer options for preventing and treating stone deterioration. In order to improve our knowledge of the role of microorganisms in the colonisation of stone heritage, an *ex-situ* collection has been created with the aim of serving as a bioresource center for the study of biodeterioration. The importance of maintaining a broad range of taxa in collections for *ex-situ* conservation accessible to researchers prompted us to perform a survey campaign along the UNESCO archaeological remains of Campania, namely Cuma, Ercolano, Nola, Oplonti, and Pompei. In a series of *in vitro* colonisation experiments, the early colonisation of stone by three main groups of microorganisms (algae, fungi, cyanobacteria) was tested and monitored for a relative short-term period. Using confocal laser scanning microscopy and computer image analysis it has been possible to depict fine structure and architecture of the studied microorganisms, in a controlled environment where the realistic conditions of the respective sampling points have been reproduced. Finally, the antimicrobial ability of two fungal metabolites was assessed to allow better conservation of works of art and to ensure suitable conditions for their conservation and their ecotoxicological characteristics were then evaluated. This work opening the way for further research in the challenging field of cultural heritage conservation suitable for their conservation control that is respectful of the

uniqueness of each artwork.

## Riassunto

Le opere d'arte in pietra di tutto il mondo rappresentano un patrimonio culturale tanto prezioso quanto fragile. Sculture, materiali da costruzione, statue, grotte, mosaici, catacombe, resti archeologici sono elementi che rendono la pietra opera d'arte unica, ma soggetta ad una colonizzazione microbica che può portare alla sua lenta, ma irreversibile scomparsa. Per garantire la trasmissione di questa eredità alle generazioni future, la conservazione dei materiali lapidei diventa cruciale e indispensabile. I biofilm che vivono all'interfaccia roccia-atmosfera sono eterogenei, sia in termini di struttura che di composizione microbica, la cui capacità di alterare le proprietà del substrato è definita biodeterioramento. Conseguentemente all'attività biologica dei microrganismi insieme agli agenti atmosferici, molti beni culturali in pietra possono perdere parte del loro valore culturale e monetario. Il presente lavoro contribuisce a una più profonda comprensione delle strategie eco-fisiologiche e strutturali dei biofilm microbici coinvolte nel deterioramento delle superfici lapidee volte a sviluppare metodi più sicuri per prevenire e trattare il deterioramento dei manufatti lapidei di un certo valore storico culturale. Al fine di migliorare la nostra conoscenza sul ruolo che ricoprono i microrganismi nella colonizzazione dei manufatti lapidei, è stata creata una collezione *ex-situ* con lo scopo di attingere ad essa come risorsa biologica per lo studio del biodeterioramento. L'importanza dell'allestire e gestire una collezione *ex-situ* che possa essere accessibile ai ricercatori di tutto il mondo, ha spinto a svolgere una campagna di campionamento presso beni culturali patrimonio dell'UNESCO in Campania, ovvero Cuma, Ercolano, Nola, Oplonti e Pompei. In una serie di esperimenti di colonizzazione *in vitro*, è stato testato e monitorato per un periodo relativamente breve lo sviluppo di biofilm su pietra originato da tre gruppi principali di microrganismi (alghe, funghi, cianobatteri). Attraverso l'uso della microscopia confocale laser e dell'analisi digitale di immagini, è stato possibile rappresentare la struttura fine e l'architettura dei microrganismi studiati, in un ambiente controllato in cui sono riprodotte le condizioni realistiche dei rispettivi punti di campionamento. Infine, è stata testata l'attività antimicrobica di due composti naturali per valutarne l'impiego nel campo della conservazione delle

opere d'arte e ne sono state poi valutate le caratteristiche ecotossicologiche. Il presente lavoro apre quindi la strada a ulteriori ricerche nel controverso ed intrigante campo della conservazione del patrimonio culturale.

**CHAPTER 1**  
**GENERAL INTRODUCTION**

### **1.1.Subaerial biofilms**

Rock surfaces exposed to the atmosphere, such as those used for the construction of buildings, monuments and bare rocks, are rapidly colonized by microbial communities forming subaerial biofilm (SAB). These communities are mainly composed of different microorganisms such as microalgae, cyanobacteria, bacteria and fungi (Gorbushina & Broughton, 2009) densely packed in self-organized structures and embedded in a matrix formed by extracellular polymeric substances (EPS).

Stone-atmosphere interface can be considered as an extreme environment characterized by severe environmental fluctuations, especially desiccation, low nutrient concentrations, large temperature variations, high exposure to wind and UV radiation (Jacob, 2018). For this reason, only microorganisms with a very broad range of tolerance to multiple and fluctuating stresses can establish themselves under these conditions (Zakharova et al., 2013).

Stone-inhabiting microorganisms namely epiliths are able to grow on the surface, while microorganisms able to grow in the substratum at depths ranging from millimeters to centimeters (Gadd et al., 2014) are named endoliths. The endolithic mode of life includes different ecological niches: chasmoendoliths and cryptoendoliths occupy pre-existing fissures and structural cavities in the rocks, whereas euendoliths grow in soluble carbonatic and phosphatic substrata dissolving the stone immediately below the surface. The first form of growth leads to a co-responsibility in the detachment of scales of material due to the pressure exerted by increasing biomass. This process can occur repeatedly, involving areas increasingly in depth (Pinna and Salvadori, 2008). The light that reaches the bulk of the stones limits the growth of phototrophic microorganisms. The presence of water in micropores, especially those with translucent walls, may enhance light penetration, increasing the light available for photosynthesis in the cryptoendolithic

habitats (Cámara et al., 2014).

### **1.1.1. Ecology of subaerial biofilms**

Terrestrial cyanobacteria and algae are pioneer organisms, which colonise habitats potentially unavailable for living organisms and transform them, giving the opportunity to other organisms to settle (Schopf et al., 1996). Typically, phototrophic biocenosis may allow the later growth of more complex communities, including the heterotrophic microbiota (Tomaselli et al., 2000). The association of phototrophic components embedded in a biofilm enriches itself with organic and inorganic substances and growth factors (Tiano, 2002) providing an excellent nutrient base for the subsequent trophic succession. However, the establishment of heterotrophic communities on rocks is possible even without the pioneering participation of phototrophic organisms and may facilitate the subsequent growth of photosynthetic populations (Roeselers et al., 2007). In this case, various organic sources are used, including airborne particles and organic vapors, organic matter naturally present in sedimentary rock (usually between 0.2% and 2%), excreted organic metabolic products and biomass from other organisms (Warscheid and Braams, 2000; Urzi, 2004).

A decisive role in the growth and development of cyanobacteria and algae is played by appropriate light conditions, temperature and humidity, which are related to the distance from larger aquatic ecosystems and vegetation (Barberousse et al., 2006). Humidity probably represents the most important factor for the colonisation of aeroterrestrial microalgae; moreover, they can quickly recover from desiccation stresses when water becomes available again, e.g., after rain events. This ability explains well the ecological success of phototrophs in thriving on building facades and roof tiles in urban areas (Häubner et al., 2006).

The availability of mineral compounds and an adequate pH substrate are also important (Grbić et al., 2010) and the stone substratum itself may act as a putative source of minerals, together with the air, that may provide

inorganic and organic compounds (Villa et al., 2015). Atmospheric gases, aerosols, pollutants and particulates can be accumulated by biofilms and serve as nutrient sources as well as inoculum (Warsheid and Braams, 2000). Although the number of studies on eukaryotes is limited, algal and fungal communities on stone revealed a lower diversity compared with those occurring in most natural systems (Cutler et al., 2013). Which microbial community dominates may depend on the substrate, the atmosphere, and abiotic stresses (Ranalli et al., 2009). Organic components in substrate or atmosphere also promote chemoorganotrophic development, which in turn leads to further organic enrichment of the system through biomass production, exudation and exopolymer synthesis (Warsheid and Braams, 2000).

### **1.1.2. Development of subaerial biofilm on lithic surfaces**

Colonisation is one of the first steps leading to the subsequent formation of a biofilm on a material, resulting at best in a reduction of its performance and, at worst, in its destruction. Morton (1994) described the phases of biofilm development as follows: (1) molecular modification of the surface, (2) reversible attack, (3) irreversible attack, (4) colonisation. The mechanisms of microbial colonisation begin when an organism finds the right conditions to attack a substrate, grow and develop. This initial cell-substrate contact is regulated by a transient chemical attraction, difficult to characterize, and dependent on environmental characteristics. Photosynthetic organisms easily grow on surfaces and can lead to the development of much more complex microbial consortia, characterized by the presence also of heterotrophic organisms, endowed with detritogenic activity even more decisive (Tiano et al., 1993; Tomaselli et al., 2000). Normally, photoautotroph microorganisms are able to lead the formation of a biofilm, which is a complex system of monolayered or multilayered cells, embedded in a polymeric matrix

extracellular hydrated (EPS) and enriched with organic and inorganic substances (Roldan et al., 2003). EPS may vary in chemical and physical properties, but it is primarily composed of polysaccharides. Some of these polysaccharides are neutral or polyanionic, as is the case for the EPS of gram-negative bacteria. The EPS matrix is also highly hydrated because it can incorporate large amounts of water into its structure by hydrogen bonding. Its production is known to be affected by nutrient status of the growth medium; excess available carbon and limitation of nitrogen, potassium, or phosphate promote EPS synthesis (Sutherland, 2001). It is known that bacteria embedded in the biofilm matrix are remarkably more tolerant to biocides, up to 1000-fold relative to planktonic cultures of the same bacterial strains, depending on the species–drug combination (Davies, 2003). Such microbial consortia can develop in any environmental context, on any solid substrate under conditions of high availability of water. Biofilm also includes cellular debris, particulate matter, atmospheric dust, spores and inorganic material of different nature absorbed by the substrate (Warscheid, 2000). The structural complexity of biofilms is maintained by the presence of EPS, having adhesive properties and indispensable in the early stages of biofilm development, as they facilitate the attachment of cells to the substrate (Decho et al., 2000; Barranguet et al., 2005). After the establishment of a biofilm community, a highly degraded stone surface with subsequent alteration of the physical condition of the rock, provide appropriate conditions for the germination of reproductive structures from higher organisms. The formation of a “proto-soil” enables the growth of cryptogams (mosses and ferns) and higher plants (Lisci et al., 2003).

### **1.2. Biological weathering of lithic surfaces**

Stone cultural heritage objects represent a challenging habitat for biological growths. The intense variability of the environmental factors (i.e., temperature and relative humidity), the exposure to intense solar

radiation and wind, low availability of nutrients and pollutants concentrations determine particularly stressful conditions (Gorbushina, 2007). Nevertheless, biological colonisation on heritage monuments is ubiquitous and has been recognized as a major mechanism of alteration of stone substrates (Palla and Barresi, 2017). Only within the last three decades this matter received serious attention from conservators and conservation scientists (Price, 1996; Schnabel, 1991). A thorough understanding of the factors and mechanisms involved in microbial biodeterioration is essential to develop appropriate methods for its control.

### **1.2.1. Biodeterioration**

For the first time in 1965, Hueck (1965, 1968) defined biodeterioration as “*any undesirable change in the properties of a material caused by the vital activities of organisms*”; till then, the weathering of stone monuments and artworks was attributed to physical agents, while later it became more and more clear that biofilms play an active role in stone decay.

The most common manifestation of microbial colonisation on lithic surfaces the biopatinas formation, able to change physical, chemical, and aesthetic appearance of substrata (Krumbein, 2003). Besides, microbial development in the lithic substrata can also induce alteration on the structural characteristic of the colonised material. Microbial colonisation of lithic surfaces is divided in: A) epilithic growth with micro-colonial appearance, B) epilithic formations with patina appearance and C) casmo-endolytic development; each category can be made up of one or more species (Cuzman et al., 2010).

Typical mechanisms of microbial weathering involve physical and biochemical destruction. Generally speaking, biodeterioration process can occur due to: (1) Mechanical processes, where the material is damaged as a direct result of the activity of an organism, such as its movement or

growth. An example of this form of biodeterioration is the damage caused to cabling as a result of insect or rodent attack. (2) Chemical assimilatory biodeterioration, perhaps the most common form of biodeterioration. It occurs when a material is degraded for its nutritive value. The breakdown of cellulosic materials by cellulolytic micro-organisms, is an example of this type of biodeterioration. (3) Chemical dissimilatory biodeterioration, which occurs when metabolic products damage a material by causing corrosion, pigmentation, or by the release of toxic metabolites into a substance. The poisoning of grain by mycotoxins is an example of this process. (4) Soiling/biofouling, the form of biodeterioration which occurs when the mere presence of an organism or its excrement renders the product unacceptable. The biofouling of ships' hulls, the formation of slime in fuel lines and corrosion within water pipelines are examples of this form of biodeterioration. Physical mechanisms of bioweathering include penetration by filamentous microorganisms (for example, certain actinobacteria, cyanobacteria, algae, fungi) along points of weakness, or direct tunnelling or boring, especially in weakened or porous substrata (Lian et al., 2008). Many cyanobacteria, not necessarily filamentous, have also been shown to have a boring ability (Cockell and Herrera, 2008). Organisms that actively bore (euendoliths) widely occur in cyanobacteria, red and green algae and fungi (Cockell and Herrera, 2008). Other physical effects on substrate integrity can be due to cell turgor pressure, and exopolysaccharide and/or secondary mineral formation (Barker and Banfield, 1996). The production of efflorescences ('salting') involves secondary minerals that are produced through the reaction of anions from excreted acids with cations from the stone. Such secondary mineral formation can cause blistering, scaling, granular disintegration and flaking or 'spalling' of outer layers. This may often be a major mechanism of stone decay (Wright, 2002). Phototrophs inhabiting anthropogenic substrates thereby contribute to their rapid biodeterioration (Tomaselli et al., 2000; Crispim and Gaylarde, 2004; Samad and Adhikary, 2008). They produce photosynthetic pigments, which change the color of

the substrates on which the cyanobacteria and algae grow. This adversely affects the aesthetic value of buildings and cultural monuments (Grbić et al., 2010; Stupar et al., 2012). When humidity changes, the hydration and volume of algal cells are also modified, causing structural microdamages to substrates (Hauer, 2010). Many phototrophs are capable of dissolving compounds contained in a substrate and penetrating into it, causing mechanical erosion (Brehm et al., 2005; Crispim and Gaylarde, 2004). During the metabolic activity of the algal cells, various types of inorganic and organic acids are produced, and algae secrete them into the external environment, causing chemical deterioration of substrates (Stupar et al., 2012). For instance, aerobic microorganisms produce respiratory carbon dioxide, which becomes carbonic acid and contributes to dissolution of stone and soluble salt formation (Griffin et al., 1991; Wakefield & Jones, 1998). The precipitation of calcium salts on cyanobacterial cells growing on limestone suggests the migration of calcium from neighboring sites (Arino et al., 1997; Crispim & Gaylarde, 2005). In addition, the production of organic acids such as lactic, oxalic, succinic, acetic, glycolic and pyruvic has been found and associated with the dissolution of calcite in calcareous stones (Danin & Caneva, 1990; Caneva et al., 1992). Endolithic photosynthetic microorganisms actively dissolve carbonates to enable penetration into the stone, enhancing stone porosity (Fernandes, 2006). Furthermore, the slimy surfaces of microbial biofilm favor the adherence of airborne particles (dust, pollen, spores, carbonaceous particles from combustion of oil and coal), giving rise to hard crusts and patinas (Saiz-Jimenez, 1995).

### **1.2.2. Bioreceptivity**

Biological colonisation of outdoor materials is closely related to abiotic factors including microclimatic conditions and material composition itself. Many groups of microorganisms are able to grow on several substrata using their mineralogical compounds, starting complex colonisation phenomena with consequent microbial proliferation

followed by biodeterioration. The microorganisms able to do so are known as biodeteriogenes. In order to explain the particular and specific interactions that occur among microorganisms and different substrata, Guillitte (1995) introduced for the first time the term “bioreceptivity”, explained as “*the aptitude of a material (or any other inanimate object) to be colonised by one or several groups of living organisms without necessarily undergoing any biodeterioration*”. It implies that there is an ecological relationship between the colonised material and the colonising organisms. Different levels of bioreceptivity can be defined: primary or intrinsic bioreceptivity is related to the initial colonization potential of a substrate. Following the action of organisms and other physical, chemical, and biological factors, this is transformed into secondary bioreceptivity; finally, the conservative treatments applied to the substrates modify their characteristics and induce a tertiary bioreception. Any building material is susceptible to irreversible alteration induced by the synergistic action of biological colonisation and weathering. The susceptibility of stone and mineral-based material to bioweathering is influenced by chemical and mineralogical composition, physical form, and geological origin (Turick and Berry, 2016). The materials, whether natural or artificial, are characterized by their own petrographic structure, texture, color, chemical and mineralogical composition. Surface roughness, porosity, hygroscopicity, chemical composition and state of conservation of the material are among the most important factors to favor bio-colonisation and can, in various ways, lead to the deterioration of a work of art (Caneva et al., 2007a). The presence of weatherable minerals in stone such as feldspars and clays may provide points of weakness and significantly increase susceptibility to attack (Warsheid and Braams, 2000). This depends on several parameters such as material composition, the status of conservation, eventual surface treatments as well as the environmental conditions in which the artifact is placed. Despite considerable research efforts, many aspects of the interaction between microbial communities and stone materials are still

unknown (Di Martino, 2016). Not surprisingly, in recent times many papers report that the biological colonisation of outdoor stones may act as a protective layer shielding the materials from other factors that cause decay, such as wind and rainwater (Pinna, 2014).

### **1.3. *In vitro* experiments for the understanding of biofilm ecology**

In general terms, deterioration can be defined as degradation of stone materials because of the action of external agents or material weakening (Sanchez-Silva and Rosowsky, 2008) together with deterioration caused by microorganisms (Guiamet et al., 2013), which grow as multispecies biofilms that develop on all types of surfaces (Romani et al., 2019). The most common approach in biodeterioration field research is usually based on the detection of microbial communities on a given work of art (Dyda, 2019; Li, 2016; Liu, 2018; Grottoli, 2020), united with the microscopical observation of the interface biofilm/material. Since deterioration of works of art is affected by many factors, studying on the decay of materials requires a combination of microbiological techniques, surface analysis and material characterization. All the aspects involved in biodeterioration can be effectively evaluated based on *in vitro* tests, simulating specific environmental conditions in which microorganisms can grow. Nowadays, tests to study biodeterioration of building materials, including a broad range of materials and microorganisms. Among them some were developed without accelerated weathering of the matrix leading to long-term experiments (Urzi and De Leo, 2007), while some other aim on qualifying aesthetic damage of external wall surface exposed to biofilm colonization (Escadeillas et al., 2007). Because of extreme variability of stone material, several studies have investigated the bioreceptivity of stone materials (among the others e.g. Saiz-Jimenez et al., 1995; Urzi and Realini, 1998; Prieto and Silva, 2005; Prieto et al., 2006; Cámara et al., 2008, 2011; Favero-Longo et al., 2009; Giannantonio et al., 2009; Fuentes 2021; Trovão, 2021). Such experimental simulations, commonly used in ecological studies, are of great interest for the case of cultural heritage since they allow experimental manipulation of the microbial ecosystem avoiding sampling and subsequent damage to cultural assets. Prospects

are oriented towards the use of strains deposited on ACUF Collection (<http://www.acuf.net/index.php?lang=it>) as models to study the biodeterioration of stone materials (Del Mondo, 2017).

#### **1.4. Traditional and modern methods to control or prevent biological development on cultural heritage**

Two main strategies to control biological colonisation on cultural heritage objects may be applied: indirect and direct methods (Pinna, 2017). The first approach is based on the fact that the microbial growth is strongly correlated to the physical and chemical characteristics of stone substrata as well as to environmental conditions (Caneva, 2008). Indirect methods act by identifying and reducing environmental conditions which directly affect the microorganism, contributing to the microbial growth. However, the use of indirect methods is not always possible, especially for outdoor monuments, since they are subjected to different climate conditions and pollution (Lo Schiavo, 2020). In restoration activities, indirect methods are often coupled with the direct ones which use mechanical, physical, chemical, and biological tools to remove the existing colonisation (Pinna, 2017). Every cultural heritage site represents diverse ecological micro-niches hosting different microbial communities able to interact with the stone substrate influencing its conservation in different ways (Tonon et al., 2019). The knowledge and monitoring of biodeterioration degree can help recognize and achieve the best conservation solutions (Schumacher and Gorbushina, 2020). This implies that each conservation procedure should be developed as a site-specific strategy for conservation of monuments taking into account the environmental parameters favoring microbial communities on cultural heritage, the nature of material subjected to biodeterioration, and microorganisms involved in the stone colonisation.

##### **1.4.1. Traditional methods**

###### **1.4.1.1. Mechanical methods**

Mechanical cleaning has been applied to building materials as the first type of treatment to remove the deteriorating biofilm and is currently often conducted

before chemical treatments. Among mechanical methods, water pressure system, sandblasting and laser cleaning are renowned. The utilization of water pressure and steam systems is the most common and easy to employ. A recent study of Sanmartín (2020a) has shown their efficacy in short term on subaerial biofilms. The limit of these methods is the difficulty of correctly regulating the water pressure sufficiently to remove the biofilm but not too high to degrade materials (Slaton and Normandin, 2005). Abrasive systems such as sandblasting methods have also shown their efficacy to clean the materials from fungi, microalgae, and bacteria (Pozo-Antonio et al., 2021), unfortunately these methods can cause damages on building materials. Furthermore, water pressure system and sandblasting methods could spread the microorganisms on the substrate (Favero- Longo and Viles, 2020), favoring rapid recolonisation. Another promising device using to mechanical cleaning of historical monuments is based on laser (Di Martino, 2016) applied in a pulse frequency. Several studies shown that laser cleaning was efficient on wide range of microalgae, fungi, bacteria and lichen (Elhagrassy et al., 2018; Speranza et al., 2013; Pozo-Antonio et al., 2019). The laser employ has many drawbacks due to the high costs (Di Martino, 2016) and difficulty to eliminate the encrusted part of the biofilm. Moreover, it may increase porosity of materials such as tiles, facilitating their recolonisation (Barberousse et al., 2006; Di Martino, 2016).

#### 1.4.1.2. Physical methods

UV treatments have showed a germicidal activity between 200-280 nm (UV-C), and they were tested quite successfully in natural caves and hypogea and show caves (Baquedano Estévez, 2019; Pfendler, 2017). The great advantage of this treatment is that it is easy to handle but needs to be performed with care by the operator when there are no visitors or other people around as their target is DNA. Moreover, they cannot be applied on mural paintings, due to ability to cause damages to the organic component and pigments. An ecologically safe alternative are thermal treatments, including microwave, heat irradiation and heat shock treatment (Tretiach, 2012; Riminesi, 2016; Mascalchi, 2020). Thanks to their low interaction with the substrate and penetration depth, they are safe for the cultural asset, for operators, and the environment. Further, they are effective against lichens

and bryophytes and partially on green algae, but they do not have any effect on most of the environmental bacteria and some black fungi. More recently, a very simple and efficient treatment is the Heat Shock Treatment (HSTs), based on the peculiarity of poikilohydric lithobionts, which are thermo-tolerant (up to 60-70°C) when dry, but become thermo-sensitive when wet. HSTs seem to be very effective against fungi and mosses but not on green algae (Bertuzzi, 2013).

#### 1.4.1.3. Chemical methods

Most of the chemical compounds used in restoration have previously been applied as cosmetic ingredients, medical care products, or used in food industry, building cleaning, agriculture not contextualized to the protection of cultural heritage. Among these, biocides represent the most used molecules which are applied in the early phases of artwork cleaning treatments, and sometimes also after restoration, to prevent or slow down the recolonisation. The BPR Regulation (EU) 528/2012, has introduced significant restrictions on the use of chemical biocides, based on their potential harm to users and other environmental issues (Commission Européenne, 2012) and more research and publications are demonstrating their toxic effects on humans and the environment. Moreover, in restoration field, research studies have demonstrated a potential risk of interference with stone materials, and an increase of bio-receptivity of the substrate (Caneva, 2008).

### **1.4.2. Recent methods**

#### 1.4.2.1 “Green Biocides”

Strict regulations on the use of traditional biocides are enforced in various countries with the purpose of preventing adverse effects on humans and the environment. Therefore, some natural compounds have been recently tested also for restoration and conservation purposes. Green biocides, such as compounds obtained from plants and or microorganisms, are an emerging and exciting research topic. Natural compounds and essential oils from plants, often already used in other application fields, in recent years have been tested as antimicrobial and for biofilm development

control in cultural heritage. Several studies on their effectiveness showed an effect against the growth of some microorganisms (among others Rotolo, 2016, Masi & Petraretti, 2021). The list of plants containing essential oils or antimicrobial compounds gets longer every year, and research on traditionally used medicinal plants can be useful in narrowing down the set of species worth of investigation (Caneva and Pieroni, 2013). Like green biocides, blue biocides, obtained from marine organisms such as jellyfish, sea-anemones, shellfish, sponges, marine plants, derive from the "Blue-Biotechnology" that use bioactive molecules (Palla, 2016). These molecules, firstly applied in quite different fields from cultural heritage conservation, are characterized by low-temperature activity, stability, and specificity of action. Several studies are focused on their proteolytic and antimicrobial activities. Molecules that show both these activities are extracted from marine invertebrate (Cnidaria) and their effectiveness is high in low temperature.

#### 1.4.2.2 Bio-cleaning

The current attention to environmental microbiology is leading to a growing body of knowledge on microbial biochemical properties. Bio-cleaning was recently employed against various forms of deterioration of both chemical and biological origin, and for removing organic compounds before conservation interventions. *Desulfovibrio vulgaris* was used in bio-cleaning treatments to remove sulphates, and comparative studies showed that its effectiveness was higher than chemical or physical treatments against black crusts on different lithotypes (Gioventù, 2011), comparing the bio-removal of black crusts on colored artistic lithotypes of the Cathedral of Florence with chemical and laser treatment. The denitrifying *Pseudomonas stutzeri* was also effectively and extensively used for removing nitrates, such as animal glue and casein proteins derived from previous restorations, from altered frescoes with an application time of 2 h (Lustrato, 2012). Different bacteria can be used in different steps of the same restoration project, and it seems possible to use two or more bacteria at the same time, such as in the combined treatment with *Cellulosimicrobium cellulans* (TBF11) for solubilizing calcium sulphates and carbonates; *Stenotrophomonas maltophilia* (UI3) for degrading proteins and *Pseudomonas koreensis* (UT30) for solubilizing inorganic compounds

and degrading protein material (Mazzoni, 2014). Obviously, the choice of bacterial strain is very important: they must be harmless, selective, and non-aggressive, environmentally compatible, low-cost and safe for the operators.

#### 1.4.2.3 Nanoparticles and Ionic Liquids

Nanotechnology is rapidly expanding and while offering technical and commercial opportunities, thus scientific community are increasingly interested in the applications of nanoparticles (Baglioni, 2015). Several nanoparticles, previously applied in stone material restoration have showed a good penetration property, significantly contribute to the consolidative/protective processes of stone materials. Among the novel compounds used in stone conservation, some self-cleaning particles, such as zinc oxide, silicon dioxide, and especially titanium dioxide (TiO<sub>2</sub>) in the anatase form, were tested in several ways of application and against several kinds of organisms. The greater advantage of TiO<sub>2</sub> is its ability of being photocatalyst under UV light, mostly UVA radiation (315–400 nm), and oxidizing various organic compounds into water and carbon dioxide (Pinna, 2017). Nowadays their application is limited because near-ultraviolet irradiation is required for photocatalytic activation. The rapid increase of nanotechnologies used in conservation field raises concerns about its potential effects on human health and the environment., as well as in terms of efficiencies against microorganisms, and long-term effects on the material. In a recent review (Lo Schiavo, 2020), a great deal of interest has been directed to ionic liquids, a class of low melting pointsalts, which can be engineered by applying Safe by Design concepts to meet green conservation criteria.

#### 1.5.Landscape ecology applied to microbial communities

The term “landscape ecology” was introduced by the German biogeographer Carl Troll (1939), arising from the European traditions of regional geography and vegetation science, and motivated particularly by the novel perspective offered by aerial photography. Landscape ecology is motivated by a need to understand the dynamics involved in ecological phenomena, promoting the development of models and theories of spatial relationships, the collection of new types of data on spatial

pattern and dynamics, and the examination of spatial scales poorly understood in ecology (Pickett and Cadenasso, 1995). The relationship between landscape structure and its ecological process is the core part of theoretical research on landscape ecology. (Lisha Zhou, 2021). Landscape is a mosaic composed of heterogeneous elements. The heterogeneity at the landscape scale includes three aspects: spatial composition, spatial configuration, and spatial correlation. Landscape ecology has been applied in many fields over the years, including microbial world. The latter is still in its infancy, in fact the current research effort on landscape ecology for microorganisms is mainly focused on pathogens and disease risk assessment, limiting itself to the study of the host-pathogen relationship and the development of methods to investigate symptoms rather than the presence of species and abundance (Cendrine, 2020). Microorganisms display a substantial spatial, this raises questions about how their distribution depends on different components of community assembly, the link with the ecological niche and coexistence mechanisms, and how community assembly is related to the functions and functioning of microbial ecosystems. Drivers of microorganism assemblages have so far mostly been analyzed at the patch scale, assuming that species niches result from the effect of the abiotic environment on species selection, disturbance or biotic interactions among microbial organisms, or with their host (Louca et al., 2018) and ignoring dispersal effects.

**CHAPTER 2**  
**AIMS OF THE WORK**

This thesis aims to contribute to a better understanding on eco-physiological and structural strategies of microbial biofilm involved in deterioration of stone surfaces, aspiring to develop safer options for preventing and treating stone deterioration and possibly suggesting new ways for further research in the challenging field of heritage conservation. To do so, three main objectives were crosswise pursued in the presented works: 1) the isolation and identification of microorganisms sampled by UNESCO archeological sites near the bay of Naples, Campania; 2) the development of *in vitro* systems simulating biodeterioration phenomenon to study the structure and ecological dynamics of microbial assemblages, transposing concepts and methods of landscape ecology; 3) Evaluation of antimicrobial activities of three allelopathic substances to allow a better preservation of stone artwork together with evaluation of their environmental compatibility, in order to develop an eco-friendly system of biofilm control that is respectful of the uniqueness of each artwork.

In recent times, culture-independent metaomic analyses are often applied for the identification and characterization of microorganisms in cultural heritage objects. Among them, the most widely used methodologies are metagenomic, metabolomic and metaproteomic methods. However, more than a detection of all the microorganisms involved in a mat, often present just in little traces, an evaluation of the microbial community on the basis of its main actors may be needed, and culture-dependent analyses offers the undoubtful advantage of providing important data concerning microbial phenotypes.

The results related to point 1 are presented in chapters 3 and 4. The study of biofilm communities through numerical ecological analyses are reported in Chapter 3 in a paper (Published in PLOS ONE, 2020) entitled “*Microbial biofilm community structure and composition on the lithic substrates of Herculaneum Suburban Baths*”.

Chapter 4 reports the results of a survey carried out in different UNESCO sites of Campania, that led to the establishment of a collection of fungal strains isolated from monuments, as described in paper (Published in Applied Science, 2021) entitled “*Community composition and Ex Situ Cultivation of Fungi associated with UNESCO Heritage Monuments in the Bay of Naples*”.

Moreover, the strains isolated, identified and maintained in culture lend the

opportunity to design a series of *in vitro* experiments, to investigate the aspects related to ecological dynamics of stone microbial colonisation and to test innovative strategies of control. It has been decided to focus on some features of subaerial biofilms such as the percentage of surface occupied by colonizers, thickness of microorganisms on lithic substrata and biofilm architecture. To do so, several techniques were used, as metallurgical microscopy, confocal laser microscopy, image segmentation analysis applying metrics of landscape ecology with opportune software. Since the field application of investigated metabolites needs the assessment of their environmental compatibility, an ecotoxicological evaluation of these compounds was also carried out. The results of these experiments have been presented in a paper (Published in *Biomolecules*, 2021) entitled Fungal Metabolites with Antagonistic Activity against Fungi of Lithic Substrata (Chapter 5) and in two manuscripts in preparation (Chapter 6 and 7).

**CHAPTER 3**  
**MICROBIAL BIOFILM COMMUNITY STRUCTURE AND COMPOSITION ON**  
**THE LITHIC SUBSTRATES OF HERCOLANEUM SUBURBAN BATHS**

## RESEARCH ARTICLE

## Microbial biofilm community structure and composition on the lithic substrates of Herculaneum Suburban Baths

Antonino De Natale<sup>1\*</sup>, Bruno Hay Mele<sup>2\*</sup>, Paola Cennamo<sup>3</sup>, Angelo Del Mondo<sup>1\*</sup>, Mariagiulia Petrarè<sup>1</sup>, Antonino Pollio<sup>1,4</sup>

**Abstract** In this work, we want to investigate the impact of different substrates and different environmental condition on the biofilm communities growing on plaster, marble, and mortar substrates inside the Herculaneum Suburban Baths. To do so, we measured environmental conditions and sampled biofilm communities along the walls of the baths and used culture-dependent and -independent molecular techniques (DGGE) to identify the species at each sampling sites. We used the species pool to infer structure and richness of communities within each site in each substrate, and confocal light scanning microscopy to assess the three-dimensional structure of the sampled biofilms. To gather further insights, we built a meta-community network and used its local realizations to analyze co-occurrence patterns of species. We found that light is a limiting factor in the baths environment, that moving along sites equals moving along an irradiation gradient, and that such gradient shapes the community structure, *de facto* separating a dark community, rich in Bacteria, Fungi and cyanobacteria, from two dim communities, rich in Chlorophyta. Almost all sites are dominated by photoautotrophs, with Fungi and Bacteria relegated to the role of rare species, and structural properties of biofilms are not consistent within the same substrate. We conclude that the Herculaneum suburban baths are an environment-shaped community, where one dark community (plaster) and one dim community (mortar) provides species to a “midway” community (marble).

## **Introduction**

The Roman city of Herculaneum was destroyed in AD 79 when the Vesuvius erupted and inundated the town with hot volcanic material, submerging houses and streets [1]. Due to their burial under a thick layer of solidified lava, the Suburban Baths of ancient Herculaneum are one of the best-conserved bathing complexes that survive from antiquity. The building that hosted the baths was probably built in the AD 40s [2] and laid at an intermediate level between the city and the former seashore line. The inside environment is highly humid, indirectly exposed to a weak light filtering from the outside, and thermally stable [3]; moreover, the public is currently not allowed to enter the site. These conditions allowed different microorganisms to quickly and permanently colonize the walls of the Baths, forming dark green or black-pigmented patinas and incrustations that extensively spread on different substrates in some of the Baths' rooms.

Biological colonisation is a complex dynamic, depending on both substrates and environmental factors [4,5]. Usually, the influence of the latter is stronger, but when light, relative humidity and temperature do not represent limiting factors, physico-chemical characteristics of substrates become crucial drivers of the assembly of microbial communities [6]. Moreover, species composition may also vary in biofilm growing very close to each other, and, apparently, in the same chemical and physical conditions [7], suggesting the involvement of species interactions and stochasticity in the community assembly process. Thus, colonisation can strongly depend on the organism that establishes the first firm relationship with the substrate, conditioning the subsequent steps of the biofilm consolidation [8]. Community-level interactions are unique to each structured community of microorganisms [9], and strongly intertwined with the architecture of the biofilm. At a fundamental level, spatial interactions among microorganisms forming biofilms on monuments can often explain important attributes of biofilms [10] and are well documented [11]. Actinobacteria and filamentous Cyanobacteria, for example, often grow in a close association, sometimes establishing a direct cell-to-cell contact and some other times sharing a matrix of extracellular polymeric substances (EPS). Such matrix represents at the same time the adhesion agent used by organisms to remain anchored to the substrate and the common ground that connects them. It also has a

potential role in modulating chemical signals at the base of microorganisms' interactions [12].

This study aims to assess the influence of substrate and microclimatic conditions on species composition and three-dimensional structure of biofilms growing in Herculaneum Suburban Baths. To do so, we measured environmental variables and collected biofilms samples from three of the substrates used in building the Baths: plaster from the *Vestibulum* (on which are still present frescoes traces), marble from the *Tepidarium*, and mortar from the swimming pool. After collection, we identified the species present in each environmental sample by coupling culture-dependent and -independent techniques and used this information to assemble a co-occurrence matrix and proceeded to analyze the structure and the richness of the communities at various sites. Then we used confocal laser Microscopy (CLSM), the election tool for non-destructive analyses of biofilm on monuments [13,14], to elucidate the spatial organization of the communities. Finally, we transformed the co-occurrence matrix into a meta-community network analyzing both its local realizations (*i.e.*, the sampled communities) and the meta-communities associated with the single substrates.

## **Material and methods**

### **Environment description and sampling**

The Herculaneum Baths architectural structure is the one generally used by Romans when building public baths (Fig 1A). The first chamber from the entrance is a *Vestibulum*, an ample room with four columns, delimitating a central square. The *Vestibulum* is followed by an *Apo- dyterium*, a *Frigidarium* and a room with a pool of cold water. Parallels to these rooms there is a day room open to the seaside landscape for conversation and relax, connected to the *Vestibulum*. Next to the "day room" is the *Caldarium*, then a room with decorations on the walls (*Tepidarium*) and finally a room with a large, heated swimming pool.

A *Laconicum*, used for saunas, is accessible from the heated pool room. Among the Suburban Baths' rooms, only the *Vestibulum*, the *Tepidarium*, and the room with the large swimming pool were colonized by conspicuous biofilms, visible on three

substrates: plaster in the *Vestibulum*, polychrome marble in the *Tepidarium*, and mortar in the swimming pool. Both plaster and mortar are non-homogeneous materials widely diffused in Herculaneum buildings: the former is made by a mixture of calcitic binder and volcanic scoriae, covered by a thin superficial layer of lime and marble powder [15], whereas the latter is prevalently composed by lime and inert volcanic aggregates with variable dimensions [16].

The general distribution of biofilms on the walls of the Suburban Thermae appeared patchy to the naked eye. Since the area is restricted to public, biofilm development and distribution is not affected by the presence of vectors. Sampling has been authorized by *Soprintendenza speciale per i beni archeologici Pompei, Ercolano e Stabia* (Via Villa dei Misteri, 1, 80045 Pompei, Naples, Italy) in the person of Arch. Giuseppe Zolfo, within an agreement with the laboratory of algal biology and ACUF collection at the Department of Biology, University of Naples “Federico II”. In every site, we measured temperature and relative humidity using a thermo-hygrometer (model HI 9564, Hanna1 Instruments, USA), and light intensity using a Climalux N light meter (Laboratori di Strumentazione Industriale s.p.a., Italy). pH on substrates was measured at sampling points using pH test paper strips, showing no consistent variation able to affect an homogeneous response of communities.

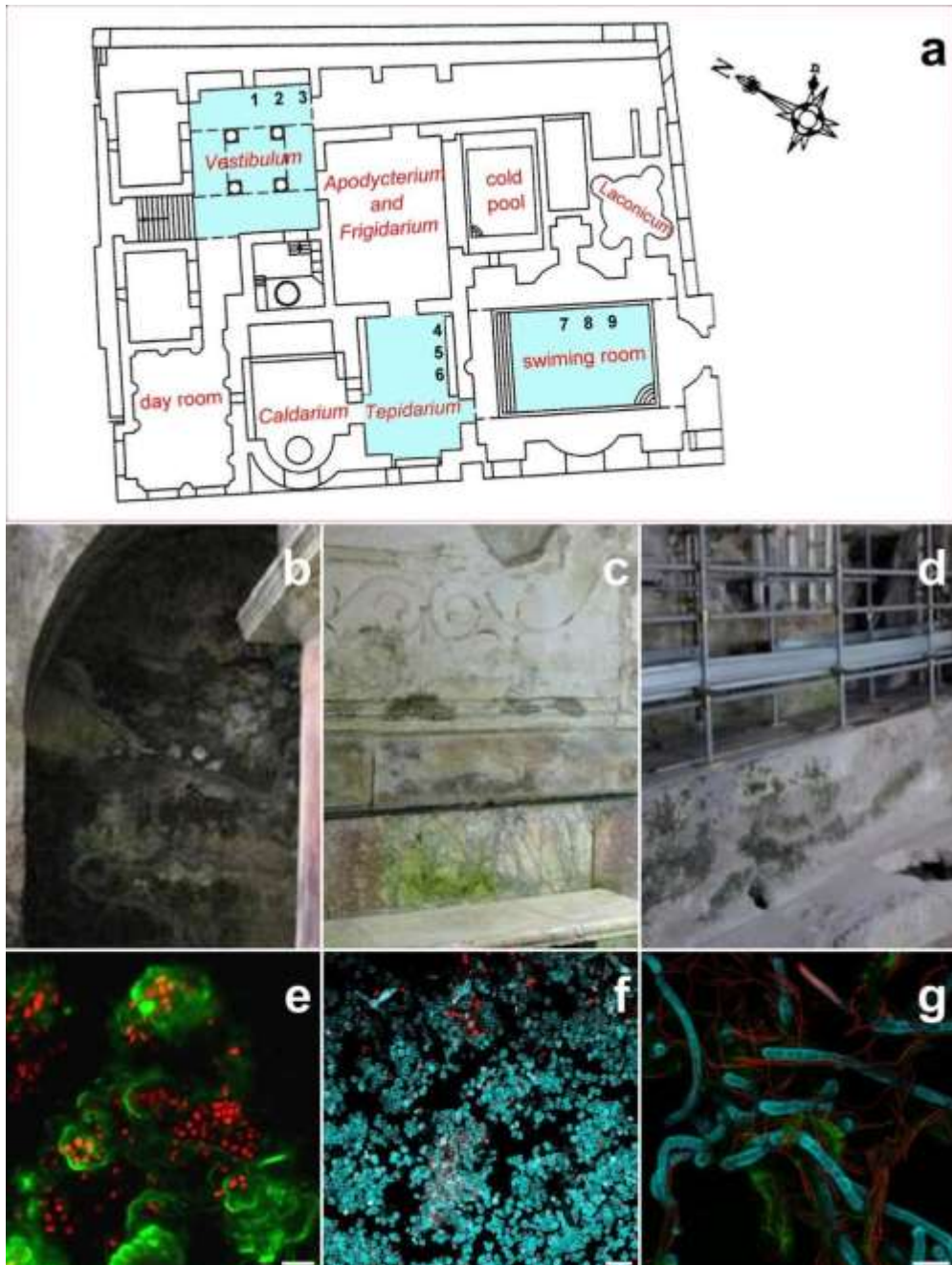


**Fig 1.** (a) Map of the Suburban Baths, with details of the *Vestibulum* (b), the *Tepidarium* (c), and of the room with a large heated swimming pool (d). Light blue highlights sampled rooms, with numbers marking the biofilm sampling sites. In following panels (e, f, g) are matched CLS-M microphotographs of sampled biofilms. Scale bar 20  $\mu\text{m}$ . Floor plan of suburban baths is not subject to copyright and has been de novo realized with freeware software Fiji.

<https://doi.org/10.1371/journal.pone.0232512.g001>

### **Biofilm sampling**

Biofilm samples were collected *in situ* during autumn 2016, using either sterile double-sided adhesive tape (1 cm wide) or by gently scraping the walls of the sampling sites with a sterile scalpel and depositing materials into sterile vials [17]; sampling was random and repeated three times per room/material (numbers in Fig 1A).

### **Culture-dependent isolation of microbial strains**

Each sample collected in the field with a sterile scalpel was suspended in a sterile isotonic solution (10 mg/ml). From this stock, serial dilutions up to  $10^{-7}$  were prepared, and 10  $\mu$ l from  $10^{-4}$  or  $10^{-6}$  dilutions were spread on 9 cm diameter Petri Dishes for the isolation of microorganisms. We used a Bold Basal Medium with the addition of sucrose 12g/L for Fungi, Bacto Yeast Extract (BYE, BD Company, USA) broth for Heterotrophic bacteria, and solidified Bold Basal Medium for Cyanobacteria and microalgae. Petri dishes were incubated at 21-22°C for heterotrophic bacteria and 25°C for fungi. The growth of colonies was daily checked for heterotrophic bacteria and every 72 hours for Cyanobacteria, microalgae and fungi. Finally, colonies from each dish were axenically picked up and transferred to Petri dishes containing the same culture media used for the isolation of colonies. We used the obtained monoclonal cultures for DNA isolation.

### **DNA-based molecular analysis**

Genomic DNA was extracted from both biofilm samples and axenic cultivated isolates using the procedure described by [18]. Biofilm samples were amplified for their rRNA genes by PCR using the universal primers for cyanobacteria 16S [19], eukaryote-specific 18S primers for algae [20], 18S and 28S primer for fungi [21].

In the case of cultivated isolates, we used the following primer combinations for amplification: ITS1 rDNA for Fungi (ITS1 5'-TCCGTAGGTGAACCTGCGG-3', [21]; ITS\_ADM 5'-TTCAAAGATTCGATGATTCAC-3'); ITS1 [21] and ITS2 rDNA for microalgae [22] and 16S rDNA for Cyanobacteria (16S\_long 16Slong\_Fw 5'-AGGATGCAAGCGTTATCCG-3'; 16Slong\_Rv, 5'-GGGGCATGCTGACTTGACG-3'). Similarly, we used different amplification protocols for biofilm samples and cultivated isolates: the formers were carried out on an estimate of 10 ng of extracted DNA, in a final volume of 50  $\mu$ L containing

five  $\mu\text{L}$  of 10X PCR buffer, 100 mM of deoxynucleotide triphosphate, 2.5 mM of magnesium chloride, 0.5 mM of primers, and 1U of Taq polymerase (Quiagen, Hilden, Germany). The PCR program consisted of an initial denaturation at 95°C for 4 min and 30 cycles including 1 min of denaturation at 94°C, 45 s of annealing at 56°C, and 2 min extension at 72°C. A final extension of 7 min at 72°C was followed by cooling at 4°C. Cultivated isolates amplifications were carried out in a 25 $\mu\text{L}$  aliquot containing approximately 100 ng DNA, a deoxynucleoside triphosphate mixture (0.2 mM each), buffer (1/10 volume of the supplied 10 $\times$  buffer), supplemented to give a final concentration of 2.5 mM  $\text{MgCl}_2$ , 1.25 U of Taq polymerase (EconoTaq, Lucigen), and 0.5 mM of each primer. The amplification was performed in an Applied Biosystem 2720 thermal cycler. The profile used was 5 min at 95°C, 15 cycles at 95°C for 30s, 55°C for 30s, 72°C for 30s, with annealing temperature increasing by 0.5°C at each cycle, plus 25 cycles with annealing temperature fixed at 55°C and a final elongation step of 7 min at 72°C followed by cooling at 4°C. The sample quality of all PCR products was evaluated through electrophoresis run on 1% (w/v) agarose gel. We obtained Denaturing Gradient Gel Electrophoresis (DGGE) profiles for microbial communities in each sampling site from the PCR products of environmental samples, following the protocol of Nubel et al. [19]. PCR products from cultivated isolates were purified them using QIAquick1 PCR Purification kit (Qiagen Inc., Valencia, CA, USA), obtaining sequence reactions with the BigDye Terminator Cycle Sequencing technology (Applied Biosystems, Foster City, CA), and purifying them in automation using the Agencourt CleanSEQ Dye terminator removal Kit (Agencourt Bioscience Corporation, 500 Cummins Center, Suite 2450, Beverly, MA, 01915, USA) and a robotic station Biomek FX (Beckman Coulter, Fullerton, CA). PCR products were analyzed using an Automated Capillary Electrophoresis Sequencer 3730 DNA Analyzer (Applied Biosystems). In both cases, we used the amplification as the sequencing primers. all sequences obtained from molecular analysis were edited using 4Peaks v1.8 software, and nucleotide sequence similarity was determined using BLASTN algorithm v 2.0 (NCBI) (S1 Table).

### **Optical, fluorescence and laser confocal microscopy**

Aliquots of the biofilm samples collected through the adhesive tape method from each sampling site were observed by optical and fluorescence microscopy (Nikon Eclipse E800) in order to distinguish the structural properties of the microbial communities.

The characterization of three-dimensional biofilm structure was obtained using Leica TCS SP5 (Leica Microsystems CMS GmbH, Mannheim, Germany) Confocal Laser Scanning Microscope (CLSM) equipped with an HCX PL APO 63.0x1.40 oil UV. We took image stacks from each strip of double-sided adhesive tape at 0.50–0.71  $\mu\text{m}$  intervals, and information acquired in the three channels simultaneously (Table 1). The substratum area of the image stack was 1024 x 1024 pixel, with the number of images in each stack varying according to the thickness of the biofilm.

We used the open-source image processing package Fiji [23]; and also <http://www.fiji.sc> for the preliminary preparation of images, according to [24] and the Comstat2 [25] plugin to determine volume and roughness of each Z-stacks [26,27]. Finally, the same plugin was applied to each stack in order to obtain the biomass associated with each color channel (Table 1). The Z-stacks in which the algal masses showed little and variable autofluorescence were deconvolved and displayed as MIPs (Maximum Intensity Projection). We manually identified and selected cell outlines to measure cell area and mean fluorescence. The Corrected Total Cell Fluorescence (CTCF) was calculated according to [28]. In all the Z-stacks assembled from the swimming pool community images, we detected a marked amount of *Scytonema julianum* filaments emitting weak self-fluorescent signals, probably due to senescence or death. To reduce the effect of dead filaments on measurements the autofluorescence of single *S. julianum* cells was equalized using auto-fluorescence values of *Leptolyngbya sp.* cells, this latter being widely present and with a uniform emission of autofluorescence (S1 Fig).

**Table 1. Fluorescence microscopy information.** Red has no labeller because pigments are observed by autofluorescence.

Channel	Wavelength	Emission	Labeller	Marker	Proxy of
Red	633	641–736		Pigments (chl <i>a</i> , phycobilins)	Phototrophs
Blue	405	415–505	Calcofluor	Bacteria, Hyphae	H. bacteria, Fungi
Green	543	553–636	Concanavalin-A	Extra-Polymeric Matrix (EPS)	EPS itself

<https://doi.org/10.1371/journal.pone.0232512.t001>

## Data analysis

All the data analysis and visualization were performed using the R environment for statistical computing [29], using the tidyverse collection of packages [30], tidygraph [31] and graph [32]. The R markdown file generating tables and figures is available as supplemental material. The substrates were ordered using the walking order of the rooms, and for each species we added two coarse levels of classification: photo/hetero-trophism and taxa. We used a Bray-Curtis distance-based nonmetric dimensional scaling (nMDS) to produce an ordination of the communities found at the nine sampling points. Pairwise distance among communities was based on differences among functional groups' relative richness (i.e., the count of species associated to each group, scaled by the total number of species determined for each site). All the environmental and structural variables measured were projected on the ordination as nonlinear surfaces to indirectly relate them to the ordination axes. The co-occurrence table that defines the sampled communities was used as a starting point for the assembly of an unweighted, undirected meta-community network that links species based on their contemporary co-occurrence in a site. A layout display was calculated using the Fruchterman-Reingold (FR) force-directed algorithm [33], that defines nodes (i.e., species) distance as inversely proportional to the number of neighbors a node has (i.e., the higher species pair co-occurrence frequency is, the lower node distance between them). We then split the meta-community network and sampled communities were plot as single graphs using the calculated FR layout. Finally, we subsetted the bath meta-community based on the three substrates, and displayed every subset as a linear graph, i.e., nodes were all put on a single line and sorted first by taxon and then by alphabetical order.

## Results

### Environment characterization of sites

The sampling campaign was focused on the three rooms of Suburban Thermae not interested by recent restoration works, where the presence of biofilms was evident at a first glance. The general distribution of biofilms appeared patchy to the naked eye. This is a common feature of microbial lithic communities, depending on variation in substrata characteristics correlated to centimeter scale variations [34]. Plotting the environmental features of samples (Table 2) shows that relative humidity (RH) is always close to saturation ( $rh > 92\%$ ) and that both humidity and temperature values partially overlaps among samples and substrates, while irradiance changes moving from the plaster substrate to wards marble and mortar is lower in the plaster site (Fig 2).

**Table 2. Mean temperature, relative humidity and light irradiance at the nine sample points.**

Each value is the mean of three measurements campaigns taken during autumn 2016.

Substratum (room)	Sample (Fig 1A)	Temperature (°C)	pH	Relative humidity (%)	Light irradiance ( $\mu\text{E m}^{-2}\text{s}^{-1}$ )
Plaster ( <i>Vestibulum</i> )	1	16.7±1.2	from 7 to 8	96±0.2	10.5±0.8
	2	17.2±2.1	from 7 to 8	95±1.5	9.0±0.4
	3	16.5±2.5	from 7 to 8	95±0.9	10.3± 1.2
Marble ( <i>Tepidarium</i> )	4	13.7±1.5	from 7 to 8	95±0.7	36±0.2
	5	15.3±0.9	from 7 to 8	94±1.7	30±0.6
	6	15.4±1.6	from 7 to 8	95±1.4	31.2±0.9
Mortar ( <i>swimming pool</i> )	7	14.3±2.0	from 7 to 8	95±0.8	22±0.4
	8	16.1±1.8	from 7 to 8	93±1.3	24±0.7
	9	15.6±2.6	from 7 to 8	94±1.5	24±1.3

<https://doi.org/10.1371/journal.pone.0232512.t002>

## Biofilm richness from molecular data

The distribution of bacteria, Cyanobacteria, Chlorophyta and Fungi species on each sample from the three selected substrates is shown in Fig 3. Globally, the most represented taxon is Chlorophyta, with thirteen species found, followed by Cyanobacteria and Fungi with ten species, and heterotrophic bacteria, with six species. All the taxa are found at least onetime on each substrate, with 50% of Cyanobacteria and Fungi being found only once.

Heterotrophic bacterial profiles were different among substrates, and almost equally distributed. The occurrence of members of *Bacillus* genus was common to all sites, with an unidentified *Bacillus* being the most diffused in the sampled areas. The remaining genera, *Paenibacillus* and *Streptomyces*, were found on plaster and marble but not on the mortar substrate.

The highest number of Cyanobacteria bands was found on plaster, with eight phylotypes, whereas the other two substrates hosted limited Cyanobacterial biodiversity. The only two species common to all three substrates were those of filamentous genera *Leptolyngbya* and *Phormidium*.

We identified thirteen different DGGE bands belonging to Chlorophyta on the three substrates, with dominance from marble and mortar (ten and eleven phylotypes, respectively). The genera most represented belong to *Chlorella* and *Chlorella*-like group. The only genera common to the three substrates were *Stichococcus*, *Pseudochlorella*, and *Microthamnion*.

Finally, we identified DGGE bands belonging to Fungi on the three substrates, with the same dominance pattern of Cyanobacteria. The genera more represented were *Aspergillus* and *Penicillium*, but no species appeared in all substrates. DGGE failed to spot one cyanobacterium (*Scytonema julianum*) and two microfungi (*Curvularia geniculata* and *Lecanicillium* sp.) in the environmental sample. Rendering the species list as an alluvial plot make possible the flows of species among substrates and shows how the species colonizing the marble substrate are also associated to plaster (for Bacteria and Fungi) and mortar (for Cyanobacteria and Chlorophyta). It is worth noting that the Fungi found on the Mortar substrate are unique to that substrate.

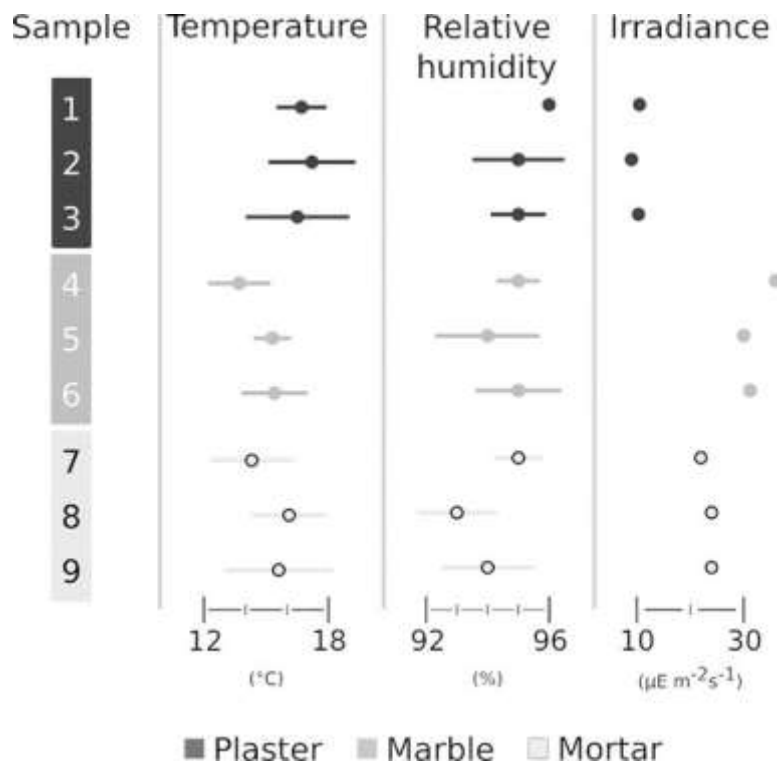
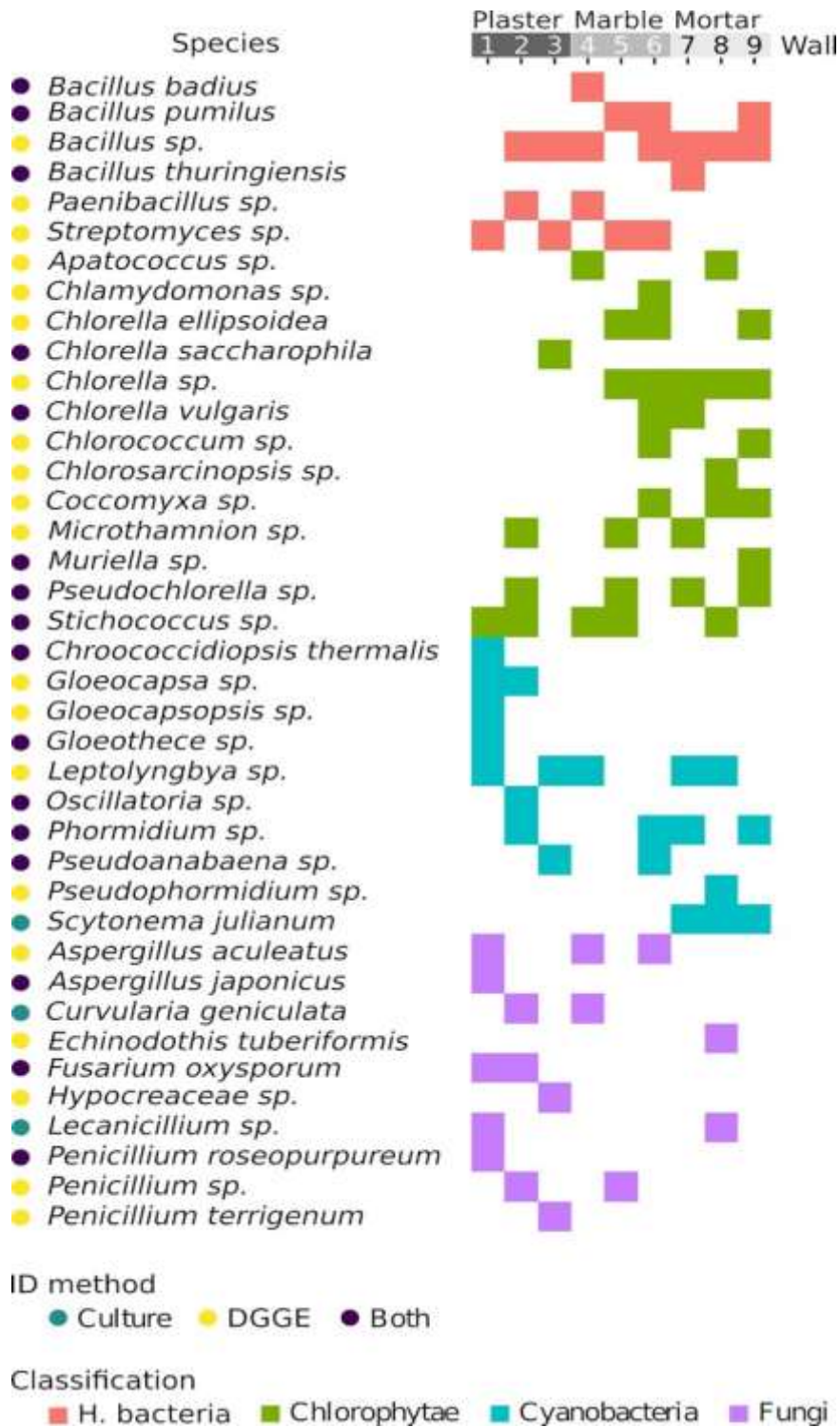


Fig 2. Scatter Plot (SP) of environmental parameters, i.e. of temperature, RH, and irradiance for all the samples of the baths.

<https://doi.org/10.1371/journal.pone.0232512.g002>



**Fig 3. List of the species identified in Herculaneum Suburban Baths samplings.** The list is ordered first by classification and then by name. Different square colors stand for different classification, while the dots at the side of species names indicate the ID method used for that species.

<https://doi.org/10.1371/journal.pone.0232512.g003>

### **Analysis of CLSM images**

After preparation, we analyzed the biofilm samples using a Confocal Light scanning Microscope (S1 Fig). The analysis permitted us to gather insights about biofilms structure and to quantify the relative abundance of and their main autotrophic and heterotrophic components (Table 3).

The low intensity of auto-fluorescence with a high Standard Deviation ( $169.75 \pm 96.32$ ) seems to indicate an advanced stage of senescence and limited cellular vitality (S1G–S1I Fig).

Plotting the structural attributes of sampled communities (S2 Fig) shows that the most samples display similar values for surface and volume to MIP ratio; at the same time, roughness and substrate coverage tends to vary among samples. Sample 7 is the one with maximum values for all the attributes.

The nMDS ordination performed on the nine sites highlight within-substrate similarities (Fig 4A).

Plaster samples are projected at equal distance between Fungi and Cyanobacteria, and display a considerable distance from Chlorophyta and Heterotrophic Bacteria. Mortar communities are characterized by the highest proximity with both Cyanobacteria and Chlorophyta, while marble samples appear to be associated to the maximal Heterotrophic Bacteria contribution to community structure. Projecting the irradiation values over the ordination highlight the light segregation of the plaster communities (all below the  $15 \mu\text{E m}^{-2}\text{s}^{-1}$  isoline), opposed to the high light condition of the marble ones. Mortar community sits in between. It is worth noting that the Cyanobacteria (and Fungi) to Chlorophyta (and heterotrophic bacteria) gradient is overlapping with the irradiance gradient. The projection of all other variables (both environmental and structural) on the ordination does not highlight any particular trend and is such reported as supplemental image (S3 Fig). The calculation of the relative abundance based of the CLSM analysis shows that all the sites are heavily dominated by photoautotroph (>93%, Fig 4B), with the only notable exception of sample 2, where fungi and heterotrophic bacteria represent the 43% of the total. The comparison of this data with the relative richness of the sites based on molecular analyses suggests that fungi and heterotrophic bacteria, while rich in terms of species, are poorly represented in terms of abundance, *i.e.*, are

rare species.

Table 3. Selected CLSM structural parameters of sampled biofilms.

Substrate	Sample	Substratum coverage (%)	Roughness (Ra)	Vol./MIP ( $\mu\text{m}^3/\mu\text{m}^2$ )	Surface ( $\mu\text{m}^2$ )		Volume (%)
plaster (Vestibulum)	1	53.68	2.91	2.85	123912.87	Phototrophs	39.84
						Fungi	1.49
						EPS	58.67
	2	20.88	13.23	8.90	97180.63	Phototrophs	29.49
						Fungi	17.28
						H. bacteria	4.83
	3	10.39	10.40	23.07	34357.94	Phototrophs	73.19
						EPS	26.81
marble (Tepidarium)	4	60.07	20.63	9.57	282924.80	Phototrophs	74.77
						Fungi EPS	1.27 23.96
	5	32.58	1.39	0.79	97183.05	Phototrophs	72.49
						Fungi	3.03
	6	37.40	18.58	0.97	217274.40	Phototrophs	98.03
						Fungi	1.97
marble (Swimming pool)	7	50.61	26.16	32.40	359188.97	Phototrophs	52.69
						EPS	47.30
	8	35.15	1.51	2.32	118733.54	Phototrophs	96.21
						Fungi	3.78
	9	8.60	0.93	2.36	27010.71	Phototrophs	77.83
						EPS	22.16

<https://doi.org/10.1371/journal.pone.0232912.t003>

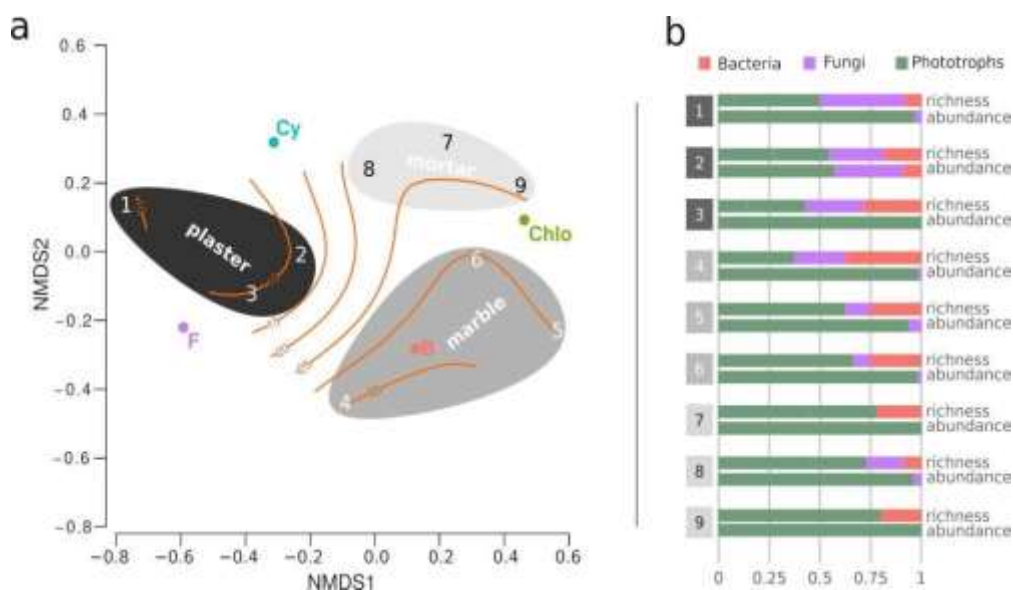


**Fig 4. Characterization of microbial community.** a) nonmetric dimensional scaling(stress = 0.03) of the communities found at the nine sampling points with respect to their relative taxa count within the different functional groups. Weighted average scores of the four functional groups are displayed as colored dots to ease the interpretation of the ordination, as well as sampling sites and substrates, following the color code presented in Fig 3. The ellipsoids visually cluster sites belonging to the same substrate, while the isolines represent irradiance values ( $\mu\text{E m}^{-2}\text{s}^{-1}$ ); b) Bar plots of relative (%) richness and abundance for all the sampling sites.

<https://doi.org/10.1371/journal.pone.0232512.g004>

### **Co-occurrences based network**

We created co-occurrence networks for each sampled community and displayed them using the FR layout algorithm (Fig 5). The three plaster communities (1–3, top row in Fig 5) are shifted toward the periphery of the network: such behavior, together with the abundance of local links (cyan edges) indicates that the community is rich in local species. At the other end of the spectrum, the three marble communities (4–6, middle row, Fig 5) tend to be concentrated in the network center: this, together with the abundance of global links (red edges), indicates that common species represent the backbone of these communities. Finally, the mortar community displays an intermediate behavior, with sample number eight being the richest in local species (cyan connections). In addition, it should be noted that mortar community displays a high level of promiscuity, *i.e.* many species are shared among single communities.

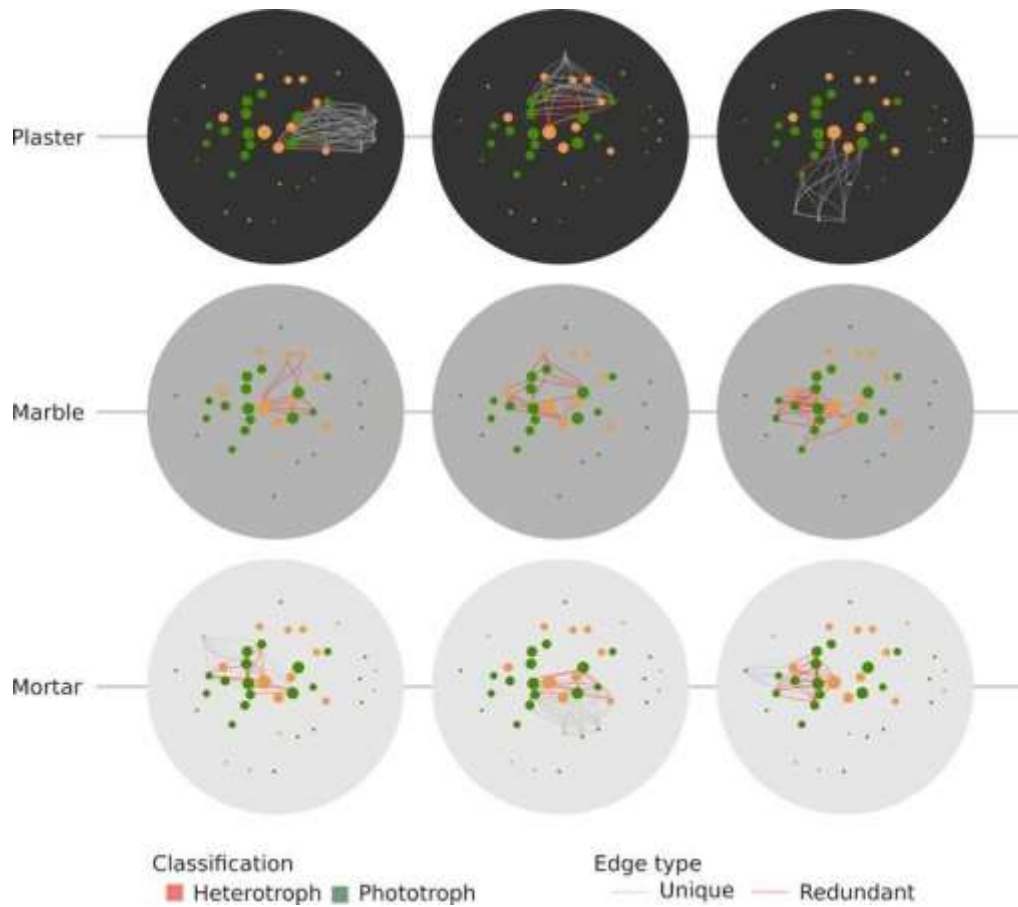


**Fig 5. Network display of the communities found in the sampled points of the Herculaneum Suburban Baths using the Fruchterman-Reingold layout (see text).** Each circle represents the community found in a single sample. Node diameter is proportional to the number of sites the species is found in, while edge color is red if the species pair is found more than once in any site, and cyan if the species pair is only found in that specific site. The substrates are color-coded as per the other figures.

<https://doi.org/10.1371/journal.pone.0232512.g005>

## **Discussion**

Microorganisms can cause severe damage to historical monuments in different ways, ranging from the corrosion of the building material of the walls to the modifications of surface colors and texture.

Heterotrophic organisms, bio-corrosive chemoorganotrophic bacteria and fungi diversely affect stone and rocks, the rate of corrosion being dependent on the geomorphology of the substratum [9,35]. The relation between lithic facies and species composition of microbial communities has been the focus of different studies, carried out on monuments of different continents. In general, some physical features of the stones, as porosity, roughness and water retention have been associated with the presence of biofilm, and, in some cases, a correlation between microbial species and different types of stone substrates has been reported [5]. Biofilm structure can be dictated also by surface and interface properties or substrata. Bio-weathering of limestones and marble used in building construction allows the acquisition of macro and micronutrients from mineral surfaces, along with some organic compounds [35,36]. Plaster and mortars in Roman houses of the Vesuvian cities were basically made of limestones, used as binder, and volcanic materials, as pumices and scoriae [37]. Major and trace elements from Herculaneum mortars evidenced the occurrence of calcium, strontium, sodium and iron [16] that can support microbial life. Also, marble shows the same structural components, being composed by limestone crystallized by heat and pressure [38]. The presence of painted walls in the Vestibulum could account for a different mineral availability. Hematite, Egyptian blue, yellow ochre, goethite, and charcoal were the pigments most frequently used to paint walls, and their chemical constituents, together with organic binders occasionally used [39] could represent a supplemental food source for pioneer microbes on the surface of the Vestibulum walls. In this respect, the possible role of micronutrient from substrate in the observed pattern of colonisation cannot be ruled out. However, the minor occurrence of heterotrophic bacteria and fungi in all biofilm samples from Herculaneum While microorganisms which live on the external surfaces of monuments must endure sharp variations of temperature, light intensity, and humidity, and are exposed to desiccation and high insolation [40], microbial

communities colonizing caves, hypogea, catacombs and similar sites, thrives in quite constant environmental conditions [41,42].

Heterotrophic bacteria and fungi, constitute most of the biodiversity in caves and are ubiquitous in different cave habitats [43,5]; actinobacteria involved in biomineralization processes are common [44,45,46], and *Bacillus* and *Paenibacillus* occurrence has been frequently reported [47,48].

The Suburban Baths of Herculaneum represent an interesting case study of hypogean biofilm communities, in which some critical environmental features such as light, temperature and humidity present limited spatial and seasonal variability and only three different substrates were available for microbial colonisation.

The results presented support the description of the Herculaneum baths as an extremely humid and thermally stable environment, where biofilm development can thrive, untouched, due to almost saturating humidity. Our results also indicate that neither species composition nor biofilm structural properties are consistent within the same substrate. This discrepancy could be due to an irradiation gradient that ranges from almost disphotic conditions to dim light, but the possible role of small-scale chemical heterogeneity cannot be ruled out due to inevitable limitations of the experimental designed. As a hypogean habitat, the bathshost four prominent groups of microorganisms: heterotrophic bacteria, fungi, green algae (Chlorophyta) and blue-green algae (Cyanophyta). All four groups are distributed among the walls in the three colonized sites, with a low contribution of heterotrophic bacterial species to richness, and a considerable, yet heterogeneous, pool of species scattered among substrates.

Actinobacteria belonging to Genus *Streptomyces* [45,46] and fungi like *Lecanicillium* can occur on different substrates of subterranean environments [47,48]. The Genus *Streptomyces* has also been found in water, rocks and soils from Spanish and Italian caves [49], and its potential role as a contributor of biotic rock-building processes has been recently proposed [50].

The fungal genera *Aspergillus*, *Penicillium* and *Fusarium*, have a cosmopolitan distribution and are common in many different habitats, including caves, where they respectively represent the first, second and fourth most frequently found taxa [51].

The community composition is seemingly influenced by the irradiation gradient and goes from being a mix of heterotrophic and dark-adapted autotrophic species (dark composition, the *Vestibulum*) to being rich in low-light adapted autotrophs (dim composition, the other sites), with the *Tepidarium* community sharing its dark-adapted species with the *Vestibulum* and its dim-adapted species with the swimming pool. It is possible to appreciate how the heterotroph/autotroph rates move from the dark vestibule extreme, where fungal richness is maximum, and cyanobacteria steadily compete with green algae, to the dim light swimming pool community, where only *E.tuberiformis* and *Lecanicillium* sp. remain as a fungus, and Cyanobacteria are relegated to a small portion of the species pool.

Fungal genera as *Lecanicillium* can occur on different substrates of subterranean environments [52], whereas *Echinodotis tuberiformis* has been described as an insect parasite and an epibiont of different flowering plant species [53,54] and could have reached the Bath with air current, or because of animal/human contamination. In a recent study carried out on two anthropogenic caves [55], we observed that blue-green unicellular and colonial Cyanobacteria dominate in almost disphotic conditions, whereas filamentous Cyanobacteria showed the highest relative abundance under dim light. In these latter conditions, Chlorophytes and other minor eukaryotic phototrophs also give a relevant contribution to stone surfaces colonisation. This trend is also confirmed in Herculaneum Suburban Baths, where unicellular Cyanobacteria genera like *Chroococciopsis*, *Gloeocapsa*, *Gloeocapsopsis*, and *Gloeotheca* occur prevalently under the very reduced light of the *Vestibulum*, whereas the filamentous *Leptolyngbya* and *Scytonema* are mainly present in the communities from *Tepidarium* and *Swimming pool*. Our analysis suggests that on the one hand, the meta-communities associated with the three substrates tend to be mostly composed of isolated communities. On the other hand, there is a single meta- community (the *Tepidarium*), sharing almost all of the species with the other two. The results gathered here support the hypothesis of the Herculaneum baths walls as communities where the low irradiance represents one of the limiting factors, influencing community composition. Indeed, while irradiance gradient influences the three meta-communities, driving the assembly of dark- (*Vestibulum*) and dim light- adapted (*Tepidarium*, *Swimming pool*)

communities, the substrate clustering emerging from the nMDS could hint at a contribution of substrate chemistry in driving community assembly.

Using a network depiction permits to appreciate the structure of the communities intuitively; furthermore, building a meta-network gives the chance to explore relationships among the populations. Even with the limit of a co-occurrence matrix, it is possible to gather interesting insights about richness by appropriately choosing the layout algorithm. Our choice of a force-directed algorithm revealed itself fundamental in expressing community structure based on the number of sites where every single species is found. Indeed, the FR-based meta-network layout shows an interesting gradient in community composition, mostly overlapping the walking order of the rooms.

## **Conclusion**

We have explored the combined effects of substrate and environmental features on microbial community composition in Suburban Baths of *Herculaneum* using molecular and CLSM data to apply numerical ecology tools. Our results indicate that micro-environmental conditions differentiate communities growing on the same substrate, and that it is possible to cluster biofilm morphology using environmental conditions. More specifically, we found that the irradiation gradient is one of the factors that contribute to the differentiation among communities in the Suburban Baths, with the low-light plaster community is rich in fungi and cyanobacteria, while the two dimly lighted communities are richer in Chlorophyceae. In conclusion, our study supports the hypothesis of a strong effect of the environment over substrate in defining community composition, and paves the way to more complex studies, where a higher sampling effort and/or a quantification of microbial abundances could further discriminate community dynamics. Biodeterioration is a prominent issue in conservation of sites and manufacts of archeological interests. Studying biofilm communities through numerical ecological analyses can represent a valuable tool to prevent their proliferation and to develop sustainable approaches to limit or eradicate them.

## References

1. Deiss JJ. Herculaneum, Italy's buried treasure. Getty Publications. 1989.
2. Guidobaldi MP. Ercolano, tre secoli di scoperte. Electa Mondadori. 2008.
3. Pesaresi P, Martelli Castaldi M. Conservation measures for an archaeological site at risk (Herculaneum, Italy): from emergency to maintenance. *Conservation and Management of Archaeological Sites*. 2008; 8(4): 215–236.
4. Barberousse H, Ruot B, Ye'pre'mianb C, Boulon G. An assessment of facade coatings against colonisation by aerial algae and Cyanobacteria. *Building and Environment*. 2007; 42(7): 2555–2561.
5. Tomaselli L, Lamenti G, Bosco M, Tiano P. Biodiversity of photosynthetic microorganisms dwelling on stone monuments. *International Biodeterioration & Biodegradation*. 2000; 46(3): 251–258.
6. Tran TH, Govin A, Guyonnet R, Grosseau P, Lors C, Garcia-Diaz E, et al. Influence of the intrinsic characteristics of mortars on biofouling by *Klebsormidium flaccidum*. *International Biodeterioration & Biodegradation*. 2012; 70: 31–39.
7. Urz'1 C, De Leo F, Bruno L, Albertano P. Microbial diversity in paleolithic caves: A study case on the phototrophic biofilms of the cave of bats (Zuheros, Spain). *Microb. Ecol.* 2010; 60:116–129. <https://doi.org/10.1007/s00248-010-9710-x> PMID: 20607532
8. Curtis TP, Sloan WT. Prokaryotic diversity and its limits: microbial community structure in nature and implications for microbial ecology. *Current Opinion in Microbiology*. 2004; 7(3): 221–226. <https://doi.org/10.1016/j.mib.2004.04.010> PMID: 15196488
9. Viles H. Ecological perspectives on rock surface weathering: towards a conceptual model. *Geomorphology*. 1995; 13: 21–35.
10. Haussler S, Fuqua C. Biofilms 2012: New discoveries and significant wrinkles in a dynamic field. *Journal of Bacteriology*. 2013; 195(13): 2947–2958. <https://doi.org/10.1128/JB.00239-13> PMID: 23625847

11. Albertano P, Urzì C. Structural interactions among epilithic cyanobacteria and heterotrophic microorganisms in Roman hypogea. *Microb. Ecol.* 1999; 38: 244–252.  
<https://doi.org/10.1007/s002489900174> PMID: 10541786
12. Paerl HW. Epi- and endobiotic interactions of cyanobacteria. In: Reisser W. (ed.), *Algae and symbioses: plants, animals, fungi, viruses, interactions explored*. Biopress, Bristol. 1992; pp. 537–565.
13. Rolda'n M, Herna'ndez Marine' M. Exploring the secrets of the three-dimensional architecture of phototrophic biofilms in caves. *International Journal of Speleology*. 2009; 38(1): 41–53.
14. Zammit G, Psaila P, Albertano P. An investigation into biodeterioration caused by microbial communities colonizing artworks in three maltese Palaeo-Christian catacombs. In: Notea A, Shoef Y. (eds.). *Non-destructive testing, microanalysis and preservation in the conservation of cultural and environmental heritage' ISAS International Seminars Ltd. 9th International Conference on NDT of Art, Jerusalem Israel, 25–30 May. 2008; pp. 1–10.*
15. Leone G, De Vita A, Magnani A, Rossi C. Thermal and petrographic characterization of Herculaneum wall plasters. *Archaeometry*. 2017; 59(4): 747–761.
16. Leone G, De Vita A, Magnani A, Rossi C. Characterization of archaeological mortars from Herculaneum. *Thermochimica Acta*. 2016;624: 86–94.
17. Urzì C, De Leo F. Sampling with adhesive tape strips: an easy and rapid method to monitor microbial colonisation on monument surfaces. *Journal of Microbiological Methods*. 2001; 44: 1–11. [https://doi.org/10.1016/s0167-7012\(00\)00227-x](https://doi.org/10.1016/s0167-7012(00)00227-x) PMID: 11166095
18. Doyle JJ, Doyle JL. Isolation of plant DNA from fresh tissue. *Focus*. 1990; 12: 13–15.
19. Nu"bel UF, Garcia-Pichel F, Muyzer G. PCR primers to amplify 16S rRNA genes from cyanobacteria. *Appl. Environ. Microbiol.* 1997; 63: 3327–3332. PMID: 9251225
20. Diez B, Pedros-Alio C, Marsh TL, Massana R. Application of denaturing gradient gel electrophoresis (DGGE) to study the diversity of marine

picoeukaryotic assemblages and comparison of DGGE with other molecular techniques. *Applied and Environmental Microbiology*. 2001; 67: 2942–2951. <https://doi.org/10.1128/AEM.67.7.2942-2951.2001> PMID: 11425706

**21.** White TJ, Bruns T, Lee S, Taylor JW. Amplification and direct sequencing of fungal ribosomal RNA genes for phylogenetics. In: Innis MA, Gelfand DH, Sninsky JJ, White TJ. (eds.) *PCR protocols: a guide to methods and applications*. Academic Press, Orlando. 1990; pp. 315–322.

**22.** Chen S, Yao H, Han J, Liu C, Song J, Shi L, et al. Validation of the ITS2 region as a novel DNA barcode for identifying medicinal plant species. *PLoS ONE*. 2010; 5(1): e8613. <https://doi.org/10.1371/journal.pone.0008613> PMID: 20062805

**23.** Schindelin J, Arganda-Carreras I, Frise E, Kaynig V, Longair M, Pietzsch T, et al. Fiji: an open-source platform for biological image analysis. *Nature Methods*. 2012; 9(7): 676–682. <https://doi.org/10.1038/nmeth.2019> PMID: 22743772

**24.** Del Mondo A, Pinto G, De Natale A, Pollio A. In vitro colonisation experiments for the assessment of mycelial growth on a tuff substratum by a *Fusarium solani* strain isolated from Oplontis (Naples, Italy) archaeological site. *International Journal of Conservation Science*. 2017;8(4): 651–662.

**25.** Heydorn A, Nielsen AT, Hentzer M, Sternberg C, Givskov M, Ersbøll BK, et al. Quantification of biofilm structures by the novel computer program COMSTAT. *Microbiology*. 2000; 146: 2395–2407. <https://doi.org/10.1099/00221287-146-10-2395> PMID: 11021916

**26.** Hartig SM. Basic Image analysis and manipulation in ImageJ. *Current protocols in Molecular Biology*. 2013; 14(14.5).

**27.** Zhang F, Kwan A, Xu A, Su el GM. A synthetic quorum sensing system reveals a potential private benefit for public good production in abiofilm. *PLoS One*. 2015; 10(7): e0132948. <https://doi.org/10.1371/journal.pone.0132948> PMID: 26196509

**28.** McCloy RA, Rogers S, Caldon CE, Lorca T, Castro A, Burgess A. Partial inhibition of Cdk1 in G2 phase overrides the SAC and decouples mitotic events. *Cell Cycle*. 2014; 13: 1400–1412. <https://doi.org/10.4161/cc.28401> PMID: 24626186

29. R Core Team. R: A language and environment for statistical computing. R Foundation for Statistical Computing. Vienna, Austria. 2018. (URL <https://www.R-project.org/>)
30. Wickham H. Tidyverse: Easily Install and Load the 'Tidyverse'. R package version 1.2.1. 2017. ([https:// CRAN.R-project.org/package=tidyverse](https://CRAN.R-project.org/package=tidyverse))
31. Pedersen TL. Tidygraph: a tidy API for graph manipulation. R package version 1.1.1. 2018. ([https:// CRAN.R-project.org/package=tidygraph](https://CRAN.R-project.org/package=tidygraph))
32. Pedersen TL, Ggraph: an implementation of grammar of graphics for graphs and networks. R package version 1.0.2. 2018. (<https://CRAN.R-project.org/package=ggraph>)
33. Fruchterman TMJ, Reingold EM. Graph drawing by force directed placement. *Software: Practice and experience*. 1991; 21.11: 1129–1164.
34. Cutler NA, Chaput DL, Oliver AE, Viles HA. The spatial organization and microbial community structure of an epilithic biofilm. *FEMS microbiology ecology*. 2015; 91(3).
35. Gadd GM. Geomycology. *Encyclopedia of Earth Sciences Series*. 2011; 416–432. [https://doi.org/10.1007/978-1-4020-9212-1\\_102](https://doi.org/10.1007/978-1-4020-9212-1_102)
36. Vaughan DJ, Patrick RAD, Wogelius RA. Minerals, metals and molecules: ore and environmental mineralogy in the new millenium. *Mineralogical Magazine*. 2002; 66: 653–676.
37. Izzo F, Arizzi A, Cappelletti P, Cultrone G, De Bonis A, Germinario C, et al. The art of building in the Roman period (89 B.C.– 79 A.D.): Mortars, plasters and mosaic floors from ancient Stabiae (Naples, Italy). *Construction and Building Materials*. 2016; 117: 129–143.
38. Van de Liefvoort S. *Marmora Splendida. Marble and marble imitation in domestic decoration—Some case studies from Pompeii and Herculaneum*. BABESCH. 2012; 87: 187–204.
39. Amadori ML, Barcellin S, Poldi G, Ferrucci F, Andreotti A, Baraldi P, et al. Invasive and non-invasive analyses for knowledge and conservation of roman wall paintings of the villa of the Papyri in Herculaneum. *Microchemical Journal*. 2015; 118: 183–92.
40. Scheerer S, Ortega-Morales O, Gaylarde C. Microbial deterioration of stone monuments—an updated overview. *Advances in Applied Microbiology*.

2009; 66: 97–139. [https://doi.org/10.1016/S0065-2164\(08\)00805-8](https://doi.org/10.1016/S0065-2164(08)00805-8) PMID: 19203650

41. Gorbushina AA. Life on the rocks. *Environmental Microbiology*. 2007; 9: 1613–1631. <https://doi.org/10.1111/j.1462-2920.2007.01301.x> PMID: 17564597

42. Albertano P. Cyanobacterial biofilms in monuments and caves. In: Whitton BA. (ed.), *Ecology of Cyano- bacteria II: Their diversity in space and time*. Springer Science+Business Media B.V. 2012; pp. 317– 338.

43. Cennamo P, Montuori N, Trojsi G, Fatigati G, Moretti A. Biofilms in churches built in grottoes. *Science of the Total Environment*. 2016; 543: 727–738. <https://doi.org/10.1016/j.scitotenv.2015.11.048> PMID: 26618300

44. Rawat S, Rautela R, Johri BN. Fungal world of cave ecosystem. In: Satyanarayana T, Deshmukh S, Johri B. (eds.) *Developments in fungal biology and applied mycology*. Springer, Singapore. 2017.

45. Tomczyk-Żak K, Zielenkiewicz U. Microbial diversity in caves. *Geomicrobiology Journal*. 2016; 33(1): 20–38.

46. Groth I, Saiz-Jimenez C. Actinomycetes in hypogean environments. *Geomicrobiology Journal*. 1999; 16: 1–8.

47. Laiz L, Pinar G, Lubitz W, Saiz-Jimenez C. Monitoring the colonisation of monuments by bacteria: Cultivation versus molecular methods. *Environmental Microbiology*. 2003; 5(1): 72–4. <https://doi.org/10.1046/j.1462-2920.2003.00381.x> PMID: 12542715

- 48.** Yasir M. Analysis of bacterial communities and characterization of antimicrobial strains from cave microbiota. *Brazilian Journal of Microbiology*. 2018; 49(2): 248–257 <https://doi.org/10.1016/j.bjm.2017.08.005> PMID: 29108974
- 49.** Sa´ez-Nieto JA, Medina-Pascual MJ, Carrasco G, Garrido N, Fernandez-Torres MA, Villalo´n P, et al. *Paenibacillus* spp. isolated from human and environmental samples in Spain. Detection of eleven new species. *New Microbes and New Infections*. 2017; 19: 19–27. <https://doi.org/10.1016/j.nmni.2017.05.006> PMID: 28702198
- 50.** Maciejewska M, Adam D, Nao´me´ A, Martinet L, Tenconi E, Całusińska M, et al. Assessment of the potential role of *Streptomyces* in cave moonmilk formation. *Frontiers in Microbiology*. 2017; 8: 1181. <https://doi.org/10.3389/fmicb.2017.01181> PMID: 28706508
- 51.** Saarela M, Alakomi H-L, Suihko M-L, Maunuksela L, Raaska L, Mattila-Sandholm T. Heterotrophic microorganisms in air and biofilm samples from Roman catacombs with a special emphasis on actinobacteria and fungi. *Int. Biodeterior. Biodegrad.* 2004; 1: 27–37.
- 52.** Vanderwolf KJ, Malloch D, McAlpine DF, Forbes GJ. A world review of fungi, yeasts, and slime molds in caves. *International Journal of Speleology*. 2013; 42(1): 77–96.
- 53.** Pusz W, Ogo´rek R, Knapik R, Kozak B, Bujak H. The occurrence of fungi in the recently discovered Jarkowicka cave in the Karkonosze Mts.(Poland). *Geomicrobiology Journal*. 2015; 32(1): 59–67.
- 54.** White JF Jr. Structure and mating system of the gramicolourous fungal epibiont *Echinodopsis tuberiformis* (Clavicipitales). *American Journal of Botany*. 1993; 80(12): 1465–1471.
- 55.** Cennamo P, Marzano C, Ciniglia C, Pinto G, Cappelletti P, Caputo P, et al. A survey of the algal flora of anthropogenic caves of Campi Flegrei(Naples, Italy) archeological district. *Journal of Caves and Krast Studies*. 2012; 74: 243–250.

## **CHAPTER 4**

### **COMMUNITY COMPOSITION AND EX SITU CULTIVATION OF FUNGI ASSOCIATED WITH UNESCO HERITAGE MONUMENTS IN THE BAY OF NAPLES**

Article

## Community Composition and Ex Situ Cultivation of Fungi Associated with UNESCO Heritage Monuments in the Bay of Naples

Mariagiulia Petrarètti <sup>1,\*</sup>, Karl J. Duffy <sup>1</sup>, Angelo Del Mondo <sup>1,2</sup>, Antonino Pollio <sup>1</sup> and Antonino De Natale <sup>1</sup>

**Abstract:** The Bay of Naples, Italy, is renowned for its archaeological heritage. However, this heritage is threatened by the combination of weathering and the biological activity of microorganisms. Fungi are among the major agents of microbial deterioration of cultural heritage since they can cause cracks and lesions in monuments due to the penetrating force of their hyphae. Such biodeterioration may weaken the stone structures and threaten the longevity of these culturally important monuments. To address this, we collected, identified, and maintained in culture filamentous fungi that colonize the external surface of monuments at five important archaeological sites near Naples, namely Cuma, Ercolano, Nola, Oplonti, and Pompei. We isolated a total of 27 fungal taxa, all of which can be cultivated in the laboratory, and form a part of our reference collection. Many of the described fungal taxa we found belong to groups that are involved in stone biodeterioration and can thus be considered as model organisms for *in vitro* studies. These results emphasize the importance of identifying and cultivating fungal stock cultures for non-invasive studies on biodeterioration. Our newly developed reference collection represents a useful resource that is available to other researchers to rapidly identify potentially hazardous fungi on other monuments.

**Keywords:** fungi; *ex situ* collection; biodeterioration; biodegradation; cultural heritage

## Introduction

Fungi play an important role in the deterioration of buildings. Deterioration caused by fungal colonisation involves both physical and chemical damage of stone surfaces, and in most cases, they take place simultaneously [1]. Physical damage is related to the ability of fungal hyphae to penetrate into the substratum, where pores and fissures provide a useful microhabitat for fungal growth. The pressure exerted by fungal growth leads to further damage due to cell turgor pressure and exopolysaccharide formation that, in addition to fungal adhesion on stone surfaces, increases mechanical pressure [2]. Moreover, chemical damage occurs due to byproducts of fungal metabolism that leads to corrosion and discoloration of stone surfaces. Fungi are able to excrete a large variety of organic acids that act as metal-chelators [3] and mediate the precipitation of secondary minerals produced through the reaction of anions from excreted acids with cations from the stone. The formation of secondary minerals, such as carbonates, oxalates, and phosphates, can cause blistering, scaling, granular disintegration, and flaking or “spalling” of outer layers, leading to stone decay [4]. There is a close relationship between material and colonizing organisms [5]; indeed, the degree of fungal colonisation of a stone surface also depends on the structure, wetness, and chemical and mineralogical compositions of the substrata as well as environmental conditions [6,7]. Different lithotypes, e.g., brick, limestone, marble, tuff, and porphyry, provide a diverse range of substrates that fungi may use to acquire nutrients and grow.

Despite the large number of studies in the literature in which damage to cultural heritage is directly associated with fungi colonisation, the occurrence of fungi on cultural heritage monuments does not necessarily mean that these fungi cause the loss of chemical and physical properties of the substrate; indeed, filamentous fungi as well as lichens could protect colonized materials, especially against environmental parameters [8], or they could bear no influence on the material properties. The multifaceted role of fungi in biodeterioration can be effectively assessed on the basis of preliminary *in vitro* tests, particularly recommended in the issues of monument protection, that require *ex situ* conservation strategies for fungal strains isolated from monuments. *Ex situ* collections may significantly improve our knowledge of the role of fungi in stone cultural heritage biodeterioration, providing the basis for an appropriate and effective maintenance

and restoration strategy. The importance of maintaining a broad range of taxa in collections for *ex situ* conservation accessible to researchers prompted us to perform a survey campaign along the archaeological remains of Campania, Italy. Campania hosts a large number of works of art and monuments made of different stone materials, spanning the last three thousand years. Despite this unique cultural heritage, a deep sampling aimed to assess the biodiversity of cultivable fungi in these historical areas has never been conducted. Using a combination of microscopical, genetic, and culture techniques, here we describe the taxonomic diversity of fungi that occur in the UNESCO heritage sites of Cuma, Ercolano, Nola, Oplonti, and Pompei, with the overall aim of developing an *ex situ* collection of fungal strains from these archeological sites.

## **2 Materials and Methods**

### *2.1 Sampling*

The sampling campaign in this study was carried out in March 2018 at some of the most important cultural heritage sites in Campania, namely the Sibyl Caves in Cuma, the Suburban Baths in Ercolano, the Roman Amphitheater in Nola, the House of Poppea in Oplonti, and the House of Fauno and the House of Castricio in Pompei (Figure 1). At every site, we measured ecological parameters, e.g., temperature and relative humidity, using a thermohygrometer (model HI 9564, Hanna® Instruments, Smithfield, RI, USA) and light intensity using a Climalux N light meter (Laboratori di Strumentazione Industriale S.p.a., Milan, Italy). We measured pH on substrates at sampling points using a pH test paper strip. All the environmental parameters are shown in Table 1. The sampling points were chosen on the basis of the visibility of the fungal presence on the surface. Biofilm samples were taken by gently scraping the walls of the sampling sites with a sterile scalpel and adhesive tape strips were also used as a non-destructive sampling method [9]. The materials were deposited into sterile vials, until arrival at the laboratory.



**Figure 1.** Location of the sampling site of UNESCO heritage monuments in the bay of Naples, Campania, Italy.

Location	Light ( $\mu\text{mol m}^{-2} \text{s}^{-1}$ )	pH	Relative Humidity	Temperature ( $^{\circ}\text{C}$ )
Cuma, Sibyl Caves	$0.8 \pm 0.01$	7/8	$50 \pm 1.2\%$	$19.2 \pm 0.3$
Ercolano, Suburban Baths	$30 \pm 0.6$	7/8	$94 \pm 1.7\%$	$15.3 \pm 0.9$
Nola Roman Amphitheater	130.84	7/8	$90 \pm 1.2\%$	$16.7 \pm 1.2$
House of Poppea, Oplonti	129.95	7/8	$95 \pm 0.9\%$	$13.2 \pm 0.9$
House of Fauno, Pompei	$46 \pm 0.6$	7/8	$58.8 \pm 0.9\%$	$18.2 \pm 0.9$
House of Castricio, Pompei	8.97	7/8	$90 \pm 1.2\%$	$18.3 \pm 0.9$

**Table 1.** Values of environmental parameters (light, pH, relative humidity, and temperature) at each sampling site.

## *2.2 Confocal Laser Scanning Microscope Analysis*

The recorded adhesive tape samples were cut into small sections (Approximately 1 x 1 cm, [9]), placed on a glass slide, and observed on a Confocal Laser Scanning Microscope (CLSM), Zeiss LSM 700 (Carl Zeiss AG, Munich, Germany, using the software Zen 2011), by capturing images with a 63x water immersion objective. Images were acquired in three channels simultaneously: the red channel was used to discriminate phototrophs containing autofluorescence pigments (chlorophyll a and phycobilins), with excitation beams at 488 and 639 nm and emissions at 590–800 nm; the green channel was used to detect extrapolymeric matrix (EPS) using concanavalin-A with Alexa 488, with the excitation beams at 488 nm and emissions at 553–636 nm; and calcofluor-white was used to evidence the bacteria and hyphae with the excitation beams at 405 and 488 nm and emissions at 415–506 nm (blue channel) [10].

## *2.3 Isolation of Fungal Strains*

After the sampling campaign, samples were inoculated on agar medium, such as Potato Dextrose Agar (PDA) prepared according to Samson et al. [11], Bold's Basal Medium (BBM) [12] added to sucrose (12 g/L) according to Jeger et al. [13], and Malt-Yeast Extract- Sucrose Agar (MEA, Difco™) prepared according to Skaar and Stenwig [14]. Incubation was carried out at 22±2 °C for 30 days. At the end of the incubation period, enumeration of microorganisms as cfu/g of sample was carried out and the several mycelia obtained were isolated with the aid of a stereomicroscope. Afterwards, fungi were separately cultivated on PDA and finally observed with a stereomicroscope.

## *2.4 Identification of Fungal Isolates*

Fungal strains were identified through a polyphasic approach that is an integrated approach of identification based on morphological and molecular features of microorganisms [15]. According to Barnett and Hunter [16] and Fassatiová and Ellis [17], the morphological identification of fungi was based on the macroscopic features of colonies growing on agar plates and the micromorphology of the reproductive structure. The morphological

analysis was then confirmed by molecular analysis. For each fungal isolate, the following procedure was applied: DNA was extracted with a modified DNA extraction protocol [18] and used for a Polymerase Chain Reaction with primers targeting the internal transcribed spacer region (ITS) (primer forward, 5'-TCCGTAGGTGAACCTGCGG-3'; primer reverse, 5'-TTCAAAGATTCGATGATTCAC-3'). The ITS is the region spanning ITS1, 5.8S rRNA, and ITS2 was recently selected to be the universal barcode marker for fungi [19]. This DNA region has enough gaps between the intraspecific and interspecific variation across the kingdom Fungi and has been shown to have a high amplification success rate in various fungal taxa, e.g., it can discriminate the majority of species in Mucorales [20]. The barcode region together with a well-curated database of DNA sequences may constitute a reliable and fast tool for culture collection in the task of providing certification of fungal cultures. The amplification reaction was carried out in a reaction volume of 25  $\mu$ L containing 2.5  $\mu$ L of 10 reaction buffer, 1.5  $\mu$ L of MgCl<sub>2</sub>, 2  $\mu$ L of dNTP, 1.5  $\mu$ L of each of the primers, and 0.2  $\mu$ L of Taq polymerase (EconoTaq, Lucigen, Middleton, WI, USA). An amount of DNA, approximately 100 ng, was added to each reaction mixture in a PCR tube. The profile used was the same described by Del Mondo 2017 [21]. Amplification was run in an Applied Biosystem 2720 thermal cycler. The amplification product was then evaluated on 1.2% (*w/v*) agarose gel in an electrophoretic purified with a QIAquick® PCR Purification kit (Qiagen Inc, Valencia, CA, USA). The sequence reaction was obtained with the BigDye Terminator Cycle Sequencing technology (Applied Biosystems, Foster City, CA, USA), purified automatically using the Agencourt CleanSEQ Dye terminator removal Kit (Agencourt Bioscience Corporation, 500 Cummins Center, Suite 2450, Beverly, MA, USA) and a robotic station Biomek FX (Beckman Coulter, Fullerton, CA, USA). The product was analyzed on an Automated Capillary Electrophoresis Sequencer 3730 DNA Analyzer (Applied Biosystems). The amplification primers were used as the sequencing primers. The obtained sequence was searched for in BLAST version 2.0 (National Center for Biotechnology Information databases) and

identified. The ITS sequences obtained in this study have been deposited in GenBank (the accession numbers are listed in Table 2).

**Table 2.** Identification of the fungal species complex level based on ITS sequences with the description of their sampling site and lithic substrate. ACUF Collection Codes and Gene Bank Accession numbers are given for each strain.

<b>Identified Species Complex Level</b>	<b>Sites</b>	<b>Source</b>	<b>ACUF Collection Code</b>	<b>Gene Bank Accession Number</b>
<i>Alternaria</i> section <i>Alternata</i>	Pompei	Mortar	033f	MW881067
	Pompei	Mortar	032f	MW881066
<i>Alternaria</i> section <i>Alternata</i>	Nola	Marble	053f	MW881087
<i>Alternaria</i> section <i>Alternata</i>	Ercolano	Plaster	017f	MW881054
<i>Alternaria</i> sp.	Ercolano	Mortar	020f	MW881053
<i>Aspergillus</i> section <i>Aeni</i>	Pompei	Mortar	039f	MW881073
<i>Aspergillus</i> section <i>Usti</i>	Ercolano	Mortar	029f	MW881060
<i>Aspergillus</i> section <i>Usti</i>	Cuma	Tuff	012f	MW881047
	Cuma	Tuff	022f	MW881049
<i>Aspergillus</i> section <i>Nigri</i>	Ercolano	Plaster	007f	MW881065
	Ercolano	Plaster	019f	MW881062

Table 2. Cont.

Identified Species Complex Level	Sites	Source	ACUF Collection Code	Gene Bank Accession Number
<i>Aspergillus</i> section <i>Circumdati</i>	Pompei	Frescos	015f	MW881099
	Pompei	Frescos	026f	MW881100
<i>Aspergillus</i> sp.	Cuma	Tuff	008f	MW881051
<i>Cladosporium</i> sp.	Pompei	Mortar	041f	MW881075
<i>Clonostachys</i> sp.	Oplonti	Mortar	005f	MW881093
	Oplonti	Mortar	056f	MW881095
	Oplonti	Mortar	010f	MW881098
	Oplonti	Mortar	021f	MW881097
<i>Clonostachys</i> sp.	Nola	Marble	042f	MW881076
	Nola	Marble	043f	MW881077
	Nola	Marble	044f	MW881078
<i>Curvularia geniculata</i> species complex	Ercolano	Plaster	023f	MW881052
<i>Fusarium oxysporum</i> species complex	Ercolano	Plaster	031f	MW881064
<i>Fusarium</i> section <i>Discolor</i>	Cuma	Tuff	009f	MW881048
<i>Fusarium oxysporum</i> species complex	Pompei	Frescos	014f	MW881102
<i>Fusarium oxysporum</i> species complex	Ercolano	Plaster	018f	MW881055
	Ercolano	Plaster	024f	MW881056
	Ercolano	Plaster	025f	MW881057
	Ercolano	Plaster	028f	MW881059
<i>Fusarium oxysporum</i> species complex	Oplonti	Mortar	054f	MW881090
	Oplonti	Mortar	055f	MW881091
	Oplonti	Mortar	001f	MW881089
<i>Fusarium solani</i> species complex	Ercolano	Plaster	016f	MW881063
<i>Fusarium</i> sp.	Oplonti	Mortar	006f	MW881088
<i>Fusarium tricinctum</i> species complex	Oplonti	Mortar	002f	MW881094
<i>Lecanicillium</i> sp.	Pompei	Frescos	013f	MW881101
<i>Lecanicillium</i> sp.	Ercolano	Mortar	027f	MW881058
<i>Lecanicillium</i> sp.	Ercolano	Plaster	030f	MW881061
<i>Neofusicoccum parvum</i> species complex	Cuma	Tuff	011f	MW881050
<i>Penicillium</i> section <i>Fasciculata</i>	Pompei	Mortar	036f	MW881070
	Pompei	Mortar	038f	MW881072
	Pompei	Mortar	035f	MW881069

Table 2. Cont.

Identified Species Complex Level	Sites	Source	ACUF Collection Code	Gene Bank Accession Number
	Pompei	Mortar	040f	MW881074
<i>Penicillium</i> sp.	Pompei	Mortar	034f	MW881068
	Pompei	Mortar	037f	MW881071
<i>Penicillium</i> section <i>Aspergilloides</i>	Nola	Marble	046f	MW881080
	Nola	Marble	047f	MW881081
	Nola	Marble	048f	MW881082
	Nola	Marble	049f	MW881083
	Nola	Marble	051f	MW881085
<i>Purpureocillium</i> sp.	Oplonti	Frescos	004f	MW881096
<i>Talaromyces</i> section <i>Talaromyces</i>	Oplonti	Mortar	003f	MW881092
<i>Talaromyces</i> section <i>Talaromyces</i>	Nola	Marble	045f	MW881079
<i>Trichoderma</i> sp.	Nola	Marble	050f	MW881084
	Nola	Marble	052f	MW881086

### 2.5 Fungal Preservation for Ex Situ Conservation

In according to the World Federation for Culture Collection Guidelines, more than one method was applied for each fungal strain for successful preservation. Our fungal strains are stored by different methods: (a) PDA on Petri dishes at a temperature range of between 22 °C and 25 °C in darkness; (b) in a corked glass tube with sterilized water at room temperature [22]; and (c) at 80 °C in glycerol (selected strains only). This method, namely cryopreservation together with freeze drying, is considered to be a long-term preservation method [23]. To maintain fungi in a viable state, to evaluate purity, and to avoid devitalization, monthly checking and refreshment of cultures were performed. All the fungal strains are maintained in the Algal Culture Collection (ACUF) at the Department of Biology, University of Naples Federico II, Italy. This collection, traditionally devoted to the maintenance of aeroterrestrial microalgae and cyanobacteria [24], has been enriched with a special section devoted to the maintenance of fungal strains isolated directly from archeological sites in Campania. Each strain is included in a private database with all the information regarding sampling sites, origin substrate, data on collection, ecological notes, cultivation and maintenance methods, phenotypic characteristics, and genomic analysis. In order to maintain the safety of the data associated with each of the

strains preserved in the collection, all computer files are duplicated and kept in a separate area. Furthermore, we deposited our isolates at the Mycotheca Universitatis Taurinensis, Turin, Italy (MUT), a renowned collection specialized in fungal preservation.

### 3 Results

#### *3.1 Description of Damage and Substrate Change*

Biological growth on stone can result in changes in surface color and structure depending on the identity of the organism and their growth and behavior. At our sampling sites, the biological colonisation on stone surfaces assumed the forms of epilithic formations with a patina aspect. In particular, these organisms formed a subaerial biofilm, which is a type of biofilm that occurs at the atmosphere–rock interface. This type of biofilm has been frequently reported in the literature on hypogean monuments, such as catacombs [25], and on walls, statues, and wetlands. These formations may have a colored patinas aspect, depending on the type of biocenosis and of the growth phase of the prevailing species. As shown in Figure 2b,d,e, the stone surface appears with a green and greenish stain, probably due to the presence of organic pigments (e.g., chlorophylls, carotenoids, melanins) [26]. In Figure 2h,k,n, the stone surface appears with a black stain and this is related to the mixed association of different fungal groups.

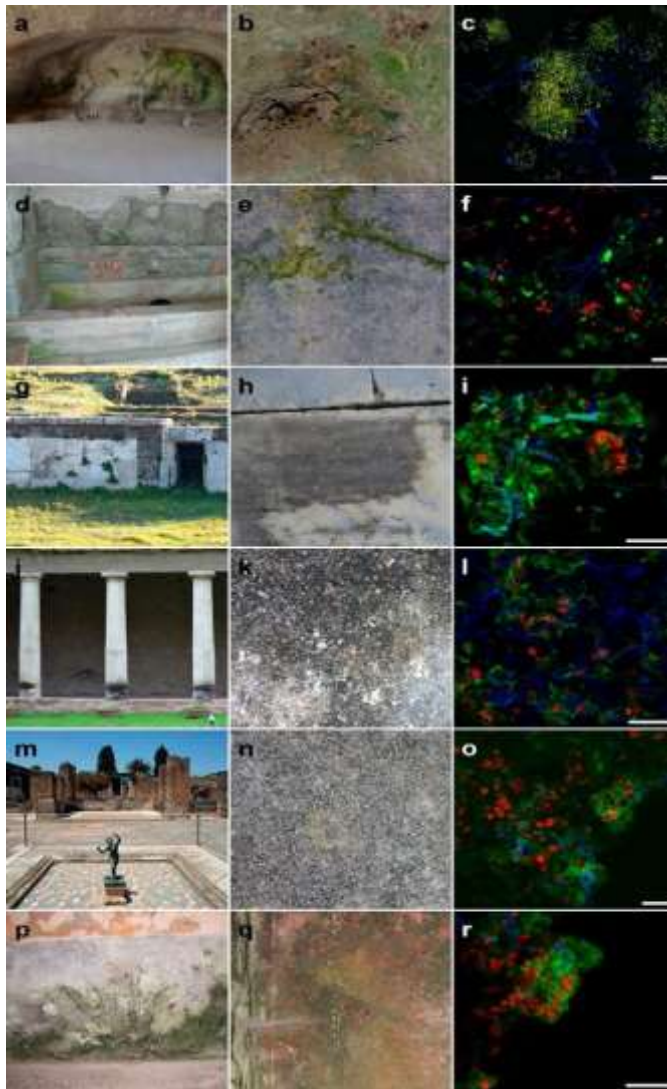


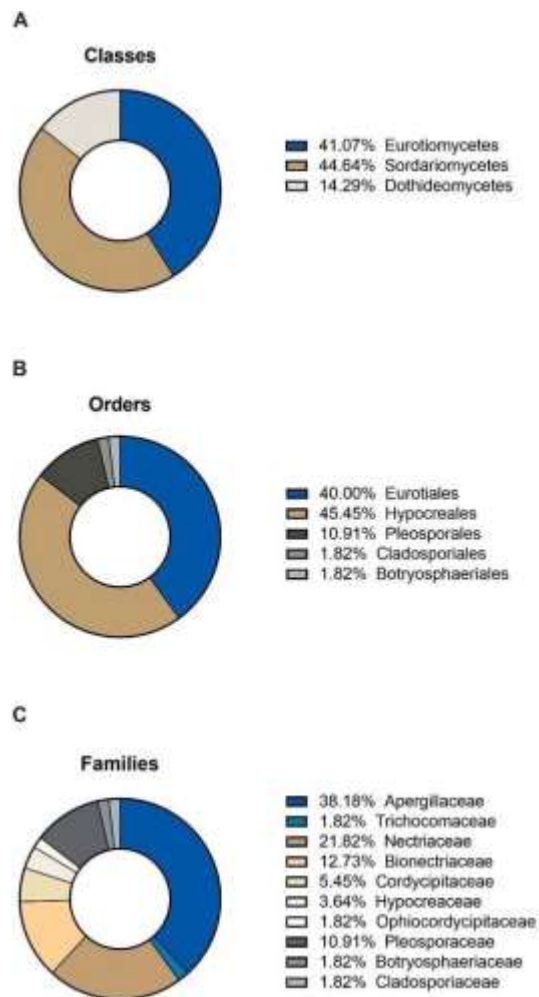
**Figure 2.** Archeological sites: Sibyl Caves in Cuma (**a**), Suburban Baths in Ercolano (**d**), the Roman Amphitheater in Nola (**g**), the House of Poppea in Oplonti (**j**), and the House of Fauno (**m**) and the House of Castricio (**p**) in Pompei; the visible alteration at the same sites (**b,e,h,k,n,q**); the recorded adhesive tape samples observed on the CLSM (**c,f,i,l,o,r**; scale bar, 50  $\mu\text{m}$ ).

### 3.2. Confocal Laser Microscopy

All the samples analyzed by CLSM revealed that many cells contained chlorophyll and phycobilin (red auto-fluorescence), which were ascribed to algae and cyanobacteria and polysaccharide polymers (e.g., cellulose and chitin) in their cell walls (blue color), which were ascribed to fungi (Figure 2c,f,i,l,o,r).

### 3.3. Molecular Identifications

Table 2 shows the identification of the isolated fungal species retrieved from the sampled UNESCO monuments, together with sites and source sampled as well as the collection code linked to the fungal strains and the GenBank accession numbers of the obtained sequences. A total of 18 fungal taxa, belonging to 3 different Classes, 5 different Orders, and 10



different Families, were obtained (Figure 3) and kept in culture.

**Figure 3.** The relative abundance of fungal isolated according to (A) classes, (B) orders, and (C) families.

Overall, the most common genera were *Aspergillus* in Cuma (60%), *Fusarium* in Ercolano (42.86%), *Penicillium* in Nola (41.67%), *Fusarium* in Oplonti (45.45%), *Penicillium* (60%) in Pompei, Fauno, and *Aspergillus* (50%) in Pompei, Castricio (Figure 4).

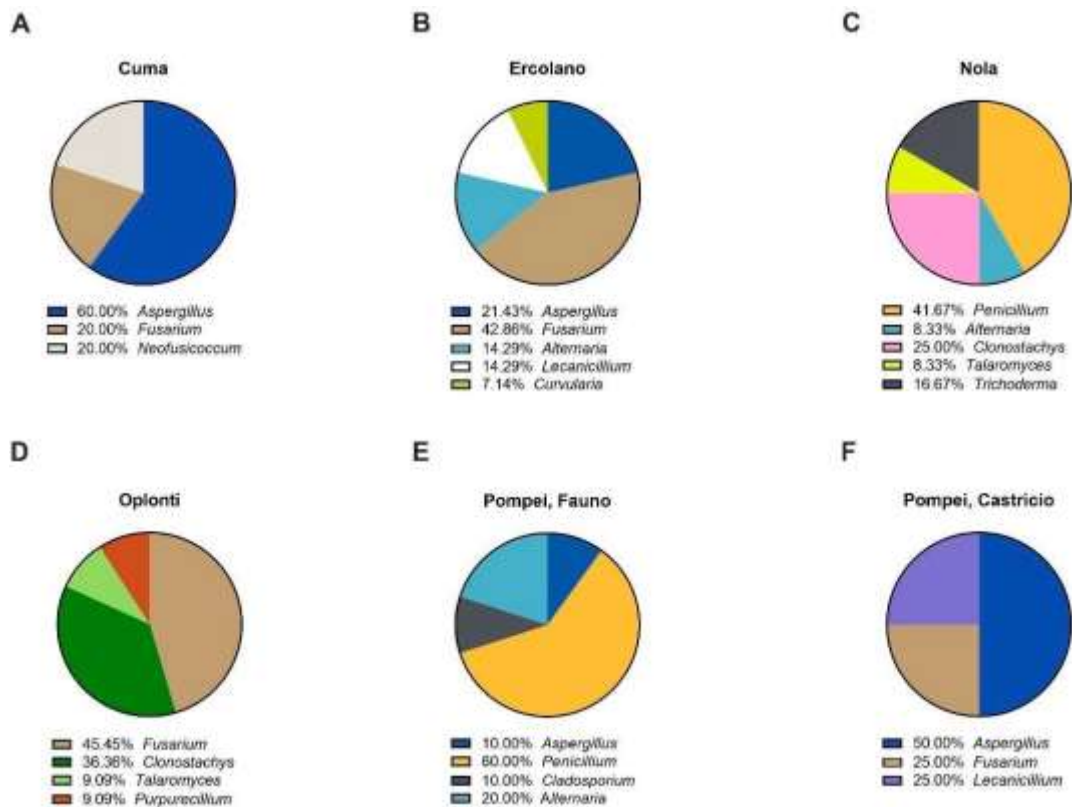


**Figure 4.** The relative prevalence of fungal genera found in: Sibyl Caves in Cuma (A), Suburban Baths in Ercolano (B), the Roman Amphitheater in Nola (C), the House of Poppea in Oplonti (D), and the House of Fauno (E) and the House of Castricio (F) in Pompei.

#### 4. Discussion

The protection of cultural heritage often involves the study of the bio-receptivity of building materials and the biodegradation potential of microorganisms involved in deterioration, which can be primarily assessed through laboratory studies. In this work, a non-destructive method was used to sample microorganisms at UNESCO cultural heritage sites in Campania, Italy. In particular, we sampled using adhesive tape sampling coupled with microscopical analysis to identify the constituent microorganisms in biofilms of these monuments, which allows us to examine the existing relationships between the surface and the colonizing microorganisms [9]. The observations made using confocal light microscopy demonstrated fungal colonisation in all the adhesive tape samples analyzed as a network of filamentous structures. Furthermore, we observed the presence of cyanobacteria and algae closely connected with filamentous structures, demonstrating that fungi actively colonize the rock as essential compounds of the biofilm sampled and not as contaminants. The isolation of fungi through culture-dependent methods, followed by maintenance of strains in culture, was aimed at obtaining quality controlled isolates for further studies on biodeterioration processes and to develop innovative strategies for their control. For each strain, we collected data related to the substrate and environmental conditions at the sampling location and this information can be used to develop future laboratory experiments simulating specific environmental conditions under which these fungi can grow. Indeed, future perspectives are directed towards using our fungi as models to perform *in vitro* experiments for understanding the patterns of microbial colonisation of stone materials [21]. The fungal isolates in this study are widespread, frequently associated with soil particles and plant material, which is probably due to their broad tolerance to different environmental conditions and allows them to colonize a large array of terrestrial habitats [27]. Molecular identification of sampled strains was performed using the internal transcribed spacer (ITS) rDNA area, which is the most widely used marker for fungi [19]. Unfortunately, for many Ascomycota genera, such as *Penicillium* and *Aspergillus*, the ITS is not variable enough to allow for species-level identification [28]. Because of the limitations associated with the chosen

molecular marker, herein we considered the species-complex level for an overview of fungal diversity on stone monuments. We recognize the necessity of further identification using taxon-specific markers (e.g., SSRs) for identifying isolates to species level as the collection grows. The genera isolated in our sampling include *Alternaria*, *Aspergillus*, *Cladosporium*, *Clonostachys*, *Curvularia*, *Fusarium*, *Lecanicillium*, *Neofusicoccum*, *Penicillium*, *Purpureocillium*, *Talaromyces*, and *Trichoderma*, which are known to be ubiquitous filamentous fungi of soil and are often airborne. Some of them were already described as colonizer, or occasionally pioneer, taxa of deteriorated monuments [29]. For most of these species, there is no representative strain of the wide range of morphology and physiology expressed within that species and therefore it is necessary to maintain a number of representative strains. Some collections, such as the CABI Bioscience Genetic Resource Collection, retain on average five strains for each species, but in some cases this number is not sufficient. This is the case for host specificity in the plant pathogen, such as *Fusarium oxysporum*, which has a large number of genetic variants [30]. Thus, *ex situ* conservation of microorganisms collected from monuments can ensure that all strains with their unique properties are preserved and maintained over time. In accordance with other studies, we observed that the genera most frequently identified as colonizers of several stone substrates are *Aspergillus*, *Fusarium*, and *Penicillium* [31]. The action of these fungi, included in the orders Capnodiales and Pleosporales, could lead to aesthetic alteration and biopitting of stone materials [32]. Moreover, some of the fungal isolates belonging to *Alternaria* section *Alternata*, *Cladosporium sp.*, *Fusarium solani* species complex, and *Penicillium* section *Aspergilloides* are known to contribute to acidification and the dissolution of stone by excreting organic acids. In particular, oxalic acid secreted by fungi can dissolve limestone calcium carbonate, producing calcium oxalates, one of the most severe biodeterioration processes affecting limestone monuments [33]. In addition, recently it has been shown that the genus *Purpureocillium* may have halotolerant characteristics [34], which may further broaden the impact these fungi have on stone structures.

## **Conclusions**

The collection and molecular identification of fungal strains and their associated

ecological data, describing their site of sampling, type of substrate, and morphological diagnostic characteristics, represent a key resource for the development of biotechnological approaches devoted to the conservation of cultural heritage. The *ex situ* conservation of fungi sampled from bio-deteriorated environments can ensure that isolates are preserved to maintain their integrity and long-term survival. This is essential for future research on the preservation of historical monuments, including the ecological differentiation of fungal communities according to sampling sites and the production of desirable end products applicable for bioremediation.

## References

1. Salvadori, O.; Municchia, A.C. The Role of Fungi and Lichens in the Biodeterioration of Stone Monuments. *Open Conf. Proc. J.* **2016**, *7*, 39–54. [[CrossRef](#)]
2. Burford, E.P.; Fomina, M.; Gadd, G.M. Fungal involvement in bioweathering and biotransformation of rocks and minerals. *Miner. Mag.* **2003**, *67*, 1127–1155. [[CrossRef](#)]
3. Sterflinger, K. Fungi as Geologic Agents. *Geomicrobiol. J.* **2000**, *17*, 97–124. [[CrossRef](#)]
4. Wright, J.S. Geomorphology and stone conservation: Sandstone decay in Stokeon Trent. *Struct. Surv.* **2002**, *20*, 50–61. [[CrossRef](#)]
5. Turick, C.E.; Berry, C.J. Review of concrete biodeterioration in relation to nuclear waste. *J. Environ. Radioact.* **2016**, *151*, 12–21. [[CrossRef](#)] [[PubMed](#)]
6. Caneva, G.; Nugari, M.P.; Nugari, M.P.; Salvadori, O. *Plant Biology for Cultural Heritage: Biodeterioration and Conservation*; Getty Publications: Los Angeles, CA, USA, 2008.
7. Gaylarde, C.; Silva, M.R.; Warscheid, T. Microbial impact on building materials: An overview. *Mater. Struct.* **2003**, *36*, 342–352. [[CrossRef](#)]
8. Pinna, D. Biofilms and lichens on stone monuments: Do they damage or protect? *Front. Microbiol.* **2014**, *5*, 133. [[CrossRef](#)]
9. Urzì, C.; De Leo, F. Sampling with adhesive tape strips: An easy and rapid method to monitor microbial colonisation on monument surfaces. *J. Microbiol. Methods* **2001**, *44*, 1–11. [[CrossRef](#)]
10. Larson, C.; Passy, S.I. Spectral fingerprinting of algal communities: A novel approach to biofilm analysis and biomonitoring. *J. Phycol.* **2005**, *41*, 439–446. [[CrossRef](#)]
11. Samson, R.A.; Hoekstra, E.S.; Frisvad, J.C.; Filtenborg, O. *Introduction to Food-Borne Fungi*; Centraalbureau voor Schimmelcultures: Delft, The Netherlands, 1996.

12. Nichols, H.W.; Bold, H.C. *Trichosarcina polymorpha* Gen. et Sp. Nov. *J. Phycol.* **1965**, *1*, 34–38. [[CrossRef](#)]
13. Jeger, M.J.; Lamour, A.; Gilligan, C.A.; Otten, W. A fungal growth model fitted to carbon-limited dynamics of *Rhizoctonia solani*. *New Phytol.* **2008**, *178*, 625–633. [[CrossRef](#)] [[PubMed](#)]
14. Skaar, I.; Stenwig, H. Malt-yeast extract-sucrose agar, a suitable medium for enumeration and isolation of fungi from silage. *Appl. Environ. Microbiol.* **1996**, *62*, 3614–3619. [[CrossRef](#)]
15. Passarini, M.R.Z.; Santos, C.; Lima, N.; Berlinck, R.G.S.; Sette, L.D. Filamentous fungi from the Atlantic marine sponge *Dracmacidon reticulatum*. *Arch. Microbiol.* **2012**, *195*, 99–111. [[CrossRef](#)] [[PubMed](#)]
16. Barnett, H.L.; Hunter, B.B. *Illustrated Genera of Imperfect Fungi, Mycol*, 3rd ed.; Burgess Publishing Company: Minneapolis, MN, USA, 1972.
17. Bushell, M.E. (Ed.) *Fassatiòv O Moulds and filamentous fungi in technical microbiology*. In *Progress in Industrial Microbiology 22*; Elsevier: Amsterdam, The Netherlands, 1986.
18. Doyle, J. DNA Protocols for Plants. In *Molecular Techniques in Taxonomy*; Springer: Berlin/Heidelberg, Germany, 1991; pp. 283–293. [[CrossRef](#)]
19. Schoch, C.L.; Seifert, K.A.; Huhndorf, S.; Robert, V.; Spouge, J.L.; Levesque, C.A.; Chen, W.; Fungal Barcoding Consortium. Nuclear ribosomal internal transcribed spacer (ITS) region as a universal DNA barcode marker for Fungi. *Proc. Natl. Acad. Sci. USA* **2012**, *109*, 6241–6246. [[CrossRef](#)] [[PubMed](#)]
20. Walther, G.; Pawłowska, J.; Alastruey-Izquierdo, A.; Wrzosek, M.; Rodriguez-Tudela, J.; Dolatabadi, S.; Chakrabarti, A.; De Hoog, G. DNA barcoding in Mucorales: An inventory of biodiversity. *Pers. Mol. Phylogeny Evol. Fungi* **2013**, *30*, 11–47. [[CrossRef](#)]
21. Del Mondo, A.; Pinto, G.; De Natale, A.; Pollio, A. In vitro colonisation experiments for the assessment of mycelial growth on a tuff substratum by a *Fusarium solani* strain isolated from the Oplonti (Naples, Italy)

- archaeological site. *Int. J. Cons. Sci.* **2017**, *8*, 651–662.
22. Smith, D.; Ryan, M.J.; Day, J.G. *The UKNCC Biological Resource: Properties, Maintenance and Management*; UKNCC Secretariat: Egham, UK, 2001; 382p.
  23. OECD. *Biological Resource Centres: Underpinning the Future of Life Sciences and Biotechnology*; OECD Publications: Paris, France, 2001;p. 66.
  24. D'Elia, L.; Del Mondo, A.; Santoro, M.; De Natale, A.; Pinto, G.; Pollio, A. Microorganisms from harsh and extreme environments: A collection of living strains at ACUF (Naples, Italy). *Ecol. Quest.* **2018**,*29*, 1–16. [[CrossRef](#)]
  25. Gorbushina, A.A. Life on the rocks. *Environ. Microbiol.* **2007**, *9*, 1613–1631. [[CrossRef](#)]
  26. Warscheid, T.; Braams, J. Biodeterioration of stone: A review. *Int. Biodeterior. Biodegrad.* **2000**, *46*, 343–368. [[CrossRef](#)]
  27. Isola, D.; Zucconi, L.; Onofri, S.; Caneva, G.; De Hoog, G.S.; Selbmann, L. Extremotolerant rock inhabiting black fungi from Italian monumental sites. *Fungal Divers.* **2016**, *76*, 75–96. [[CrossRef](#)]
  28. Seifert, K.A.; Samson, R.A.; Dewaard, J.R.; Houbraken, J.; Lévesque, C.A.; Moncalvo, J.-M.; Louis-Seize, G.; Hebert, P.D.N. Prospects for fungus identification using CO1 DNA barcodes, with *Penicillium* as a test case. *Proc. Natl. Acad. Sci. USA* **2007**, *104*, 3901–3906. [[CrossRef](#)][[PubMed](#)]
  29. Del Mondo, A.; De Natale, A.; Pinto, G.; Pollio, A. Correction to: Novel qPCR probe systems for the characterization of subaerial biofilms on stone monuments. *Ann. Microbiol.* **2019**, *69*, 1097–1106. [[CrossRef](#)]
  30. Kirk, P.M.; Cannon, P.F.; David, J.C.; Stalpers, J.A. *Dictionary of the Fungi*, 9th ed.; CABI Publishing: Wallingford, UK, 2001; p. 55.
  31. Saarela, M.; Alakomi, H.-L.; Suihko, M.-L.; Maunuksela, L.; Raaska, L.; Mattila-Sandholm, T. Heterotrophic microorganisms in air and biofilm samples from Roman catacombs, with special emphasis on

- actinobacteria and fungi. *Int. Biodeterior. Biodegrad.* **2004**, *54*, 27–37. [[CrossRef](#)]
32. Sterflinger, K. Fungi: Their role in deterioration of cultural heritage. *Fungal Biol. Rev.* **2010**, *24*, 47–55. [[CrossRef](#)]
33. Gadd, G.M. Geomycology: Biogeochemical transformations of rocks, minerals, metals and radionuclides by fungi, bioweathering and bioremediation. *Mycol. Res.* **2007**, *111*, 3–49. [[CrossRef](#)] [[PubMed](#)]
34. Arpini, C.M.; Nóbrega, Y.C.; Casthologe, V.D.; Neves, D.S.; Tadokoro, C.E.; Da Costa, G.L.; Oliveira, M.M.E.; Santos, M.R.D.D. *Purpuricillium lilacinum* infection in captive loggerhead sea turtle hatchlings. *Med Mycol. Case Rep.* **2019**, *23*, 8–11. [[CrossRef](#)]

**CHAPTER 5**

**FUNGAL METABOLITES WITH ANTAGONISTIC ACTIVITY  
AGAINST FUNGI OF LITHIC SUBSTRATA**

Article

## Fungal Metabolites with Antagonistic Activity against Fungi of Lithic Substrata

Marco Masi <sup>1,\*</sup>, Mariagiorgia Petraretti <sup>2,†</sup>, Antonino De Natale <sup>2</sup>, Antonino Pollio <sup>2</sup> and Antonio Evidente <sup>1</sup>

**Abstract:** Fungi are among the biotic agents that can cause deterioration of building stones and cultural heritage. The most common methods used to control fungal spread and growth are based on chemical pesticides. However, the massive use of these synthetic chemicals produces heavy environmental pollution and risk to human and animal health. Furthermore, their use is time dependent and relies on the repetition of treatments, which increases the possibility of altering building stones and culture heritage through environmental contamination. One alternative is the use of natural products with high antifungal activity, which can result in reduced toxicity and deterioration of archeological remains. Recently, three fungal strains, namely *Aspergillus niger*, *Alternaria alternata* and *Fusarium oxysporum*, were isolated as damaging agents from the external tuff wall of the Roman remains “Villa of Poppea” in Oplontis, Naples, Italy. In this manuscript, three selected fungal metabolites, namely cyclopaldic acid, cavoxin and *epi*-epoformin, produced by fungi pathogenic for forest plants, were evaluated as potential antifungal compounds against the above fungi. Cavoxin and *epi*-epoformin showed antifungal activity against *Aspergillus niger* and *Fusarium oxysporum*, while cyclopaldic acid showed no activity when tested on the three fungi. The same antifungal activity was observed *in vitro* experiments on infected stones of the Neapolitan yellow tuff (NYT), a volcanic lithotype widely diffused in the archeological sites of Campania, Italy. This study represents a first step in the use of these two fungal metabolites to allow better preservation of artworks and to guarantee the conditions suitable for their conservation.

**Keywords:** fungal metabolites; antifungal activity; cultural heritage; fungi; stone biodeterioration; stone biodegradation

## 1. Introduction

Fungi are among the major agents of microbial deterioration of building stones and cultural heritage. Deterioration caused by fungal colonisation involves aesthetic, physical and chemical damage of stone surfaces, which, in most cases, take place simultaneously [1]. Besides aesthetic damage due to color change, black spots and patina formation, fungi can deeply colonize cracks and fissurations because of the extraordinary penetrating power of fungal hyphae into the substratum, causing breaking and lesions in artwork. Fungi are able to excrete a large variety of organic acids that are able to act as metal-chelators, mediating the precipitation of secondary minerals like carbonates, oxalates and phosphates, which can cause blistering, scaling and granular disintegration, leading to stone decay [2]. For these reasons, it is important to find solutions to the deterioration of stone surfaces that do not compromise the readability and structure of artworks. Synthetic pesticides, including fungicides, are massively used in agriculture, forests, parks, and archeological areas. The heavy pollution, essentially of soil and water, due to the worldwide use of these chemicals has prompted the search for eco-friendly alternatives based on bioactive natural substance formulations. This also satisfies the requests of people and authorities who ask for safe products to avoid the contamination of food and lower the risk to human and animal health [3–5]. Plants, microorganisms, lichens, and algae are producers of metabolites possessing diverse biological activities, such as phytotoxic, antiviral, anticancer, antitumor, algicide, enzyme-inhibiting, immunostimulant, antiplatelet aggregation, cytotoxic, antiplasmodium, antibacterial, and antifungal activities [6–9]. Several secondary metabolites with antimicrobial activity have already been isolated from different fungi [10–14]. These metabolites belong to diverse structural classes of naturally occurring compounds (e.g., alkaloids, anthraquinones, poliketides, terpenes, steroids), and most of them possess original modes of action to overcome antimicrobial resistance [15–19]. Recently, three fungal strains, namely *Aspergillus niger*, *Alternaria alternata* and *Fusarium oxysporum*, were isolated as damaging agents from the external tuff wall of the Roman remains, “Villa of Poppea” in Oplontis, Naples, Italy. This manuscript reports the assessment of *in vitro* systems to study the early steps of fungal colonisation of stone (Neapolitan

yellow tuff, a volcanic lithotype widely diffused in the archeological sites of Campania, Italy) and to test the antifungal properties of three fungal metabolites, namely cavoxin, *epi*-epoformin and cyclopaldic acid, for their potential fungicidal activity.

## 2. Material and methods

### 2.1 General Chemical Procedure

Electrospray ionization mass spectrometry (ESI MS) and liquid chromatography/mass spectrometry (LC/MS) analyses were performed using an LC/MS TOF system Agilent 6230B (Agilent Technologies, Milan, Italy), HPLC 1260 Infinity. A Phenomenex (Bologna, Italy) Luna (C18 (2) 5 mm, 150–4.6 mm column) was used to perform the high performance liquid chromatography (HPLC) separations. Bruker 400 Anova Advance (Karlsruhe, Germany) was used to record the <sup>1</sup>H NMR spectra at 400 MHz in CDCl<sub>3</sub> at 298 K. Analytical, preparative, and reverse phase thin layer chromatography (TLC) were carried out on silica gel (Merck, Kieselgel 60, F254, 0.25, 0.5 mm, and RP-18 F254s, respectively) plates (Merck, Darmstadt, Germany). The spots were visualized as previously described [20]. Column chromatography (CC) was performed using silica gel (Kieselgel 60, 0.063–0.200 mm) and C18-reversed phase silica gel (230–400 mesh) (Merck, Darmstadt, Germany). Sigma Aldrich Co. (St. Louis, MO, USA) supplied all the reagents and the solvents.

### 2.2 Fungal metabolites

Cavoxin was obtained as previously reported [21] from *Phoma cava* (CBS (Centraalbureau voor Schimmelcultures), The Netherlands, 535.66). The fungus was grown in flasks containing 300 mL of a semisynthetic liquid medium incubated at 25 °C and 200 rpm for 5 days. The cultures were filtered, and the filtrate was lyophilized. The solid residue corresponding to 9 L of culture filtrate was dissolved in distilled water and extracted with CHCl<sub>3</sub>. The organic extract was chromatographed on a Sephadex LH-20 column eluted with CHCl<sub>3</sub>- *i*PrOH (9:1,

v/v), obtaining cavoxin as a homogeneous oil, which was crystallized from EtOAc-petroleum ether (1:1, v/v) as pale-yellow needles (979 mg). Cyclopaldic acid was obtained from *Seirdium cupressi* as previously reported [22]. The strain of *S. cupressi* was isolated in Kos (Greece) and deposited in the collection of Dipartimento di Patologia Vegetale, University of Bari, Italy, as DPG10. It was grown as stationary culture in 1 L Roux flasks containing 150 mL Czapek's medium with the addition of 2% corn meal and incubated at 23 °C for 30 days in the dark. The culture filtrates were acidified to pH 4 and extracted with *t*-butylmethyl ether. The combined organic extracts afforded an oil, which was washed with CHCl<sub>3</sub>, leaving a white amorphous substance. The latter gave cyclopaldic acid (750 mg) by crystallization from MeOH-CHCl<sub>3</sub> (1:1,v/v). *epi*-epoformin was obtained from *Diplodia quercivora* as previously described [23]. A strain of *D. quercivora* was isolated from a symptomatic branch of *Quercus canariensis* in a natural area in Tunisia and deposited in the collection of the Dipartimento di Agraria, University of Sassari, Italy, as BL9. The fungus was grown in 2 L Erlenmeyer flasks containing 400 mL of Czapek medium amended with corn meal and incubated at 25 °C for 3 weeks in darkness. The culture filtrates (6.7 L) were acidified to pH 4 and extracted exhaustively with EtOAc. The organic extracts were purified on silica gel and successively on reverse-phase column chromatography, yielding *epi*-epoformin (276.1 mg) as a white solid. The purity of cavoxin, cyclopaldic acid, and *epi*-epoformin (>98%) was ascertained by HPLC, <sup>1</sup>H NMR and ESI MS spectra.

### 2.3 Antifungal Test-Well Diffusion Assay

A conidia suspension of the test fungi was obtained from a 6-day-old colony grown in solid-medium potato dextrose agar (PDA) treated with PBS-Tween20 solution 0.5%, by scraping from the agar surface with a sterile spatula. Conidia were suspended in physiological solution (0.9% NaCl) to a final concentration of 1x10<sup>6</sup> conidia/mL. 50 μL of the final conidia suspension was spread onto the PDA until the suspension was completely absorbed. Then, filter paper discs 13 mm in diameter, previously absorbed with 20 μL of each chemical compound at the

desired concentration, were placed on the agar surface. Finally, the Petri dishes were incubated at  $22 \pm 2$  °C in darkness for 3 days with control fixed every 24 h. The natural biocides selected for this study were cavoxin, cyclopaldic acid and *epi*-epoformin. All of these were tested in several concentrations, namely 0.25, 0.50 and 1.0 mg/L. Then, the eventual diameters of inhibition growth zones were measured. Pentachloronitrobenzene (PCNB) was used as positive control [24], while empty filter paper discs were used as negative control. Filter paper discs absorbed with 20 µL of methanol were used to verify the eventual interference with fungal growth.

#### 2.4 Lithotypes and Microorganisms

The selected fungal strains were *Aspergillus niger* (008f), *Alternaria alternata* (015f) and *Fusarium oxysporum* (014f), obtained from ACUF, Algal Collection of University of Naples Federico II, Italy. A new section of this collection, which has been traditionally devoted to the maintenance of aeroterrestrial microalgal and cyanobacteria strains [25], was recently created to keep fungal strains that have been isolated directly from archeological sites in Campania. In particular, these strains were collected from the external tuff walls of “Villa of Poppea” in Oplontis (Naples, Italy). The identification of fungal strains was assessed on the basis of morphological observations coupled with molecular analysis. DNA was extracted with a modified Doyle and Doyle DNA extraction protocol [26] and used for a polymerase chain reaction using ITS spacers as target primer (primer forward 5'-TCCGTAGGTGAACCTGCGG-3'; primer reverse 5'-TTCAAAGATTCGATGATTCAC-3'). The PCR products were evaluated on agarose gel in an electrophoretic run and purified using a QIAquick® PCR Purification kit (Qiagen Inc., Valencia, CA, USA). The sequence reaction was obtained with BigDye Terminator Cycle Sequencing technology (Applied Biosystems, Foster City, CA, USA), using the amplification primers as the sequencing primers, and purified using the Agencourt CleanSEQ Dye terminator removal kit (Agencourt Bioscience Corporation, 500 Cummins Center, Suite 2450, Beverly, MA, USA) and a robotic station Biomek FX (Beckman Coulter, Fullerton, CA, USA). The product was analyzed by an Automated Capillary Electrophoresis

Sequencer 3730 DNA Analyzer (Applied Biosystems). Nucleotide sequence similarity was determined using BLAST version 2.0 (<https://blast.ncbi.nlm.nih.gov> (accessed on 26 January 2021)). The obtained sequences were identified as *Aspergillus niger*, *Alternaria alternata* and *Fusarium oxysporum*. The stone selected for the *in vitro* biodeterioration test was the Neapolitan yellow tuff (NYT), a volcanic lithotype widely diffused in the archeological sites of Campania, which is known for its porosity and great water absorption coefficient, both of which support the colonisation of microorganisms [27].

### 2.5. *In Vitro Biodeterioration Test*

In order to reproduce the biological damage caused by fungi on stone, a series of *in vitro* tests was performed by inoculating the selected fungal strains on stone. NYT tiles (3 x 3 cm) were placed in Petri glass dishes and inoculated with a standardized inoculum of the test fungi [28]. The dishes were incubated at 22±2 °C for 20 days with 90–100% of relative humidity to reproduce the environment in which the fungal strains occurred. For each fungal strain, four glass Petri dishes were prepared containing three tuff tiles. In order to evaluate the potential degradation activity of metabolites considered in this study, NYT tiles were also inoculated with fungi together with the tested metabolites at a concentration of 1 mg/mL. To evaluate the fungal growth, the experiments were monitored for 20 days. Once the measurements were taken, the tuff tiles were discarded. Each set of measurements was performed for 20 days at an interval of 5 days in the following way: (1) quantification of the fungal covered area on tiles by recording digital images; (2) measurement of the fungal thickness on tiles with a metallurgical microscope with an objective 6.5×.

### 2.6. *Laboratory Strains and Culturing Conditions*

All the NYT tiles used in the experiments were washed, dried, and displaced in triplicate in Petri glass dishes. On the bottom of each plate was placed a filter paper disc flooded with sterile distilled water in order to guarantee 90–100% of relative humidity. The tiles were then inoculated with 70 µL of sterile Bold's Basal Medium

(BBM) [29] with 12 g/L of sucrose added [30] in order to provide an equal starting nutrient source for all the fungal strains. For the experiment aimed at evaluating the antifungal activity of metabolites considered in this study, together with fungal growth medium, an amount of 70  $\mu$ L of the metabolites at a concentration of 1 mg/mL was inoculated. In all the experiments, for each selected strain, an inoculum of 5000 conidia suspended in 5  $\mu$ L of sterile distilled water was inoculated in the middle of each tile, as previously reported [28]. Two other glass chambers were prepared with tuff tiles watered with (1) distilled water instead of the nutritive medium and (2) methanol and kept until the end of the experiment as controls. To evaluate the fungal growth, every 5 days three tuff tiles per strain from each of the four glasses chambers were analyzed, and once the measurements were taken, they were discarded. During the whole time of observation, the potential occurrence of bacteria was microscopically checked by sampling at regular times the fungal population growing on the tiles. No significant bacterial growth was observed throughout the experiments. All the described procedures took place under a laminar flow hood, and all the materials used were sterilized.

### *2.7. Evaluation of Fungal Growth*

The fungal growth and thickness on the tuff tiles were determined after 5, 10, 15 and 20 days of incubation. Tuff tiles were photographed and recorded every 5 days with a digital camera (Nikon D5100 50 mm objective). The lens of the camera was always kept at the same distance from the samples inside a laminar flow hood, with the lids of the Petri dishes off. The digitized images were analyzed using Trainable Weka Segmentation [31,32], a plugin of open-source software of digital image analysis, namely Fiji [33]. Colony growth on the tuff tiles was also determined by measuring fungal thickness on the same samples used for the quantification of covered areas at each incubation period. To determine the thickness values, the procedure was followed according to Bakke and Olsson [34], with a metallurgical microscope (Leitz Wetzlar Ortholux Microscope) with an objective 6,5x. In this set of experiments, each tile was virtually divided into three zones, ranging from the middle to the external borders of the tile, as described by Del Mondo et al. [28]; these zones were central, median and distal. The results obtained by the triplicates

for any given set of measurements for both the thickness and surface data were used as means for each observation point and then plotted with their respective standard errors.

### 2.7. Statistical Analysis

Statistical analyses were carried out by two-way analysis of variance (ANOVA), and means were compared by Dunnett's test, using Prism software, from three independent replicate values. The value of  $p \leq 0.05$  was considered statistically significant, as noted by an asterisk accompanying means in figures.

### 3. Results and discussion

The fungal metabolites were selected to assay their antifungal activity among a plethora of natural substances isolated and purified in our laboratory at the Department of Chemical Science of University of Naples Federico II in Naples, Italy. In the literature data, the most promising appeared to be the three fungal metabolites cavoxin [21], cyclopaldic acid [22], and *epi*-epoformin [23] (1–3, respectively, in Figure 1).

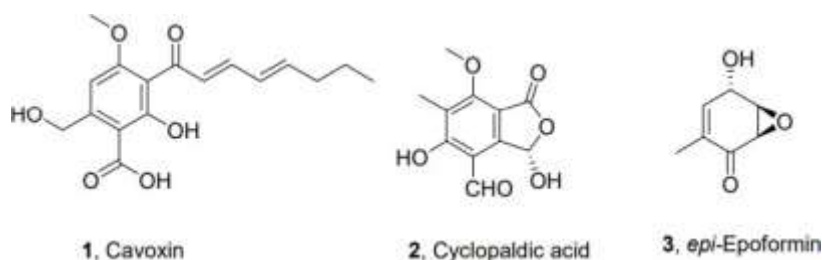


**Figure 1.** Structures of cavoxin, cyclopaldic acid and *epi*-epoformin (1–3).

The three metabolites were isolated and purified as phytotoxins from pathogens of forest plants as *Phoma cava*, *Seiridium cupressi* and *Diplodia quercivora*, which are the causal agent of chestnut (*Castanea sativa*) and cypress (*Cupressus sempirens* L.) canker diseases [21– 23]. In particular, cavoxin showed antifungal

activity against *Aspergillus niger* and *Penicillium roqueforti*, and thus was bioformulated in PBS for intelligent food packaging to protect bread bakery products [35]. Cyclopaldic acid was active against *Botrytis cinerea*, *Fusarium solani* and *Geotrichum candidum* in a structure activity relationships study [36]. Furthermore, cyclopaldic acid and *epi*-epoformin showed antifungal activity against *Puccinia triticina* and *Uromyces pisi*, two rusts pathogens for *Pisum sativum* and other legumes [37]. The antifungal activity of cavoxin, cyclopaldic acid and *epi*-epoformin was first tested against *A. niger*, *A. alternata* and *F. oxysporum* by the paper disk diffusion assay. Cavoxin and *epi*-epoformin inhibited *A. niger* and *F. oxysporum*, while cyclopaldic acid did not show any activity on the three strains. In particular, cavoxin and *epi*-epoformin inhibited the growth of *A. niger* and *F. oxysporum* after 72 h at different concentrations, while no activity was shown against *A. alternata*. For this reason, the strain was discarded from *in vitro* analysis. The sensitivity of *A. niger* and *F. oxysporum* was concentration-dependent, and cavoxin was shown to be more effective than *epi*-epoformin (Figure 2). Digital image analysis complemented with metallurgical microscopy was employed for evaluating the growth of fungal strains on tuff tiles and the potential biocide activity of cavoxin and *epi*-epoformin. The condition selected for the experiments supported a visible fungal growth within the timecourse of the experiments (20 days). The development of *A. niger* and *F. oxysporum* growth on tuff tiles, coupled with the respective metallurgical microscopy images, after 20 days both in presence and absence of the tested compounds (cavoxin and *epi*-epoformin) are shown in Figure 3. In controls, *F. oxysporum* and *A. niger* formed compact mycelia that had partly overgrown the surface of tiles. A radial development of the fungal mycelia was observed, and it was possible to establish a temporal sequence of tile colonisation, with fungal hyphae progressively extending from the zone of the inoculum to the median and distal regions of the tiles. At later stages of colonisation, *F. oxysporum* and *A. niger* respectively occupied about 60% and 70% of the tile surfaces (Figures 4 and 5). A corresponding increase of thickness was also observed, but *F. oxysporum* attained an average thickness of about 150 µm in central and median regions of the tiles, whereas *A. niger* achieved about 300 µm in the central region

and 200  $\mu\text{m}$  in the medial one (Figures 6 and 7).

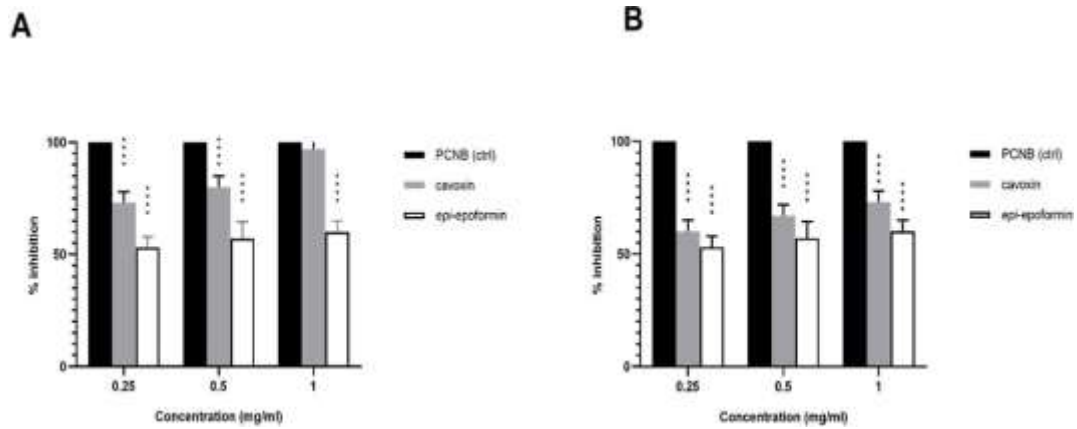


**Figure 2.** Percentage of inhibition, normalized to the positive control (PCNB) (black bar), of cavoxin (grey bar) and *epi*-epoformin (white bar), against *A. niger* (A) and *F. oxysporum* (B). Data shown are means  $\pm$  SD of three independent experiments.

\*\*\*\* indicates  $p < 0.0001$ .

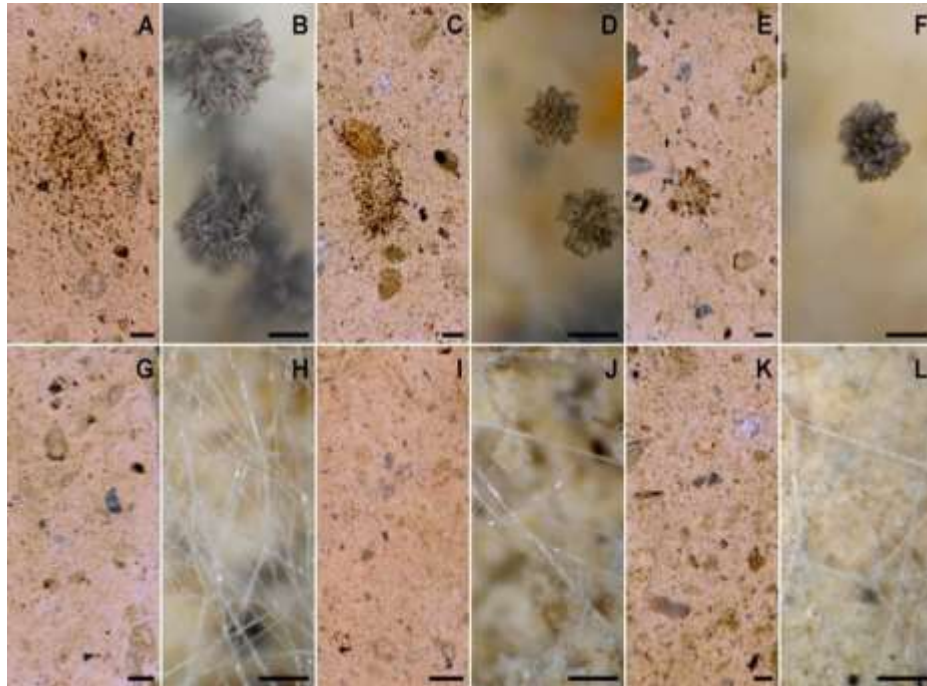


**Figure 3.** Development of fungal growth on tuff tiles at 20 days after inoculation of *A. niger* (A: control, C: with cavoxin, and E: with *epi-epoformin*) and *F. oxysporum* (G: control, I: with cavoxin, and K: with *epi-epoformin*) coupled with the respective metallurgical microscopy images (B, D, and F for *A. niger* and H, J, and L for *F. oxysporum*); scale bar on tuff tiles is 2 mm, scale bar for metallurgical microscopy is 50  $\mu$ m.

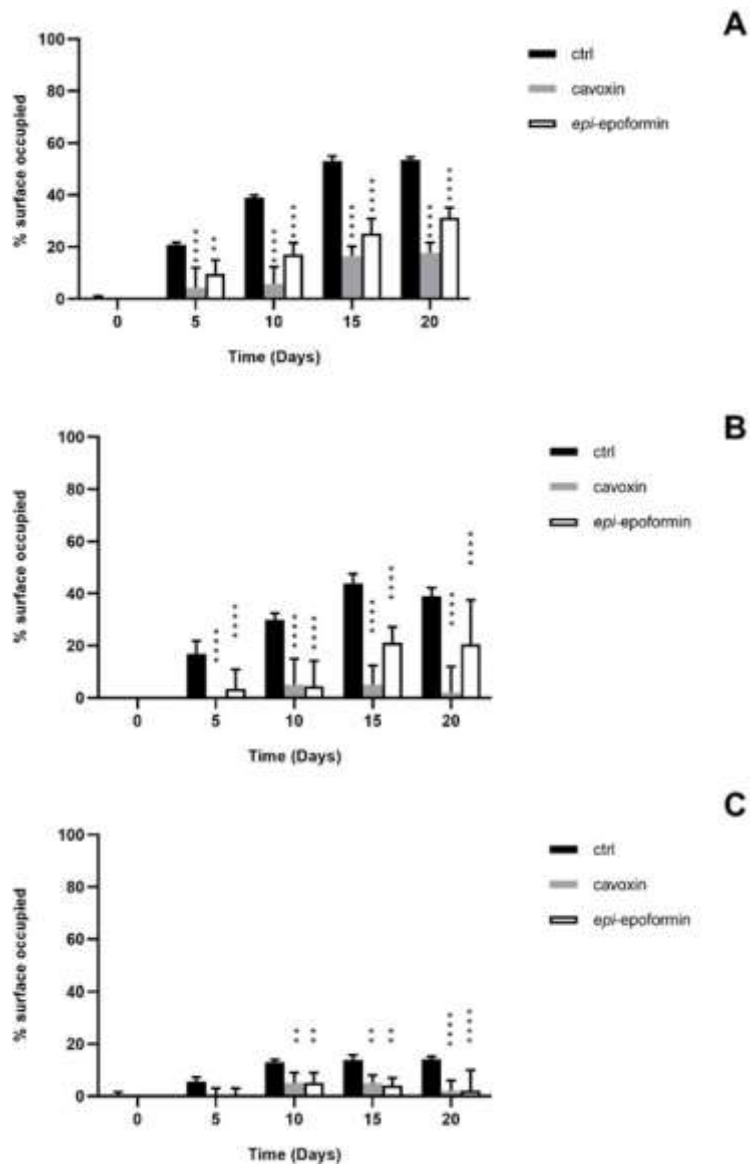


**Figure 4.** Percentage of surface occupied by *F. oxysporum* on central region (A), median region (B), and distal region (C) of the tuff tile. Untreated (black bar), treated with cavoxin (grey bar), treated with *epi-epoformin* (white bar). Data shown are means  $\pm$  SD of three independent experiments. \*\* indicates  $p < 0.005$ , and \*\*\*\* indicates  $p < 0.0001$ .

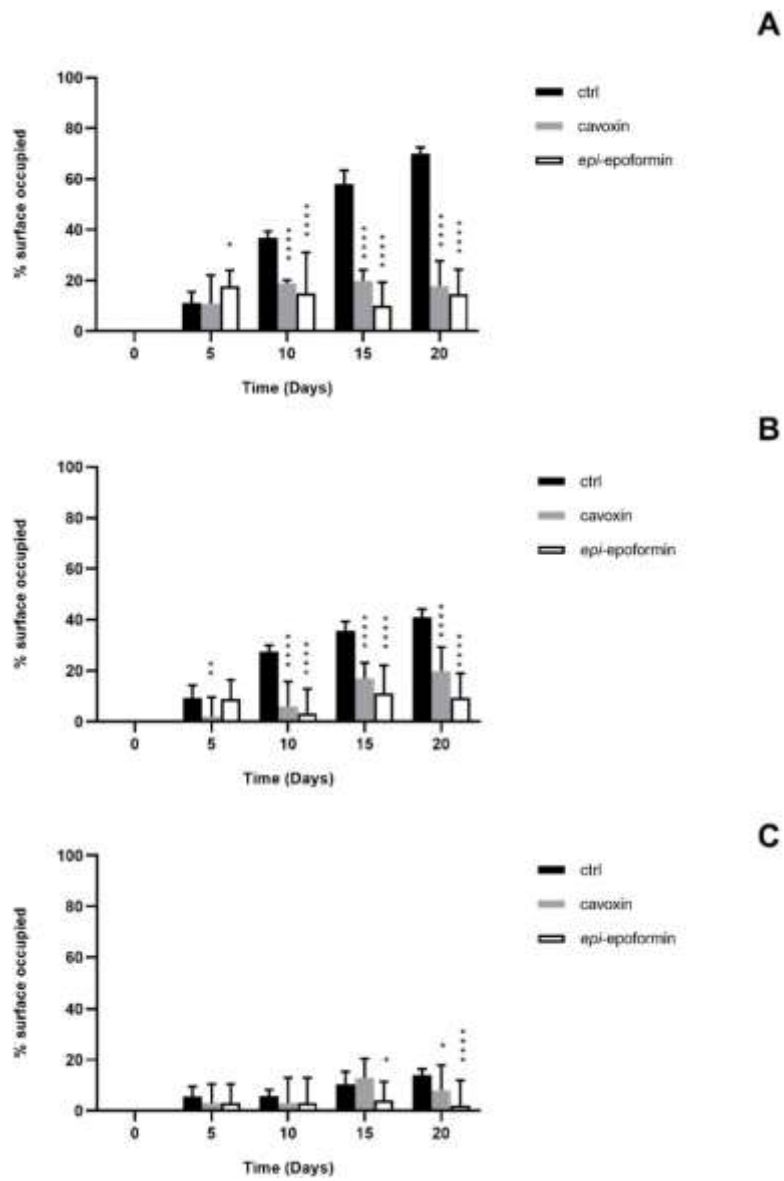


**Figure 5.** Percentage of surface occupied by *A. niger* on central region (A), median region (B), and distal region (C) of the tuff tile. Untreated (black bar), treated with cavoxin (grey bar), treated with *epi-epoformin* (white bar). Data shown are means  $\pm$  SD of three independent experiments.  
 \* Indicates  $p < 0.05$ , \*\* indicates  $p < 0.005$ , and \*\*\*\* indicates  $p < 0.0001$ .

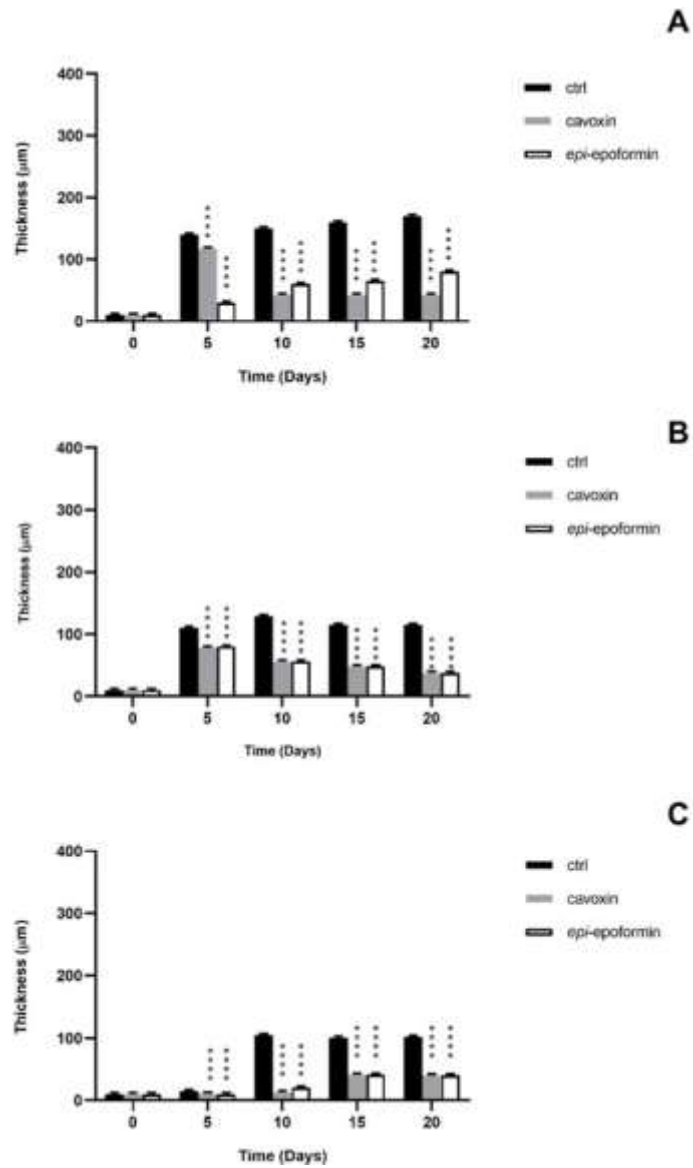


**Figure 6.** Thickness of *F. oxysporum* on central region (A), median region (B), and distal region (C) of the tuff tile. Untreated (black bar), treated with cavoxin (grey bar), treated with *epi-epoformin* (white bar). Data shown are means  $\pm$  SD of three independent experiments. \*\*\*\* indicates  $p < 0.0001$ .

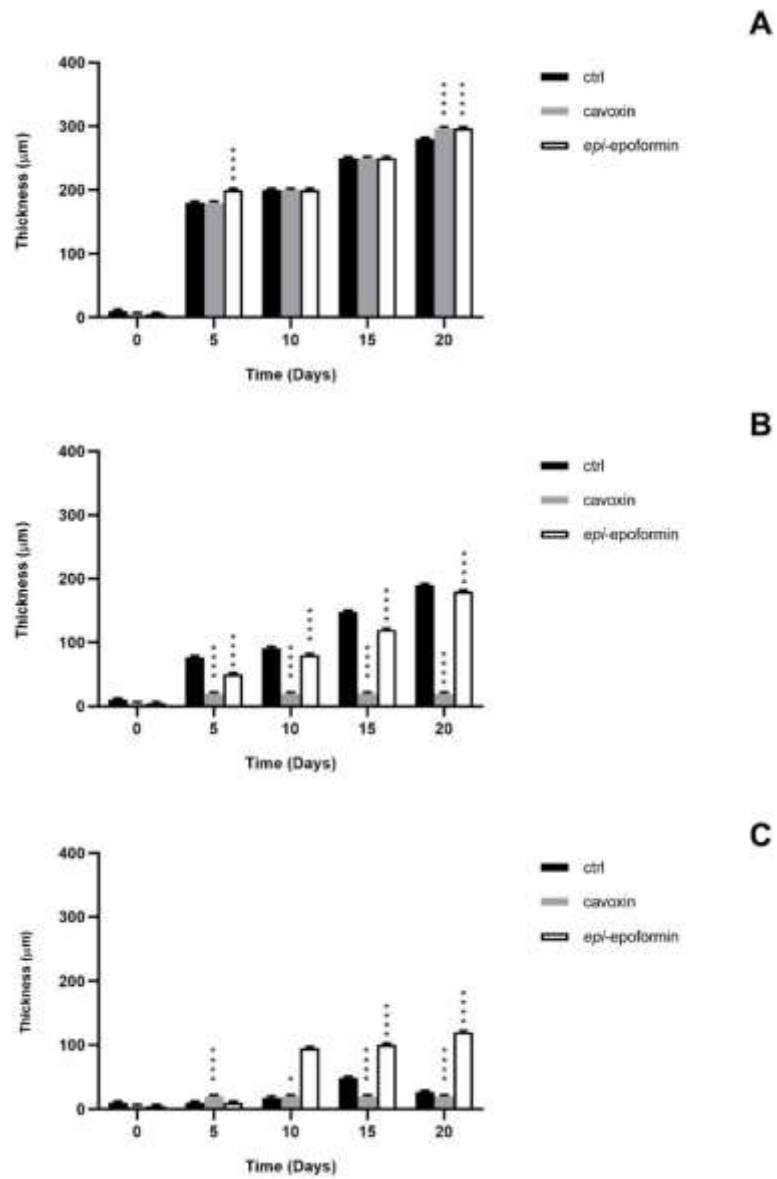


**Figure 7.** Thickness of *A. niger* on central region (A), median region (B), and distal region (C) of the tuff tile. Untreated (black bar), treated with cavoxin (grey bar), treated with *epi-epoformin* (white bar). Data shown are means  $\pm$  SD of three independent experiments. \* Indicates  $p < 0.05$ , \*\*\*\* indicates  $p < 0.0001$ .

The ability of *Aspergillus* sp. to rapidly produce large biomasses firmly adhering to substratum has been reported, as has the ability to withstand different humidity and temperature conditions [38,39]. Both fungi showed a very reduced thickness in distal regions of the tiles, where the hyphal network presented numerous large voids (not shown), as previously reported [28]. The treatment with cavoxin and *epi*-epoformin was very effective against the growth of *A. niger* and *F. oxysporum* on tuff tiles, drastically reducing the colonisation of both fungi. In the treated tiles, both surface coverage and thickness decreased in all the regions (central, medial, distal) of the tiles. In the experiments with *F. oxysporum*, the maximum superficial coverage observed corresponded to about 30% for tiles treated with *epi*-epoformin and was reduced to 20% for those with cavoxin. Similar results were obtained with *A. niger*, whose coverage did not exceed a 20% of tile surface in the presence of each compound. Laboratory-based stone colonisation experiments using different fungal isolates as target organisms are well-established tests to assess the efficacy of the control techniques implemented for the conservation of stone artworks [40,41]. Different approaches have been attempted to eradicate the biofilms growing on artworks, ranging from ultraviolet rays and laser cleaning to ice cleaning systems and microwaves [42]. In addition, the application of protective products and/or hydrophobic agents does not prevent stone colonisation by fungi, and the combined application of biocides is required [43]. In terms of the use of biocides, by far the most frequently adopted strategy of control, synthetic chemicals or mixtures derived from plant preparations (essential oils or water extracts) have been frequently tested [44]. Both can be effective but present some points of weakness. They have a time-limited action on biofilms, depending on environmental parameters such as humidity and temperature [45]. Moreover, it is well known that the application of many biocides on stone surfaces may increase stone tertiary bio-receptivity [46] due to their composition, which might be utilized by microorganisms as nitrogen and carbon sources [47]. This is one of the reasons why the use of traditional biocides to reduce the phenomenon of biodeterioration of stone monuments is increasingly discouraged [44]. In this respect, the investigation of fungal active metabolites opens a promising avenue of research.

Due to the amazing number of chemically different substances produced by fungi, it is possible to design biocides targeting specific microbial communities, using combinations of antifungal natural products that selectively inhibit the growth of individual fungal species within the biofilm.

#### **4. Conclusions**

This study represents a first step in the use of fungal metabolites to allow a better preservation of artwork and to guarantee the conditions suitable for their conservation. The results obtained with *epi*-epoformin and cavoxin confirm that fungi are an untapped source of effective substances to halt or reduce biodeterioration. However, a prerequisite of their application will be to assess their possible detrimental effects on different lithic materials as well as environmental compatibility, in order to develop an eco-friendly system of biofilm control that is respectful of the uniqueness of each artwork.

## References

1. Salvadori, O.; Municchia, A.C. The role of fungi and lichens in the biodeterioration of stone monuments. *Open Conf. Proc. J.* **2016**, *7*, 39–54. [[CrossRef](#)]
2. Gadd, G.M. Geomicrobiology of the built environment. *Nat. Microbiol.* **2017**, *2*, 1–9. [[CrossRef](#)]
3. Evidente, A.; Abouzeid, M.A.; Andolfi, A.; Cimmino, A. Recent achievements in the bio-control of *Orobanche* infesting important crops in the Mediterranean basin. *J. Agric. Sci. Technol. A* **2011**, *1*, 461–483.
4. Cimmino, A.; Masi, M.; Evidente, M.; Superchi, S.; Evidente, A. Fungal phytotoxins with potential herbicidal activity: Chemical and biological characterization. *Nat. Prod. Rep.* **2015**, *32*, 1629–1653. [[CrossRef](#)]
5. Matassini, C.; Parmeggiani, C.; Cardona, F. New frontiers on human safe insecticides and fungicides: An opinion on trehalase inhibitors. *Molecules* **2020**, *25*, 3013. [[CrossRef](#)]
6. Marrone, P.G. Pesticidal natural products—status and future potential. *Pest Man. Sci.* **2019**, *75*, 2325–2340. [[CrossRef](#)]
7. Turner, W.B.; Aldridge, D.C. *Fungal Metabolites II*; Academic Press: London, UK, 1983.
8. Osbourn, A.E.; Lanzotti, V. *Plant-Derived Products*; Springer: Dordrecht, Germany, 2009.
9. Dewick, P.M. *Medicinal Natural Products—A Biosynthetic Approach*; Wiley and Sons Ltd.: Chichester, UK, 2009.
10. Coleman, J.J.; Ghosh, S.; Okoli, I.; Mylonakis, E. Antifungal activity of microbial secondary metabolites. *PLoS ONE* **2011**, *6*, e25321. [[CrossRef](#)]
11. Kumar, S.; Kaushik, N. Metabolites of endophytic fungi as novel source of biofungicide: A review. *Phytochem. Rev.* **2012**, *11*, 507–522. [[CrossRef](#)]
12. Wang, Y.T.; Xue, Y.R.; Liu, C.H. A brief review of bioactive metabolites derived from deep-sea fungi. *Mar. Drugs* **2015**, *13*, 4594–4616. [[CrossRef](#)]
13. Roscetto, E.; Masi, M.; Esposito, M.; Di Lecce, R.; Delicato, A.;

- Maddau, L.; Calabrò, V.; Evidente, A.; Catania, M.R. Anti-biofilm activity of the fungal phytotoxin sphaeropsidin A against clinical isolates of antibiotic-resistant bacteria. *Toxins* **2020**, *12*, 444. [[CrossRef](#)] [[PubMed](#)]
14. Masi, M.; Maddau, L.; Linaldeddu, B.T.; Scanu, B.; Evidente, A.; Cimmino, A. Bioactive metabolites from pathogenic and endophytic fungi of forest trees. *Curr. Med. Chem.* **2018**, *25*, 208–252. [[CrossRef](#)][[PubMed](#)]
  15. Hasan, S.; Ansari, M.I.; Ahmad, A.; Mishra, M. Major bioactive metabolites from marine fungi: A Review. *Bioinformation* **2015**, *11*, 176. [[CrossRef](#)] [[PubMed](#)]
  16. Reveglia, P.; Cimmino, A.; Masi, M.; Nocera, P.; Berova, N.; Ellestad, G.; Evidente, A. Pimarane diterpenes: Natural source, stereochemical configuration, and biological activity. *Chirality* **2018**, *30*, 1115–1134. [[CrossRef](#)] [[PubMed](#)]
  17. Kot, A.M.; Błaz'ejak, S.; Kieliszek, M.; Gientka, I.; Brys', J.; Reczek, L.; Pobiega, K. Effect of exogenous stress factors on the biosynthesis of carotenoids and lipids by *Rhodotorula* yeast strains in media containing agro-industrial waste. *World J. Microbiol. Biotechnol.* **2019**, *35*, 1–10. [[CrossRef](#)]
  18. Masi, M.; Evidente, A. Fungal bioactive anthraquinones and analogues. *Toxins* **2020**, *12*, 714. [[CrossRef](#)]
  19. Reveglia, P.; Masi, M.; Evidente, A. Melleins—Intriguing natural compounds. *Biomolecules* **2020**, *10*, 772. [[CrossRef](#)]
  20. Masi, M.; Meyer, S.; Clement, S.; Andolfi, A.; Cimmino, A.; Evidente, A. Spirostaphylotrichin W, a spirocyclic  $\gamma$ -lactam isolated from liquid culture of *Pyrenophora semeniperda*, a potential mycoherbicide for cheatgrass (*Bromus tectorum*) biocontrol. *Tetrahedron* **2014**, *70*, 1497–1501. [[CrossRef](#)]
  21. Evidente, A.; Randazzo, G.; Iacobellis, N.S.; Bottalico, A. Structure of cavoxin, a new phytotoxin from *Phoma cava* and cavoxone, its related chroman-4-one. *J. Nat. Prod.* **1985**, *48*, 916–923. [[CrossRef](#)]
  22. Graniti, A.; Sparapano, L.; Evidente, A. Cyclopaldic acid, a major phytotoxic metabolite of *Seiridium cupressi*, the pathogen of a canker disease of cypress. *Plant Pathol.* **1992**, *41*, 563–568. [[CrossRef](#)]

23. Cala, A.; Masi, M.; Cimmino, A.; Molinillo, J.M.; Macias, F.A.; Evidente, A. (+)-*epi*-Epoformin, a phytotoxic fungal cyclohex enepoxide: Structure activity relationships. *Molecules* **2018**, *23*, 1529. [[CrossRef](#)] [[PubMed](#)]
24. Guo, Z.; Chen, R.; Xing, R.; Liu, S.; Yu, H.; Wang, P.; Li, C.; Li, P. Novel derivatives of chitosan and their antifungal activities in vitro. *Carb. Res.* **2006**, *341*, 351–354. [[CrossRef](#)] [[PubMed](#)]
25. D’Elia, L.; Del Mondo, A.; Santoro, M.; De Natale, A.; Pinto, G.; Pollio, A. Microorganisms from harsh and extreme environments: A collection of living strains at ACUF (Naples, Italy). *Ecol. Quest.* **2018**, *29*, 63–74. [[CrossRef](#)]
26. Doyle, J.J.; Doyle, J.L. Isolation of plant DNA from fresh tissue. *Focus* **1990**, *12*, 13–15.
27. Kastenmeier, P.; Di Maio, G.; Balassone, G.; Boni, M.; Joachimski, M.; Mondillo, N. The source of stone building materials from the Pompeii archaeological area and its surroundings. *Period. Mineral.* **2010**, 39–58. [[CrossRef](#)]
28. Del Mondo, A.; Pinto, G.; De Natale, A.; Pollio, A. In vitro colonisation experiments for the assessment of mycelial growth on a tuff substratum by a *Fusarium solani* strain isolated from the oplontis (Naples, Italy) archaeological site. *Int. J. Conserv. Sci.* **2017**, *8*, 651–662.
29. Nichols, H.W.; Bold, H.C. *Trichosarcina polymorpha* gen. et sp. Nov. *J. Phycol.* **1965**, *1*, 34–38. [[CrossRef](#)]
30. Jeger, M.J.; Lamour, A.; Gilligan, C.A.; Otten, W. A fungal growth model fitted to carbon limited dynamics of *Rhizoctonia solani*. *New Phytol.* **2008**, *178*, 625–633. [[CrossRef](#)]
31. Vyas, N.; Sammons, R.L.; Addison, O.; Dehghani, H.; Walmsley, A.D. A quantitative method to measure biofilm removal efficiency from complex biomaterial surfaces using SEM and image analysis. *Sci. Rep.* **2016**, *6*, 32694.
32. Arganda-Carreras, I.; Kaynig, V.; Rueden, C.; Eliceiri, K.W.; Schindelin, J.; Cardona, A.; Sebastian Seung, H. Trainable Weka Segmentation: A machine learning tool for microscopy pixel classification. *Bioinformatics* **2017**, *33*, 2424–2426. [[CrossRef](#)]
33. Schindelin, J.; Arganda Carreras, I.; Frise, E.; Kaynig, V.; Longair, M.; Pietzsch, T.;

- Preibisch, S.; Rueden, C.; Saalfeld, S.; Schmid, B.; et al. Fiji: An open-source platform for biological image analysis. *Nat. Methods* **2012**, *9*, 676–682. [[CrossRef](#)] [[PubMed](#)]
34. Bakke, R.; Olsson, P.Q. Biofilm thickness measurements by light microscopy. *J. Microb. Methods* **1986**, *5*, 93–98. [[CrossRef](#)]
35. Santagata, G.; Valerio, F.; Cimmino, A.; Dal Poggetto, G.; Masi, M.; DiBiase, M.; Malinconico, M.; Lavermicocca, P.; Evidente, A. Chemico-physical and antifungal properties of poly (butylene succinate)/cavoxinblend: Study of a novel bioactive polymeric based system. *Eur. Polym.J.* **2017**, *94*, 230–247. [[CrossRef](#)]
36. Sparapano, L.; Evidente, A.A. Biological activity of cyclopaldic acid, a major toxin of *Seiridium cupressi*, its six derivatives, and iso- cyclopaldic acid. *Nat. Toxins* **1995**, *3*, 156–165. [[CrossRef](#)] [[PubMed](#)]
37. Barilli, E.; Cimmino, A.; Masi, M.; Evidente, M.; Rubiales, D.; Evidente, A. Inhibition of early development stages of rust fungi by the two fungal metabolites cyclopaldic acid and *epi-epoformin*. *Pest Man. Sci.* **2017**, *73*, 1161–1168. [[CrossRef](#)]
38. Mishra, N. Influence of temperature and relative humidity on fungiflora of some species in storage. *Z. Lebensm. Unters. Forsch.* **1981**, *172*, 30–31. [[CrossRef](#)]
39. Siqueira, V.M.; Lima, N. Biofilm formation by filamentous fungus recovered from a water system. *J. Mycol.* **2013**, 152941. [[CrossRef](#)]
40. Shirakawa, M.A.; Beech, I.B.; Tapper, R.; Cincotto, M.A.; Gambale, W. The development of a method to evaluate bioreceptivity of indoor mortar plastering to fungal growth. *Int. Biodeter. Biodegr.* **2003**, *51*, 83–92. [[CrossRef](#)]
41. Wiktor, V.; De Leo, F.; Urzì, C.; Guyonnet, R.; Grosseau, P.H.; Garcia-Diaz, E. Accelerated laboratory test to study fungal biodeterioration of cementitious matrix. *Int. Biodeter. Biodegr.* **2009**, *63*, 1061–1065. [[CrossRef](#)]
42. Caneva, G.; Terscari, M. Stone biodeterioration: Treatments and preventive conservation. In Proceedings of the 2017 International Symposium of Stone Conservation, Conservation Technologies for Stone Cultural Heritages: Status and

Future Prospects, Seoul, Korea, 21 September 2017; ISBN 978-89-299-1102-793600.

43. De Leo, F.; Urzì, C. Fungal colonisation on treated and untreated stonesurfaces. In *Molecular Biology and Cultural Heritage*; Swets & Zeitlinger BV: Lisse, The Netherlands, 2003; pp. 213–218.
44. Fidanza, M.R.; Caneva, G. Natural biocides for the conservation of stone cultural heritage: A review. *J. Cult. Herit.* **2019**, *38*, 271–286. [[CrossRef](#)]
45. Young, M.E.; Alakomi, H.L.; Fortune, I.; Gorbushina, A.A.; Krumbein, W.E.; Maxwell, I.; McCullagh, C.; Robertson, P.; Saarela, M.; Valero, J.; et al. Development of a biocidal treatment regime to inhibit biological growths on cultural heritage: BIODAM. *Environ. Geol.* **2008**, *56*, 631–641. [[CrossRef](#)]
46. Miller, A.Z.; Sanmartìn, P.; Pereira-Pardo, L.; Dionisio, A.; Macedo, M.F.; Priteo, B. Bioreceptivity of buildings stones: A review. *Sci. Total Environ.* **2012**, *426*, 1–12. [[CrossRef](#)] [[PubMed](#)]
47. Bastian, F.; Jurado, V.; Novakova, A.; Alabouvette, C.; Saiz-Jimenez, C. The microbiology of lascaux cave. *Microbiology* **2010**, *156*, 644–652. [[CrossRef](#)] [[PubMed](#)]

**CHAPTER 6**  
**A BIOLOGICAL AND QUANTITATIVE STUDY ON IN VITRO COLONISATION**  
**OF NEAPOLITAN YELLOW TUFF BY *BRACTEACOCCLUS MINOR*, *FUSARIUM***  
***OXYSPORUM* AND *NOSTOC COMMUNE***

## **Abstract**

To integrate the understanding of biodeterioration on artistic-historical heritages due to the vital activity of microorganisms, we performed *in vitro* experiments inoculating *Nostoc commune* strain, *Fusarium oxysporum* strain and *Bracteacoccus minor* strain collected from the UNESCO site of archaeological park of Pompeii (Naples, Italy), on Neapolitan Yellow Tuff (NYT) tiles for 50 days in a low-carbon environment. We documented microbial growth using photomicrography-based image analyses, integrating our findings with landscape metrics to evaluate the spatial arrangement and the ecological relationships between microorganisms during growth. To our knowledge, this study represents the first attempt to characterize the ecology of microbial biofilm growing on cultural heritage using metrics, normally applied on landscape ecology referred to large geographical areas. Our results confirm that *in vitro* accelerated tests, coupled with microscopical observations, computer image analysis and landscape metrics, are useful tools to evaluate and quantify the amount and the spatial arrangement of microorganisms on a stone substratum, especially in the early steps of microbial colonisation.

**Keywords:** accelerated-test, biodeterioration, image analysis, CSLM, landscape metrics

## Introduction

Microorganisms, may colonise and degrade building materials, including cultural heritage and artworks made of stone [1]. Microorganisms, especially fungi can penetrate the substratum, causing cracks and lesions to the artwork, due to the extraordinary penetrating power of hyphae, while also discoloring the surface and forming patinas over it, thus contributing to superficial spoiling [2, 3]. Biological colonisation on stone surfaces is a complex dynamic, depending on both substrates and environmental factors [4,5]. Usually, the influence of the latter is stronger, but when light, relative humidity and temperature do not represent limiting factors, physicochemical characteristics of substrates become crucial drivers of the assembly of microbial communities [6]. Thus, colonisation can strongly depend on the organisms that establishes the first firm relationship with the substrate, conditioning the subsequent steps of the biofilm consolidation [7]. The ecological success of biofilms growing on lithic surfaces is the result of a balance between the ecological interactions of different microbial species [8] which strongly influence the architecture of biofilms. Such structural arrangements often explain important attributes of deteriogenic biofilms [9], therefore their knowledge is essential for any predictive model of biofilm formation and for the design of strategies to remove biofilm infections. Here we present an *in vitro* laboratory test coupled with metallurgical, confocal microscopy and image analyses to study the initial steps of microbial colonisation on stone and to better understand how spatial structure of these communities influences the ecology and community diversity of biofilms growing on lithic surfaces. We chose strains sampled in the House of Marco Castricio (Pompei) due to their easy cultivability. *In vitro* experiments are useful to assess microbial bioreceptivity and biodeteriogenic abilities of different lithotypes [10, 11, 12], setting an artificial close system in which several environmental parameters may be varied by the operator. Despite their great usefulness, to our knowledge, there is no current report in literature taking into account the penetration into substratum concerned with

investigating the ecological interactions between 3 diverse microbial species including autotrophic and heterotrophic species in a closed system in which material and ambient condition are fully standardized. We followed microbial growth for 50 days within glass Petri dishes containing Neapolitan Yellow Tuff tiles with low sucrose supply as a unique carbon source and saturated relative humidity. We monitored coverage dynamics of the spreading colonies and described the spatial arrangement through metallurgical microscopy and CLSM microscopy stack reconstruction. We integrated these spatial measures with the use of landscape metrics, to quantify the amount and the spatial arrangement of habitable patches. This novel approach to the assessment of biodeteriogenic potential of microorganisms allowed us to highlight some features of microbial colonisation on stone, advancing our understanding of the dynamics of physical spoiling of ancient building materials.

## **Materials and Methods**

The experiment rationale was to monitor the growth and fine structure of biofilm forming by *Bracteacoccus minor*, *Fusarium oxysporum* and *Nostoc commune* strain on Yellow Neapolitan tuff, under controlled, non-limiting conditions, every ten days for fifty days.

### **Petrographic analysis, roughness and porosity**

In many archaeological sites, the employment of local stone for architectural purposes is widespread: this is the case of Campania region (Italy), where the use of volcanic products was encouraged by their abundance and workability. Among these, the Neapolitan Yellow Tuff (NYT) typically presents itself as an assemblage with prevailing epigenetic phases (phillipsite, chabazite and analcime), feldspar, and minor amounts of mica, hydrated iron oxides and volcanic glass [13]. For these reasons, the selected stone for the *in vitro* biodeterioration test was the NYT, known for its porosity and great water absorption coefficient, both of which support the colonisation of

microorganisms [14, 15]. We produced fifteen tiles from material extracted from the Neapolitan Yellow Tuff (NYT) caves of Quarto (Napoli, Italy). We performed all measurements in triplicate. We evaluated each tile's roughness parameters with an ALPA© RT-20 handheld rugosimeter, following standard ISO (ISO 4287:1984) protocols. We measured roughness profile from 1600 sample points for each tile to determine average roughness (Ra), root mean square surface roughness (Rq), mean roughness depth (Rz), maximum roughness (Rt), and averagedensity (Da). We acquired the data using the Measurement Studio Lite software (ver. 1.0.3.96, Metrology Systems, Turin, Italy, <http://www.sminstruments.com/it/prodotti/rugosimetri/software-measurement-tudio.html>). Finally, we calculated water absorption coefficient (WAC) (mean  $\pm$  SD) following [16].

### **Origin, culture and identification of the strains**

All the experiments were performed using the strains: ACUF\_169 (*Bracteacoccus minor*); ACUF\_812 (*Nostoc commune*); ACUF\_014f (*Fusarium oxysporum*), collected from the tuff walls at the House of Marco Castricio in Pompei Archaeological Park, Naples, Italy [17, 18]. The identification of strains was performed through a polyphasic approach that is an integrated approach of identification based on morphological and molecular features of microorganisms [19]. Further confirmation of the observations and the assessment of the species was obtained through molecular analysis. DNA was extracted following Doyle and Doyle DNA extraction protocol [20] and used for a Polymerase Chain Reaction with primers targeting ITS rDNA for fungus (primer Fw 5'-TCCGTAGGTGAACCTGCGG-3'; primer Rv5'-TTCAAAGATTCGATGATTCAC-3'), 16S rDNA for Cyanobacteria identification (primer forward 5'-AGGATGCAAGCGTTATCCG-3' ; primer reverse 5'-GGGGCATGCTGACTTGACG-3') and finally RbCL for microalgae (primer forward 5' - TTYATGCGTTGGAGAGAYCG - 3'; primer reverse 5' - GTGCATAGCWCGGTGAATRTG - 3') as described by Del Mondo 2018 [21]. The amplification product was then evaluated by agarose gel electrophoresis and purified with QIAquick® PCR Purification kit (Qiagen Inc, Valencia, CA, USA).

Sequence reaction was obtained with the BigDye Terminator Cycle Sequencing technology (Applied Biosystems, Foster City, CA), purified in automation using the Agencourt CleanSEQ Dye terminator removal Kit (Agencourt Bioscience Corporation, 500 Cummins Center, Suite 2450, Beverly MA 01915 - USA) and a robotic station Biomek FX (Beckman Coulter, Fullerton, CA). Product was analyzed on an Automated Capillary Electrophoresis Sequencer 3730 DNA Analyzer (Applied Biosystems). The amplification primers were used as the sequencing primers. The obtained sequence was loaded in BLAST version 2.0 (National Center for Biotechnology Information databases) and identified as *Bracteacoccus minor*, *Fusarium oxysporum* and *Nostoc commune* with a similarity score of 100%.

### **In vitro NYT colonisation of *Bracteacoccus minor*, *Nostoc commune* and *Fusarium oxysporum***

An *in vitro* approach has been settled (**Fig.1**) in order to reproduce dispersal, growth and ecological succession of microorganisms on lithic substrata. At this aim three strains from ACUF collection, previously isolated from archeological sites, were used to perform in *in vitro* microcosm experiment: 1) ACUF\_169 (*Bracteacoccus minor*); 2) ACUF\_812 (*Nostoc commune*); 3) ACUF\_014f (*Fusarium oxysporum*). All the *in vitro* tests were performed by inoculating the selected strain on NYT tiles (3 x 3 cm) placed in triplets in five Petri dishes (100 x 15 mm), one for each time point, and tyndallised the dishes. The tuff tiles were inoculated with a standardized inoculum of the test fungi [22], algae and cyanobacteria [23]. The dishes were incubated at  $22 \pm 2$  °C for 50 days maintaining at saturated relative humidity with sterile filter paper disks soaked in sterile distilled water. The tiles were then watered with 2 mL of a nutritive medium composed of BBM (Bold's Basal Medium) [24] plus the addition of sucrose 12g/L as low carbon supply [25]. In the first experimental condition the growth of single microorganisms was evaluated, in the second experimental condition the growth of autotrophic and heterotrophic microorganisms in pairs was evaluated, thus one-time cyanobacteria and fungus strain were inoculated together in the middle of the tuff tile; in another set conditions algae and fungus were inoculated together in the middle of the tuff tile.

A petri dish missing of the inoculum was prepared in the same manner and kept for 50 days as a control.

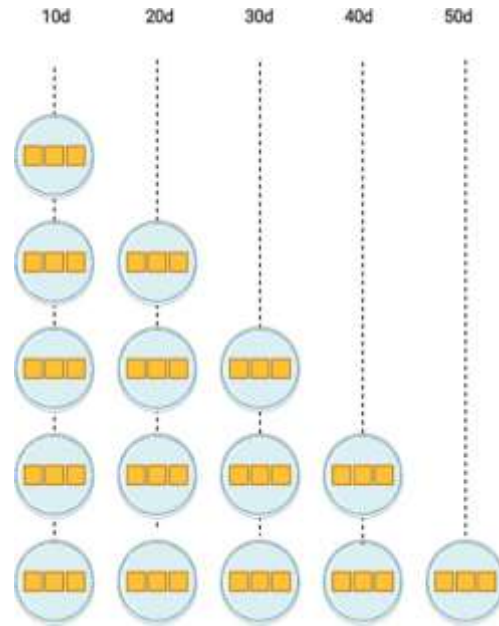


**Fig. 1 - Experimental strategy**

Five petri dishes containing NYT tiles in triplicates were inoculated on day 0 using 5000 *F.oxysporum* spores as control; five petri dishes containing NYT tiles in triplicates were inoculated on day 0 using  $1 \times 10^4$  cells of *N.commune* as control; five petri dishes containing NYT tiles in triplicates were inoculated on day 0 using  $1 \times 10^4$  cells of *B.minor* as control. Five petri dishes containing NYT tiles in triplicates were inoculated on day 0 using 5000 *F.oxysporum* spores together with  $1 \times 10^4$  cells of *B.minor*. Five petri dishes containing NYT tiles in triplicates were inoculated on day 0 using 5000 *F.oxysporum* spores together with  $1 \times 10^4$  cells of *N.commune*. The growth of microorganisms was followed for 50 days using photographic documentation, while a destructive sampling of the tiles was made with a 10 days interval to determine CLSM scan.

We obtained *F. oxysporum* conidia from a five-day old colony treated for one minute with PBS-Tween20 solution at the final concentration of 0.5% and mechanically scraped with a sterile glass handle; the suspension was filtered through sterile gauze and then diluted. We determined the number of conidia per

milliliter through a direct microscopic count in a counting chamber (Burker blood-counting chamber, HBG – German). Subsequently, we injected 5000 conidia suspended in 0.9% of NaCl solution in the middle of each tile. A 20 µl aliquot of a *N. commune* and 20 µl aliquot of a *B. minor* liquid cultures in the exponential growth phase (equivalent to  $1 \times 10^4$  cells), was inoculated on the center of the NYT and porphyry blocks, in a laminar flow hood, as previously described [23]. To evaluate the biofilm growth and structure, the experiments were monitored for 50 days. Once the measurements were taken, the tuff tiles were discarded. Each set of measurements was performed for 50 days at an interval of 10 days in the following way: (1) quantification of the microbial covered area on tiles by recording digital images with a Nikon D5100 camera with 50 mm objective; (2) measurement of the biofilm thickness on tiles with a metallurgical microscope with an objective 6.5× (3) observation of biofilm structure with CLSM. Calcofluor white staining for fluorescence microscopy observation was used for fungus. Red autofluorescence was detected for algae and cyanobacteria.

### **Metallurgical, CLSM observations and image analyses**

The microbial growth, thickness and spatial arrangement on the tuff tiles were determined after 10, 20, 30, 40 and 50 days of incubation. Every 10 days, each tuff tile was photographed as the triplicate of each tile at different experimental conditions with a digital camera (Nikon D5100 50 mm objective). The lens of the camera was always kept at the same distance from the samples inside a laminar flow hood, with the lids of the Petri dishes off. The digitized images were analyzed using Trainable Weka Segmentation [26], a plugin of open-source software of digital image analysis, namely Fiji [27] to evaluate the colonised areas in each photograph. Microbial thickness on the tuff tiles was also determined with a metallurgical microscope (Leitz Wetzlar Ortholux Microscope) equipped with an Ultropak 6.5x objective, following the procedure described by Bakke and Olsson [28]. Measurements were performed at ten points of each tile: the center (2 points), middle (4 points) and periphery (4 points) of the tile. Finally, every 10 days, the microbial fine structure on the substratum were also analysed in three points (center, middle and periphery) with a Zeiss LSM 700 Confocal Laser Scanner Microscope

(CLSM), acquiring z-stack images using a 10× objective (**Fig.2**).

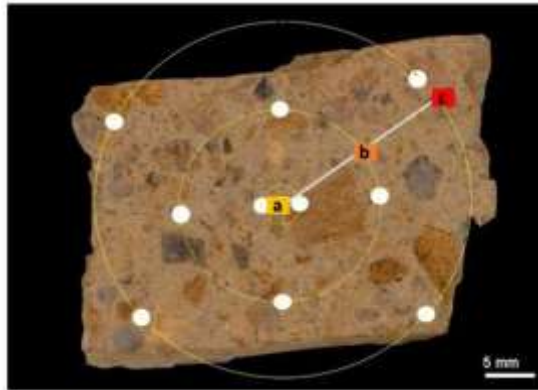


**Fig. 2 - Sampling points on NYT tile** The observation points were classified as central (a), middle (b) and periphery (c) region.

The fluorescence of hyphae was recorded with an excitation beam at 405-458 nm and emission at 415-505 nm (blue channel) using calcofluor white 1% to stain the hyphae. The red channel was used for autofluorescence pigment (chlorophyll a and phycobilins) with excitation beams at 488-639 nm and emission at 590–800 nm (red channel). To discriminate cyanobacteria an emission filter was set at 610-650 nm (red-cyanochannel); for green algae a second filter was used with an emission of 675-700 nm (Red Channel). We formed stacks by using images captured at 13.46  $\mu\text{m}$  intervals. The methodology used for the observation, acquisition and analysis of the microbial biofilms agree with a formerly validated protocol [23]. The substratum area of the image stack was  $512 \times 512$  pixels. On each sample, three Z-stacks were registered randomly. The number of images in each stack varies according to the microbial mat's thickness. The package Fiji was used to obtain 2D maximum intensity projections (MIPs). The images were previously converted to 8-bit and then resampled by using the tool Threshold [29, 30]. The MIPs constructed from the confocal Z-stacks were rasterized in standard cells in which landscape metrics quantifying the amount and the spatial arrangement of habitable patches were applied. The results obtained by the triplicates for any given set of measurements for both the surface, thickness and spatial arrangement data were used as means for each observation point and then plotted with their respective

standard errors.

### **Landscape temporal dynamics**

Geographic areas represented by contiguous presence data (cells scored as ‘1’) and entirely surrounded by absence cells (i.e., scored as ‘0’) represent a habitat patch. To retrieve information about aggregation, shape and subdivision of patches, as well as to evaluate their degree of fragmentation in each time bin, we calculated the following six landscape metrics using the ‘landscape metrics’ R package: total patch area, number of patches, mean patch area, mean Euclidean nearest-neighbour distance, aggregation index and division index. The number of patches represents a simple measure of the fragmentation extent, while the mean patch area gives information about how the habitat patches of a particular landscape are growing or merging over time [31-32]. Division index yields the probability that two randomly selected cells are not located in the same patch. Mean Euclidean nearest-neighbour distance accounts for the number of highly isolated patches, whereas aggregation index evaluates the frequency with which patch pairs occur side by side in the landscape [33]. We selected these metrics as they can be successfully used to compare fragmentation among different landscapes and, in our case, different time bins [34-35]. These metrics were calculated for each species in each 1 ka time bin (limited to the temporal range of the species fossils), each replicated date and binarization threshold, combining all the results in a single dataset. The outcomes were used to describe the temporal dynamics of habitat patch configuration during the last 200 ka by fitting linear mixed models (LMMs), where each of the landscape metrics was used as the response variable and the time (in kilo years, from 200 to 2 ka), as the explanatory variable. Response variables were first transformed using a logarithmic transformation to improve normality. In addition, since we were interested in testing for different temporal dynamics of spatial patch configuration for extinct and extant species, LMMs were fitted putting the ‘time’ explanatory variable in interaction with the species status (i.e. extinct or extant). This setup allowed LMMs to fit two different landscape metrics versus time relationships for extinct and extant species. As we did not have an a priori expectation about the shape of the relationship between landscape metrics and time, we accounted for

possible non-linear patterns by fitting LMMs with linear, linear + quadratic and linear + quadratic + cubic relationships. To avoid overly complex or overfitted models, LMMs including quadratic and cubic terms were compared with linear terms using AIC. To account for differences in metric values among the different species, replicated datasets and binarization thresholds, we included such factors as random effects in LMMs, allowing the models to vary their intercepts accordingly. Models' goodness of fit was assessed by calculating the conditional coefficient of determination for LMM [36]. Furthermore, we evaluated the LMMs' predictive accuracy by calculating Pearson's correlation coefficient between observed and predicted values of the outcome under a fivefold cross-validation scheme. All the statistical analyses were run by using the 'lme4', 'MuMIn' and 'performance' R packages. To assess the relative contribution of the landscape metrics and functional traits (body mass and diet, [37-38] in discriminating between extinct and extant species, we ran a Random Forest classification model [39] using the 'caret' R package [40]. In this model, we used the status of each species ('extinct' versus 'extant') as the response variable, while the landscape metrics, body mass, diet, time in kilo-years, replicated datasets and binarization thresholds were included as explanatory variables. Before entering the RF model, the six landscape metrics were checked for multicollinearity (Zuur et al. 2010), retaining aggregation index, mean patch area, mean Euclidean nearest-neighbor distance, number of patches and division index. We evaluated the RF model's ability to correctly classify a species as extinct or extant according to the abovementioned covariates by calculating the AUC under a five-fold cross-validation scheme. In particular, we optimally tuned RF settings by testing for different combinations of the number of variables randomly selected at each node, depth of the classification trees created by the algorithm and splitting rule parameters (Gini index and ExtraTrees algorithm). All RF candidate models were run allowing a maximum of 1000 trees. Once optimally tuned, the RF model was used to quantify the relative importance of each covariate, expressed as the mean decrease accuracy (i.e., how much accuracy the model loses by excluding each variable in turn). We cumulated the mean decrease in accuracy across variables in four macro-categories: landscape metrics, diet, mass and other effects (i.e., time in kiloyears, replicated datasets and binarization thresholds). In

addition, we generated partial dependence plots according to Greenwell [41], to depict the shape of the relationship between each explanatory variable and the probability of a given species being classified as ‘extinct’ while holding the values of other variables constant.

### **Data analysis**

Comparative analysis was performed using the analysis of variance (ANOVA) followed by the Bonferroni post hoc comparisons or the Tukey test for multiple comparison test. A  $p$ -value less than 0.05 was considered as statistically significant. All the data analysis and visualization were performed using the R environment for statistical computing [42], using the tidyverse collection of packages [43], tidygraph [44] and graph [45].

## Results

### Characterisation of NYT samples

The tiles of Neapolitan Yellow Tuff used in this study were analysed for water absorption coefficient, porosity and roughness as described in Materials and methods. Data regarding tuff characterisation are consistent with the properties and description of this building material and measured values for petrographic characterisation are shown in **Table 1**.

WAC (g dm <sup>-2</sup> min <sup>-1/2</sup> )	<u>Porosity</u>				<u>Roughness</u>			
	<u>Densit</u>	<u>Porosit</u>	<u>Average</u>	<u>Total pore</u>	<u>Ra</u>	<u>Rq</u>	<u>Rz</u>	<u>Rt</u>
	<u>y</u>	<u>y</u>	<u>pore</u>	<u>area</u>				
	(g cm <sup>-3</sup> )	(%)	<u>diameter</u>	(m <sup>2</sup> /g)				
			(nm)					
49.28 <sup>-5</sup>	1.461	56.63	247.8	9.47	19.3	23.2	85.6	101.83
					2	1	8	

**Table 1 – Petrographic features of Neapolitan yellow tuff (NYT).**

### **Colonisation dynamic of *Bracteacoccus minor*, *Fusarium oxysporum* and *Nostoc commune* in the accelerated test on NYT**

The overall spreading of *Bracteacoccus minor* (ACUF\_169); *Fusarium oxysporum* (ACUF\_014f) and *Nostoc commune* (ACUF\_812) on tuff tiles was documented during all the experiment. Beside the monitoring of the whole colonisation grown on NYT tiles, also microscopic variations of microbial colonisation on tuff tile were observed, taking into account the thickness and spatial arrangement of the colony on ten local spots for each tile, classified as center, middle and periphery (Figure 2). The results show a progressively extending from the zone of the inoculum to the median and distal regions of the tiles in control experiments. At later stages of colonisation, *B.minor*, *F.oxysporum* and *N.commune* respectively occupied about 88%, 58% and 40% of the tile surfaces (**Figure 3**).

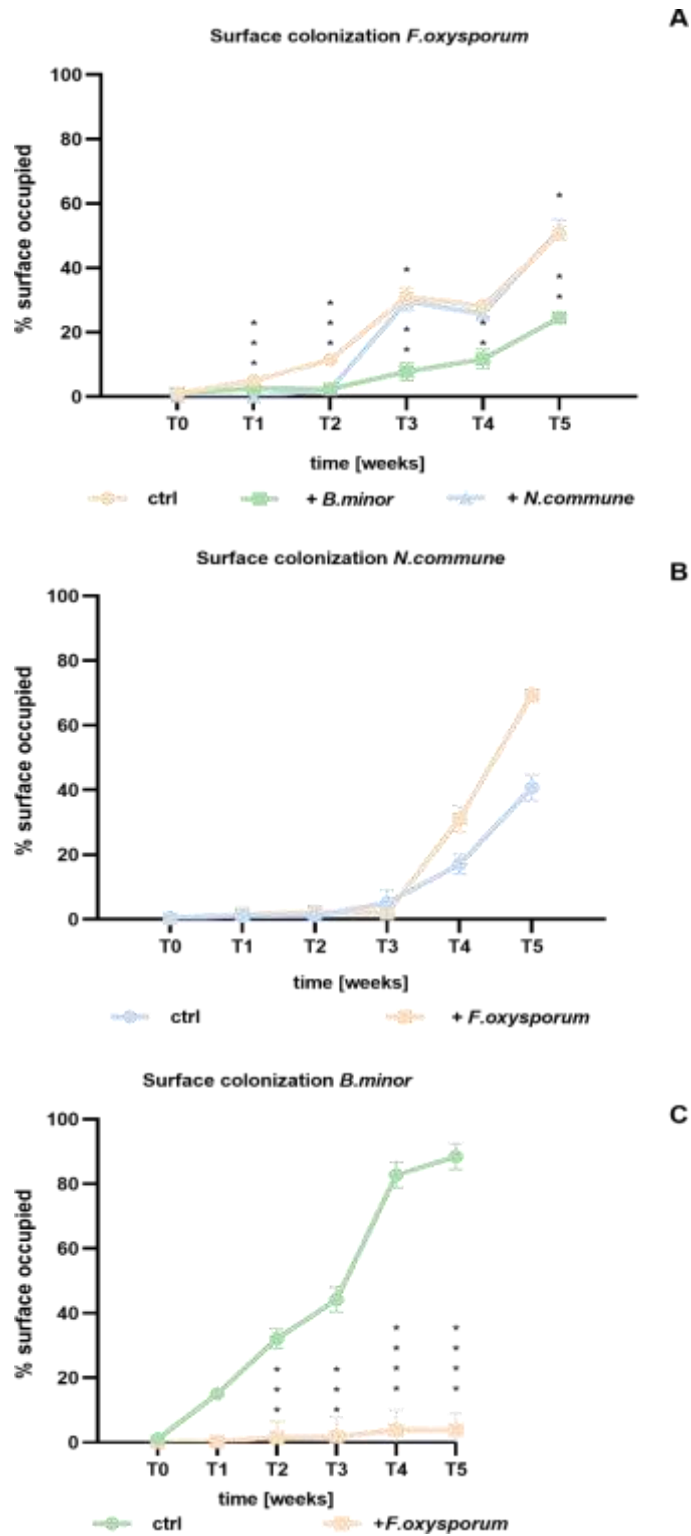


**Figure 3.** Percentage of surface occupied by *F. oxysporum* (A), *N.commune* (B), and *B.minor* (C) of the tuff tile. Data shown are means  $\pm$  SD of three independent experiments. \* indicates  $p < 0.05$ , \*\* indicates  $p < 0.005$ , and \*\*\*\* indicates  $p < .0001$

A corresponding increase of thickness (**Figure 4**) was also observed, but *F. oxysporum* attained an average thickness of about 150  $\mu\text{m}$  in central and median regions of the tiles, whereas *N.commune* achieved about 300  $\mu\text{m}$  in the central region and 200  $\mu\text{m}$  in the medial one. Furthermore, there was a 96% decrease in the colonised area for *B.minor* when interacting with the *F.oxysporum*. Also a 91% decrease in the thickness reached by *B.minor* when interacting with *F.oxysporum*. While, 53% decrease in the thickness reached by *F.oxysporum* when interacting with *N.commune* was observed. Image analysis performed on the whole colony developing on tuff tiles showed a continuous growth for single microorganisms, with a particular capacity to form local aggregation on stone for *B.minor* and *N.commune*.

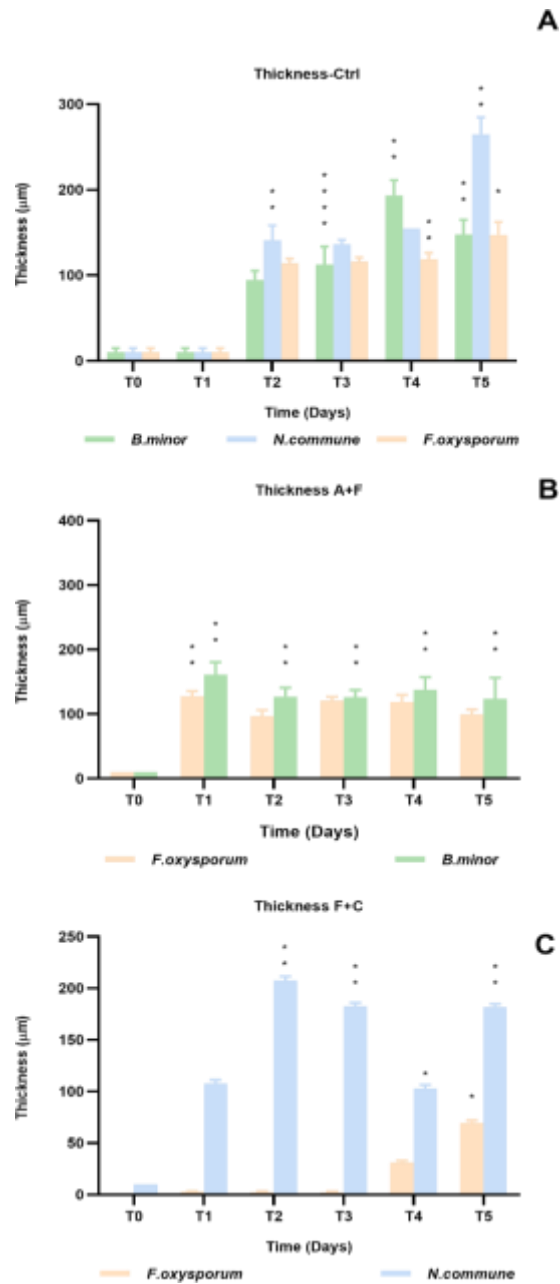


**Figure 4.** Thickness of *B.minor*, *F.oxysporum* and *N.commune* in control experiments (A), *F.oxysporum* and *B.minor* in interaction experiments (B), and *F.oxysporum* and *N.commune* in interaction experiments (C) of the tuff tile. Data shown are means  $\pm$  SD of three independent experiments. \* indicates  $p < 0.05$ , \*\* indicates  $p < 0.005$ , \*\*\* indicates  $p < 0.0001$

In order to determine the ecological relationship of microorganisms over time, landscape metrics were applied on MIPs recorded from Z-stack of tuff tiles at each control time. The results shows no similarity in the spatial arrangement for fungus *F.oxysporum* and algae *B.minor* when in control experiments and in interaction experiments, while highlight similarity was observed in the structural arrangement of cyanobacteria *N.commune* in control experiments and in interaction with fungus *F.oxysporum*. Referred to *N.commune*, in both cases the number of patches, total patch area, meanpatch distance, contiguity index and aggregation index increasing and/or decreasing in the same way. The last phase of the measured dynamics (between thirtieth and fiftieth days) shows a decreasing of number of patches, total patch area and contiguity index, displaying the ability of *N.commune* to grow in few and few aggregate structures. Collaterally, at the same time for a halting phase for cyanobacteria, *F.oxysporum* increasing the surface of colonized area and its aggregation index while number of patches, mean patch distance and contiguity index tends to slightly decrease (**Figure 5**).

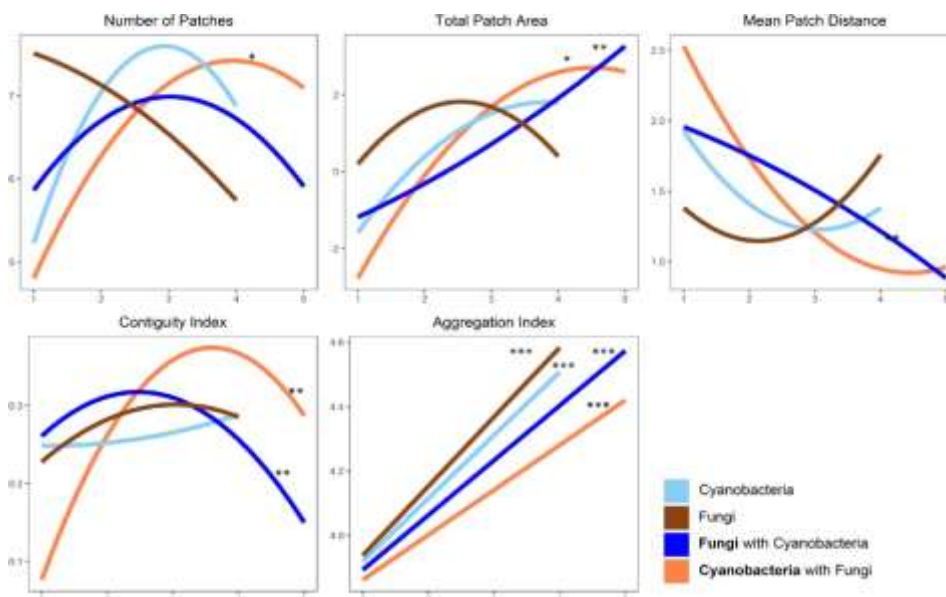


**Figure 5.** The relationship between landscape metrics (logged values) and time fitted by LMMs, plotted for interaction fungus + cyanobacteria.

The similarity between *B.minor* breaks in the control experiment and experiment in interaction with *F.oxysporum*: the latter's colonisation starts to increase, while

the colonisation ability of *B.minor* drastically decline. *F.oxysporum*, together with *B.minor*, continues to increase number of patches, total patch area, contiguity index and aggregation index on the tuff tile, while mean patch distance remain on steady state. While, all the metrics referred to *B.minor* together with *F.oxysporum*, continue to decrease, albeit number of patches slightly increase (Figure 6).

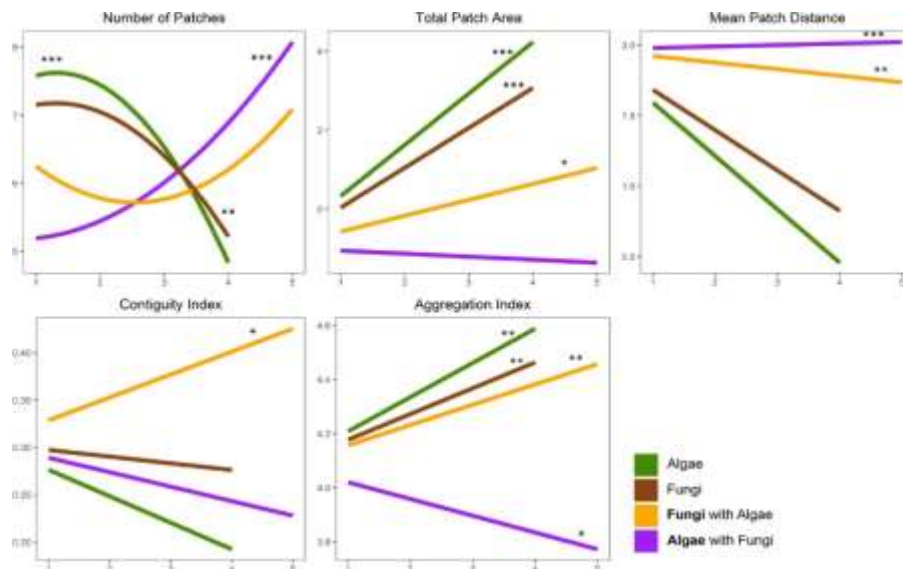


**Figure 6.** The relationship between landscape metrics (logged values) and time fitted by LMMs, plotted for interaction fungus + algae.

Taken together these findings suggest that penetration and development of hyphal fungal network during the colonisation progresses inside the pores and the cracks into the substratum with a non-equal rate over the time in different experimental conditions but shows a trend that is patchy but directionally spread from the inoculum area to the periphery.

## Discussion

In the present study a biological and quantitative survey on *in vitro* colonisation of NYT by *Bracteacoccus minor*, *Fusarium oxysporum* and *Nostoc commune* was performed, thereby confirming the use of closed system experiments for the understanding the early establishment of microbial biofilm on stone. In close system experiments there is no external perturbation, although in open systems fluctuating conditions and

atmospheric weather can leave serious marks on the development of subaerial biofilm mats. In natural environment fungal colonisation on stone surfaces may occur earlier than phototrophs. This can be possible due to atmospheric deposition of organic compounds that have a nutritive potential to pioneer microorganisms, especially for filamentous fungi as *F.oxysporum*, which can also take advantage of favorable porous substrates and bloom in a few days if small nutrients are provided. In particular, the network of fungal hyphae already established on stone seems to be able to host other microorganisms, influencing the growth and spatial arrangement of photosynthetic populations [42]. Thus, in our experimental conditions, we reproduce biodeterioration phenomena in a low-carbon environment ( $0.88 \text{ mg cm}^{-3}$ ). In this conditions, the development of microbial communities on the NYT has been shown to be adequate for the substrate topography and filling of depressions, fissures and intergranular spaces, especially for filamentous fungus *F.oxysporum*. The latter's which seems to take advantage of small nutrients provided in NYT porous substratum, influencing the subsequent development of the phototrophic community. A combination of metallurgical and CLSM microscopy techniques has been successfully applied to assess the early steps of microbial colonisation on stone substratum, especially to evaluate thickness and structural texture of the subaerial biofilm. On the other hand, surface overlay of monospecific algal, cyanobacterial and fungal colony and the surface overlay of fungal and cyanobacterial or fungal and algal couple were measured with computer image analysis, allowing also to analyze spatial arrangement and ecological interaction between microorganisms, using landscape metrics. To our knowledge this study represents the first attempt to characterize the ecology of microbial biofilm growing on cultural heritage monuments using landscape ecology metrics. The understanding of microbial early colonisation dynamics, especially for fungi, on stone surfaces may also be considered as a useful system to study biodeterioration both for their damaging power and for the ability to favor the establishment of heterologous communities over the time. Image segmentation analysis provided a useful tool for an easy and fast determination of microbial overlay

on stone surface, and the correlation with other biomass indicators may hopefully lead to the use of image analysis also for an in field application devoted to the monitoring of natural microbial mats.

## References

- [1] Pyzik, A., Ciuchcinski, K., Dziurzynski, M., & Dziewit, L. (2021). The Bad and the good—Microorganisms in cultural heritage environments—An update on biodeterioration and biotreatment approaches. *Materials*, *14*(1), 177.
- [2] Sterflinger K (2010) Fungi: Their role in deterioration of cultural heritage. *Fungal Biol Rev* 24:47-55.
- [3] Onofri S, Zucconi L, Isola D, Selbmann L (2014) Rock-inhabiting fungi and their role in deterioration of stone monuments in the Mediterranean area. *Plant Biosyst* 148(2), 384–391.
- [4] Barberousse H, Ruot B, Ye´pre´mianb C, Boulon G. An assessment of facade coatings against colonisation by aerial algae and Cyanobacteria. *Building and Environment*. 2007; 42(7): 2555–2561.
- [5] Tomaselli L, Lamenti G, Bosco M, Tiano P. Biodiversity of photosynthetic microorganisms dwelling on stone monuments. *International Biodeterioration & Biodegradation*. 2000; 46(3): 251–258.
- [6] Tran TH, Govin A, Guyonnet R, Grosseau P, Lors C, Garcia-Diaz E, et al. Influence of the intrinsic characteristics of mortars on biofouling by *Klebsormidium flaccidum*. *International Biodeterioration & Bio- degradation*. 2012; 70: 31–39
- [7] Curtis TP, Sloan WT. Prokaryotic diversity and its limits: microbial community structure in nature and implications for microbial ecology. *Current Opinion in Microbiology*. 2004; 7(3): 221–226. <https://doi.org/10.1016/j.mib.2004.04.010> PMID: [15196488](https://pubmed.ncbi.nlm.nih.gov/15196488/)
- [8] Viles H. Ecological perspectives on rock surface weathering: towards a conceptual model. *Geomorphology*. 1995; 13: 21–35.
- [9] Haussler S, Fuqua C. Biofilms (2012): New discoveries and significant wrinkles in a dynamic field. *Journal of Bacteriology*. 2013; 195(13): 2947–2958. <https://doi.org/10.1128/JB.00239-13> PMID: [23625847](https://pubmed.ncbi.nlm.nih.gov/23625847/)
- [10] Miller AZ, Rogerio-Candelera MA, Laiz L, Wierzchos J, Ascaso C, Sequeira Braga MA, Hernández-Mariné M, Maurício A, Dionísio A, Macedo MF, Saiz-Jimenez C (2010) Laboratory-induced endolithic growth in calcarenites:

biodeteriorating potential assessment. *Microb Ecol* 60:55-68.

[11] Wiktor V, De Leo F, Urzì C, Guyonnet R, Grosseau Ph, Garcia-Diaz E (2009) Accelerated laboratory test to study fungal biodeterioration of cementitious matrix. *Int Biodeterior Biodegrad* 63:1061-1065.

[12] Casanova Municchia A, Percario Z, Caneva G (2014) Detection of endolithic spatial distribution in marble stone. *J Microsc* 256(1):37-45.

[13] De Gennaro M, Langella A (1996) Italian zeolitized rocks of technological interest. *Mineralium Deposita*, 31(6), 452–472. doi:10.1007/bf00196127

[14] Kim M, Or D (2016) Individual-Based Model of Microbial Life on Hydrated Rough Soil Surfaces. *PLoS ONE* 11(1): e0147394. doi:10.1371/journal.pone.0147394

[15] Guillitte O, Dreesen R (1995) Laboratory chamber studies and petrographical analysis as bioreceptivity assessment tools of building materials. *Sci Total Environ* 167:365–74.

[16] Del Mondo A, Pinto G, De Natale A, Pollio A (2017) Microcosm experiment for the assessment of mycelial growth on a tuff substratum by a *Fusarium solani* strain isolated from Oplontis (Naples, Italy) archaeological site. *Int J Conserv Sci* 8(4):651-662.

[17] D’Elia L, Del Mondo A, Santoro M, De Natale A, Pinto G, Pollio A (2018) Microorganisms from harsh and extreme environments: a collection of living strains at ACUF (Naples, Italy). *Ecol Quest*, <http://dx.doi.org/10.12775/EQ.2018.023>

[18] Petraretti, M., Duffy, K. J., Del Mondo, A., Pollio, A., & De Natale, A. (2021). Community Composition and Ex Situ Cultivation of Fungi Associated with UNESCO Heritage Monuments in the Bay of Naples. *Applied Sciences*, 11(10), 4327.

[19] Passarini, M. R., Santos, C., Lima, N., Berlinck, R. G., & Sette, L. D. (2013). Filamentous fungi from the Atlantic marine sponge *Drummacidon reticulatum*. *Archives of Microbiology*, 195(2), 99-111.

[20] Doyle JJ, Doyle JL (1990) Isolation of plant DNA from fresh tissue. *Focus* 12:13-15.

[21] Del Mondo A, De Natale A, Pinto G, Pollio A (2019) Correction to: Novel

qPCR probe systems for the characterization of subaerial biofilms on stone monuments. *Annals of Microbiology*. doi:10.1007/s13213-019-01480-9

[22] Masi, M., Petraretti, M., De Natale, A., Pollio, A., & Evidente, A. (2021). Fungal metabolites with antagonistic activity against fungi of lithic substrata. *Biomolecules*, 11(2), 295.

[23] Del Mondo, A., Pinto, G., De Natale, A., & Pollio, A. (2017). In vitro colonisation experiments for the assessment of mycelial growth on a tuff substratum by a *Fusarium solani* strain isolated from the Oplontis (Naples, Italy) archaeological site. *International Journal of Conservation Science*, 8(4).

[24] Nichols HW, Bold HC (1965) *Trichosarcina polymorpha* gen. et sp. Nov. *J Phycol* 1:34-38.

[25] Jeger MJ, Lamour A, Gilligan CA, Otten W (2008) A fungal growth model fitted to carbon-limited dynamics of *Rhizoctonia solani*. *New Phytol* 178(3):625-633.

[26] Arganda-Carreras I, Kaynig V, Rueden C, Eliceiri KW, Schindelin J, Cardona A, Seung HS (2017) Trainable Weka Segmentation: a machine learning tool for microscopy pixel classification. *Bioinform* 33(15):2424-2426.

[27] Schindelin, J.; Arganda-Carreras, I.; Frise, E.; Kaynig, V.; Longair, M.; Pietzsch, T.; Preibisch, S.; Rueden, C.; Saalfeld, S.; Schmid, B.; et al. Fiji: An open-source platform for biological image analysis. *Nat. Methods* **2012**, 9, 676–682.

[28] Bakke, R.; Olsson, P.Q. Biofilm thickness measurements by light microscopy. *J. Microb. Methods* **1986**, 5, 93–98.

[29] [Kuehn M](#), [Hausner M](#), [Bungartz H-J](#), [Wagner M](#), [Wilderer PA](#), [Wuertz S](#) (1998) Automated confocal laser scanning microscopy and semiautomated image processing for analysis of biofilms. *Appl Environ Microbiol* 64:4115-4127.

[30] Lepanto P, Lecumberry F, Rossello J, Kierbel A (2014) A confocal microscopy image analysis method to measure adhesion and internalization of *Pseudomonas aeruginosa* multicellular structures into epithelial cells. *Mol Cell Probes* 28:1

[31] Hesselbarth, M. H., Sciaini, M., With, K. A., Wiegand, K., & Nowosad, J. (2019). Landscape metrics: an open-source R tool to calculate landscape metrics. *Ecography*, 42(10), 1648-1657.

[32] McGarigal, K., Cushman, S. A., & Ene, E. (2012). FRAGSTATS v4: spatial

pattern analysis program for categorical and continuous maps. *Computer software program produced by the authors at the University of Massachusetts, Amherst. Available at the following web site: <http://www.umass.edu/landeco/research/fragstats/fragstats.html>.*

[33] Zatelli, P., Gobbi, S., Tattoni, C., Cantiani, M. G., La Porta, N., Rocchini, D & Ciolli, M. (2019). Relevance of the cell neighborhood size in landscape metrics evaluation and free or open-source software implementations. *ISPRS International Journal of Geo-Information*, 8(12), 586.

[34] He, H. S., DeZonia, B. E., & Mladenoff, D. J. (2000). An aggregation index (AI) to quantify spatial patterns of landscapes. *Landscape Ecology*, 15(7), 591-601.

[35] Cornejo-Denman, L., Romo-Leon, J. R., Hartfield, K., van Leeuwen, W. J., Ponce-Campos, G. E., & Castellanos-Villegas, A. (2020). Landscape dynamics in an iconic watershed of Northwestern Mexico: Vegetation condition insights using landsat and planetscope data. *Remote Sensing*, 12(16), 2519.

[36] Nakagawa, S., & Schielzeth, H. (2013). A general and simple method for obtaining R<sup>2</sup> from generalized linear mixed-effects models. *Methods in ecology and evolution*, 4(2), 133-142.

[37] Koch, P. L., & Barnosky, A. D. (2006). Late Quaternary extinctions: state of the debate. *Annual Review of Ecology, Evolution, and Systematics*, 37.

[38] Galetti, M., Moleón, M., Jordano, P., Pires, M. M., Guimaraes Jr, P. R., Pape, T. & Svenning, J. C. (2018). Ecological and evolutionary legacy of megafauna extinctions. *Biological Reviews*, 93(2), 845-862.

[39] Breiman, L. (2001). Random forests. *Machine learning*, 45(1), 5-32.

[40] Kuhn, M., Wing, J., Weston, S., Williams, A., Keefer, C., & Engelhardt, A. (2018). caret: classification and regression training (R package). *R package version*, 6-0.

[41] Greenwell, B. M. (2017). pdp: An R package for constructing partial dependence plots. *R J.*, 9(1), 421.

[42] Team, R. C. (2014). R: A language and environment for statistical computing. R Foundation for Statistical Computing, [on line]. Vienna, Austria.

[43] Wickham, H. (2017). The tidyverse. *R package ver*, 1(1), 836.

[44] Pedersen, T. L. (2018). Tidygraph: a tidy API for graph manipulation. R

package version, 1(0).

[45] Pedersen, T. L. (2018). ggraph: An Implementation of Grammar of Graphics for Graphs and Networks. R package version 1.0. 2.

[46] Roeselers G, van Loosdrecht MCM, Muyzer G (2007) Heterotrophic pioneers facilitate phototrophic biofilm development. *Microb Ecol* 54:578-585.

**CHAPTER 7**  
**AN ECOTOXICOLOGICAL EVALUATION OF FOUR FUNGAL METABOLITES**  
**WITH POTENTIAL**  
**ANTI-FOULING PROPERTIES FOR STONE-BUILT CULTURAL HERITAGE**

## **Abstract**

Biocides based on chemical toxic compounds have been commonly used to mitigate damages caused by microbial fouling on stone cultural heritage. However, in the last few years, the use of commercial and traditional biocides has been banned and/or limited due to their dangerous profile for environment and human health. The current state of the art highlights an urgent need to develop proper mitigation strategy for microbiologically contaminated historic materials based on eco-friendly solutions. Natural products could be a suitable alternative having low toxicity and stability if compared to synthesized compounds. In this manuscript, the ecotoxicological profile of four selected fungal metabolites, namely cavoxin, *epi*-epoformin, seiridin and sphaeropsidone was evaluated. A battery of ecotoxicological tests using bacteria (*Aliivibrio fischeri*), crustacean (*Daphnia magna*), algae (*Raphidocelis subcapitata*), and nematode (*Caenorhabditis elegans*) revealed a lower toxicity of this compounds, especially when compared with Preventol® and Rocima® (commercial biocides). Most of these solutions developed in laboratory settings appear very promising, although their efficiency and ecotoxicological features remain to be further tested before being widely marketed.

**Keywords:** cultural heritage – biodeterioration – natural compounds – antifouling – biofilm – cavoxin – *epi*-epoformin – sphaeropsidone – seiridin

## **Introduction**

The growth of lithobionts on cultural heritage stone surfaces has long been associated with biodeterioration, defined as “any undesirable change in the properties of a material caused by the vital activities of organisms” [1], and recognized as a threat to conservation [2]. It has been demonstrated that such damages and alterations on rock surfaces highly depend on colonizing organisms, including vascular plants [3], bryophytes [4], lichenized and non-lichenized fungi [5], microalgae, photo and chemolithotrophic bacteria which growth are variably favored by environmental conditions [6-7]. The bio-deteriorative ability of lithobionts is related to 1) mechanical damage such as breakage and loss of cohesion of the substrate; 2) chemical alteration due to ability of microorganisms, especially fungi, to excrete organic acids; 3) aesthetic damages through the formation of patinas and crusts [8]. To guarantee the preservation and transmission to future generations of stone cultural heritage, controlling bio-deterioration is duties of utmost importance shared and signed at global level [9]. It has been demonstrated that biological growth can also have a bio-protective role on stone cultural heritage [10]. As such, approaches in restoration activity to intervene or not should be acquired on a case by case basis [11].

In restoration activities, two main strategies are used to remove and / or control microbial growth on cultural heritage assets, i.e., indirect and direct methods, often coupled. The indirect approach is based on the control of micro-environmental parameters unfavorable to biological growth [8]. Any cultural heritage site represents different ecological microinches [12], hosting different lithobiontic communities that interact with the substrate influencing its conservation in different ways [13]. The knowledge and monitoring of environmental parameters, especially for deteriorogenic species, can help to recognize and reach the best conservation solutions [14-15]. However, the use of indirect methods is not always possible in crypts, hypogea and outdoor monuments, where parameters such as humidity, temperature and nutrients are not easy to control [16-17-18]. Direct intervention to clean up cultural heritage includes physical, chemical, and mechanical strategies. Among these, chemicals such as biocides have been widely used to kill unwanted organisms on cultural heritage and remain the most widely used practical solution [19]. Unfortunately, several biocides commonly used for this purpose

have proved to be a potential danger to human health and the environment, due to their acute toxicity, their suspected teratogenic activity, and their environmental risk. Recent studies have also highlighted a potential risk of interference with stone materials and an increase in the bio-receptivity of the substrate when using biocides. In addition, some obsolete biocides led to corrosion of the minerals, causing rust or black spots. Currently, extensive research is ongoing and long overdue, aiming to find alternative and eco-friendly substances or methods to reduce biodeterioration phenomena. In the restoration field, "natural compounds", that is compounds that are not molecules synthesized by industrial processes but directly produced by organisms, appear to be very promising tools for addressing biodeterioration problems. The use of natural bioactive compounds is hypothesized to be less toxic than purely synthetic alternatives. The scientific literature on natural biocides that can be used against the biodeterioration of the stone cultural heritage is extensive [20]. More than sixty natural substances, mainly essential oils and substances of plant and lichen origin have been tested for this type of application. However, in most cases, adequate information is still lacking for many substances, such as specific efficacy on biodeteriogens at low doses, performance over time, absence of interference with materials and other potential hazards. Recently, three metabolites produced by fungi pathogenic for forest plants, were evaluated as potential antifungal compounds against *Aspergillus niger*, *Alternaria alternata* and *Fusarium oxysporum*, isolated as damaging agents from the external tuff wall of the Roman remains "Villa of Poppea" in Oplontis, Naples, Italy. Among them cavoxin and *epi*-epoformin showed antifungal activity against *A. niger* and *F. oxysporum* on infected stones of the Neapolitan yellow tuff (NYT), a volcanic lithotype widely diffused in the archeological sites of Campania, Italy [21]. However, their environmental compatibility is one of the most important prerequisites for their application as well as their possible detrimental effects on different lithic materials. For this purpose, five living organisms, the bacterium *Aliivibrio fischeri*, the alga *Raphidocelis subcapitata*, the crustacean *Daphnia magna* and the nematode *Caenorhabditis elegans* were used as bioindicators for ecotoxicology evaluation of these compounds. Furthermore, other two promising fungal natural products, namely sphaeropsidone and seiridin, that already showed antifungal properties and other interesting activities (Table 1) were also evaluated.

**Table 1. Classes, Sources, and Biological Activities of Fungal Metabolites (1-4)Used in this Study.**

<b>Compound</b>	<b>Class of Natural Compound</b>	<b>Fungal Source</b>	<b>Biological activity</b>	<b>Literature n.</b>
Cavoxin (1, Figure 1)	Aromatic acid	<i>Phoma cava</i>	Antifungal  Antirust  Phytotoxic	Schrader et al., 2010 Santagata et al. 2017 Barilli et al., 2019 Masi et al. 2021  Barilli et al. 2016  Evidente et al., 1985
<i>epi</i> -Epoformin (2, Figure 1)	Cyclohexen epoxide	<i>Diplodia quercivora</i>	Phytotoxic, antifungal and zootoxic  Antifungal  Antirust  Phytotoxic	Andolfi et al., 2014  Masi et al. 2021  Barilli et al. 2016 Barilli et al. 2017  Cala et al., 2018
Sphaeropsidone (4, Figure 1)	Cyclohexen epoxide	<i>Diplodia cupressi</i>	Antifungal  Phytotoxic  Induction of haustorium formation in parasitic plant	Evidente et al., 2011  Evidente et al., 1998 Evidente et al., 2011  Fernández-Aparicio et al., 2016

Seiridin ( <b>3</b> , Figure 1)	Furanone	<i>Seiridium cupressi</i>	Antifungal  Bactriostatic  Antifeedant  Phytotoxic	Sparapano et al., 1986 Sparapano and Evidente 1995b  Aznar-Fernandez et al. 2019  Evidente et al., 1986
---------------------------------	----------	---------------------------	----------------------------------------------------------------------	------------------------------------------------------------------------------------------------------------------------

## Materials and methods

### Instruments and chemicals

Column chromatography (CC) was performed using silica gel (Merck, Kieselgel 60, 0.063–0.200 mm). Analytical and preparative TLC were performed on silica gel plates (Merck, Kieselgel 60, F254, 0.25 and 0.5 mm respectively); the spots were visualized by exposure to UV light (254 nm) and/or iodine vapors and/or by spraying first with 10% H<sub>2</sub>SO<sub>4</sub> in MeOH, and then with 5% phosphomolybdic acid in EtOH, followed by heating at 110 °C for 10 min. <sup>1</sup>H NMR spectra were recorded at 500 MHz, in CDCl<sub>3</sub> or CD<sub>3</sub>OD on a Varian spectrometer and the same solvents were used as internal standards. ESI mass spectra were performed using the LC/MSTOF system AGILENT 6230B, HPLC 1260 Infinity. A JASCO P-1010 digital polarimeter was used to measure the optical rotations. The HPLC system (HITACHI) consisted of a pump (5160) and a spectrophotometric detector (5410). The HPLC separations were performed using a Merck (Darmstadt, Germany) C18 reversed-phase column Lichrocart (250 × 4.6 mm i.d.; 5 μm). Sigma-Aldrich Co. supplied all the reagents and the solvents.

## Isolation of selected compounds

Cavoxin, *epi*-epoformin, sphaeropsidone and seiridin (1-4, Figure 1) were purified, as previously described, from the culture filtrates of *Phoma cava* [22], *Diplodia quercivora* [23], *Seiridium cardinale* [24], and *Diplodia cupressi* [25], respectively. The purity of the compound was >98% as ascertained by <sup>1</sup>H NMR and HPLC analyses.

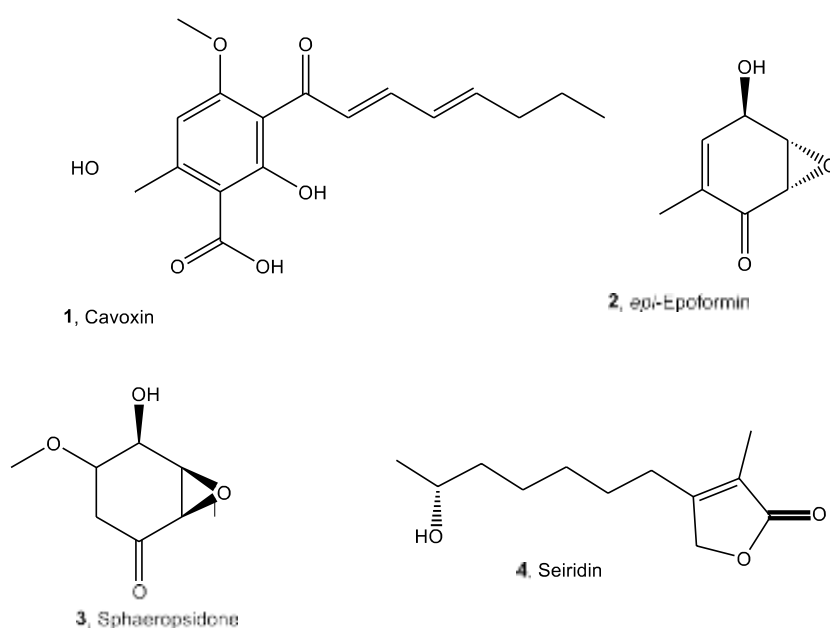


**Figure 1.** Chemical structures of compounds 1-4.

## Isolation and Purification of Cavoxin

The fungus *Phoma cava* was cultured in flasks containing 300 ml of a semisynthetic liquid medium incubated at 25° and 200 rpm for 5 days. The cultures were filtered, and the filtrate was lyophilized. Lyophilized solid residue corresponding to 9 liters of culture filtrate was dissolved in distilled H<sub>2</sub>O (1 liter) and extracted with CHCl<sub>3</sub> (4 X 500 ml). After the extraction, the aqueous phase had no phytotoxic activity. The organic extracts were combined, dried (Na<sub>2</sub>S<sub>4</sub>), filtered, and then evaporated under reduced pressure. The residue (1.762 g), which had a good phytotoxic activity, was chromatographed on Sephadex LH-20 column. The former compound eluted with CHCl<sub>3</sub>-iPrOH (9:1) was cavoxone, while the successive toxic eluate

contained cavoxin. After removal of the solvent under reduced pressure, both compounds were obtained as a homogeneous oil. Cavoxin crystallized as pale-yellow needles (979 mg, 108 mg/liter) from EtOAc-petroleum ether (40-70°).

### **Isolation and Purification of *epi*-epoformin**

The fungus *Diplodia quercivora* was cultured in flasks containing 300 ml of a semisynthetic liquid medium incubated at 25° and 200 rpm for 5 days. The culture filtrates (6.7 L) were acidified to pH 4 with 2 M HCl and extracted exhaustively with EtOAc. The organic extracts were combined, dried with Na<sub>2</sub>SO<sub>4</sub>, and evaporated under reduced pressure to give a brown oil residue (1.14 g). This latter was fractionated through chromatography column on silica gel, eluted with CHCl<sub>3</sub>:i-PrOH (95:5). Eight homogeneous fraction groups were collected. The residue of the fourth fraction (474.6 mg) was purified by CC on reverse phase eluted with Me<sub>2</sub>CO:H<sub>2</sub>O (7:3), yielding 1 (276.1 mg) as a white solid. The spectroscopic data of 1 are as follows: HRMS, m/z (M<sup>+</sup>) calcd for C<sub>7</sub>H<sub>9</sub>O<sub>3</sub> 141.0552, found 141.0601 [M + H]<sup>+</sup>; IR<sub>ν</sub><sub>max</sub> 3357 (O-H), 1674 (C=O) cm<sup>-1</sup>, [α]<sub>D</sub> 20 = +139.3° (c = 0.08). <sup>1</sup>H-NMR (400 MHz, CDCl<sub>3</sub>, δ, ppm): 6.46 (brs, 1H, H-3), 4.67 (brs, 1H, H-4), 3.78 (m, 1H, H-5), 3.53 (m, 1H, H-6), 1.86 (s, 3H, H-7).

### **Isolation and Purification of Seiridin**

Culture filtrates (10 liters) of *Seiridium cardinale* were adjusted at pH 4 with 0.1N HCl and extracted with r-BuOMe (4X2.5 liters). The combined extracts were dried (Na<sub>2</sub>SO<sub>4</sub>) and evaporated under reduced pressure to afford a brown oily residue (2.0 g). This was fractionated by column chromatography on SiO<sub>2</sub> using CHCl<sub>3</sub>:iPrOH (9:1) as eluent. After inspection by tic, homogeneous fractions were pooled and assayed for their phytotoxicity. Three groups of fractions displayed activity, the most potent containing two products with R<sub>f</sub> value of 0.51 and 0.56 on tic run with petroleum ether-Me<sub>2</sub>CO (6:4). Separation of the products was achieved by chromatography of the mixture (736 mg) on a SiO<sub>2</sub> column run with the same solvent system; the products were finally purified by preparative tic with the same solvent system to afford seiridin (495 mg, 49.5 mg/liter) as pure compound.

## **Isolation and Purification of Sphaeropsidones**

The fungus *Diplodia cupressi* was grown in 2 L Erlenmeyer flasks containing 400 mL of modified Czapek medium supplemented with 2% corn meal (pH 5.7). Each flask was seeded with 5 mL of a mycelia suspension and then incubated at 25°C for 4 weeks in darkness. The culture filtrates (15 L) were acidified and extracted with EtOAc. The organic extract, obtained as a brown-red oil (9.2 g), having a high phytotoxic activity, was chromatographed on a silica gel column eluted with CHCl<sub>3</sub>-i-PrOH (19:1), affording nine groups of homogeneous fractions. The residues (3.6 g) of fractions 4-7 were combined and further purified by a silica gel column, eluted with CHCl<sub>3</sub>-i-PrOH (9:1), yielding six groups of homogeneous fractions. The residue of fraction 3 was crystallized from EtOAc-n-hexane (1:5), yielding sphaeropsidone (1, R<sub>f</sub> 0.40, 2.3 g, 153.3 mg/L) as white needles. The mother liquors were further purified by silica gel CC, eluted with petroleum ether-acetone (7:3), affording episphaeropsidone (2, R<sub>f</sub> 0.53, 725 mg, 48.3 mg/L) as a homogeneous oil. The residue (775.5 mg) of fraction 8 from the first column containing two more polar metabolites (R<sub>f</sub> 0.21 and 0.14) was purified by silica gel CC, eluted with CHCl<sub>3</sub>-i-PrOH (9:1), to afford five groups of homogeneous fractions. The residues (150 and 102.4 mg) of fractions 3 and 4 were independently purified by two further steps of preparative TLC on silica gel, using CHCl<sub>3</sub>-i-PrOH (9:1) and petroleum ether-acetone (7:3), to give chlorosphaeropsidone and epichlorosphaeropsidone (chlorosphaeropsidone, and its 6-epimer, 80 and 57 mg, 5.3 and 3.8 mg/L, respectively) as homogeneous oils.

## ***Stability studies on the selected compounds***

### **Qualitative analysis**

10 mg of pure cavoxin, *epi*-epoformin, sphaeropsidone and seiridin (**1-4**, Figure 1) were separately added to 100 mL of the corresponding culture medium BBM. After 72 h (corresponding to the longest time used for the algal inhibition test) the metabolites were extracted from 50 mL of the culture media with EtOAc (3 x 50 mL) obtaining 4.90, 4.89, 4.80 and 4.95 mg for **1-4**, respectively. The four extracts were analyzed by TLC eluted with CHCl<sub>3</sub>-*iso*PrOH 95:5 (v/v) in comparison with standard samples of compounds **1-4**. 50 mL of culture media, without any

compound added, were extracted in the same conditions obtaining 0.19 mg of organic extract.

### **Quantitative analysis**

The HPLC analysis was carried out on the same solution of BBM containing compounds **1-4** after 72 h. The mobile phase used to elute the samples in isocratic mode was MeCN–H<sub>2</sub>O 70/30 (v/v) at a flow rate of 0.5 mL/min. Detection was performed at 286, 237, 257, and 215 nm, corresponding to the maximum UV absorption of cavoxin (**1**) [22], *epi*-epoformin (**2**) [26], sphaeropsidone (**3**) [27], and seiridin (**4**) [24], respectively. BBM medium without the compounds was analysed in the same conditions. Samples were injected using a 10- $\mu$ L loop and monitored for 25 min. The same conditions were used to obtain the calibrations curves for compounds **1-4** which were accurately weighed ( $\pm 0.0001$  mg) and separately dissolved in MeCN in the range between 1 and 0.0001  $\mu$ g/mL. Each analysis was performed in triplicate. The limit of detection (LOD) was extrapolated from the calibration graphics according to the guidelines provided by IUPAC while the validation of the HPLC method (in terms of limit of quantitation (LOQ), intra- and inter-assay precision, and accuracy) was achieved following the rules reported in the “Guidance for Industry-Bioanalytical Method Validation” of the Food and Drug Administration (FDA, USA), as previously reported [28].

### **Ecotoxicity analysis**

The algal growth inhibition test (72 h) with *R. subcapitata*, was carried according to ISO [29]. The algal density was determined by spectrophotometric analysis (DR5000, Hach Lange GmbH, Weinheim, Germany) at 670 nm. The percentage growth inhibition (GI, %) was calculated as the difference between the growth rate of the control group and of the sample and expressed as the mean ( $\pm$ SD). Toxicity tests were carried out in triplicate. The bioluminescence inhibition test (30 min) was detected with the *A. fischeri* (NRRLB-11177) supplied by MicroBioTest, Gent, Belgium, and according to ISO [30]. The bioluminescence was determined by luminometer Microtox (Model 500 analyzer, New Castle, DE, USA) at 490 nm.

To provide the required osmotic pressure for the bacterium, the test was conducted using a saline water solution (2% sodium chloride, NaCl). Toxicity tests were performed in triplicate with a control, and the percentage luminescence inhibition (LI, %) was expressed as the ratio of the decrease in bacterial light production to the remaining light.

The immobility test (24 h) with *D. magna* was conducted according to ISO [31]. *D. magna* were selected from laboratory stock cultures at Hygiene Laboratory of the Department of Biology of the University of Naples Federico II in ISO medium and daily fed with microalgae *R. subcapitata*. Groups of 5 neonates (third brood, <24 h old) in 10 ml ISO medium were exposed to each compound (n = 4 test groups per concentration) [29]. After exposure, any immobility and abnormal appearance was recorded at stereomicroscope (LEICA EZ4-HD).

Mortality tests (24 h) with *C. elegans* (wild-type strain N2 variant Bristol), were performed using an age-synchronous L4-larval nematodes. Ten organisms were placed into 24-well tissue culture plates containing 0.5 mL of each sample. All treatments were done in triplicate and without feeding. After exposure, the number of dead worms was determined by stereomicroscope (LEICA EZ4-HD).

## Results and Discussion

The stability of compounds **1-4** in BBM culture medium after 72 h (corresponding to the longest time used for the algal inhibition test) was evaluated by qualitative and quantitative analyses following the procedures described in Materials and Methods section. For the qualitative analysis the solutions of BBM containing the four metabolites were extracted three times with EtOAc and the corresponding organic extracts were analyzed by TLC in comparison with standard samples of compounds **1-4**. Among the metabolites only cavoxin (**1**) was not detected in the corresponding organic extract whose chromatographic profile showed the presence of other compounds (probably degradation products).

To confirm the stability of the other compounds (**2-4**), and the result obtained with cavoxin, a quantitative analysis was carried out by HPLC. Standard samples of compounds **1-4**, isolated from the corresponding natural sources, were used to obtain HPLC calibration curves (Table 2) for their quantitative determination in

BBM solutions after 72 h, as described in Materials and Methods section. The retention times were highly reproducible, varying less than 0.500 min. Linear regression curves (absolute amount against chromatographic peak area) for **1-4** were obtained based on weighted values calculated for 7 concentrations of the standards. The quantitative determination of the metabolites was calculated by interpolating the mean area of the chromatographic peak using the equation from the calibration curve. The chromatographic profiles of standard samples of compounds **1-4** and those of the solutions obtained adding to BBM the same compounds after 72 h are reported in Figure 2.

The peak of cavoxin was absent in the corresponding chromatographic profile (Figure 2E) confirming the result obtained with the qualitative analysis. Instead, the peaks of compounds **2-4** in the chromatograms (Figure 2F-2H) were almost coincident to retention times of the standards (Figure 2B-2D) and the % of compounds present in the culture medium after 72 h is reported in Table 2. Furthermore, when BBM medium without the compounds was analysed in the same conditions, no significative peaks were observed in correspondence of the retention times of compounds **1-4**. The results showed that compounds **2-4** were still present in high concentrations ( $\geq 90\%$ ) in BBM solution at 72 h confirming their stability in these conditions.

In Figure 3, the results about the GI (%) of *R. subcapitata* were reported for Cavoxin (Figure 3 A), *epi*-epoformin (Figure 3 B), Seiridin (Figure 3 C), and Sphaeropsidone (Figure 3 D). The EC<sub>50</sub>, EC<sub>10</sub>, and EC<sub>5</sub> values were summarized in Table 3. No significative effects were detected at the first lowest exposure concentrations for Cavoxin, *epi*-epoformin and Sphaeropsidone, and also the other concentrations for Seiridin. Results with *R. subcapitata* showed that the relative toxicity order was *epi*-epoformin > Sphaeropsidone > Cavoxin > Seiridin. For cavoxin, biostimulation effects were detected at the first lowest exposure concentration. Algae growth impairment occurred for *epi*-epoformin and sphaeropsidone between 3.125 and 25 mg/L (nominal concentrations), and for cavoxin between 25 and 50 mg/L. For *R. subcapitata* exposed to cavoxin, all concentrations evidenced a concentration-response and the effects ranged

**Table 2.** Analytical characteristics of the calibration curves<sup>a</sup> and quantification of compounds **1-4** culture medium (BBM) after 72 h.

Compound	Rt (min)	R <sup>2</sup>	Detection limit (µg)	Compound detected (µg) in 10 µL	% of compound present in the culture medium after 72 h
Cavoxin ( <b>1</b> )	4.790	0.9998	0.0001	n.d. <sup>b</sup>	0
<i>epi</i> -Epoformin ( <b>2</b> )	1.830	0.9997	0.0001	0.00095 ± 0.0001	95
Sphaeropsidone ( <b>3</b> )	3.200	0.9998	0.0001	0.00092 ± 0.0002	92
Seiridin ( <b>4</b> )	4.080	0.9996	0.0003	0.00090 ± 0.0003	90

<sup>a</sup> Calculated in the form  $y = a + bx$ , where  $y$  is the chromatographic peak area and  $x$  is the µg of compound with a number of data points = 21; <sup>b</sup> n.d. = not detected.

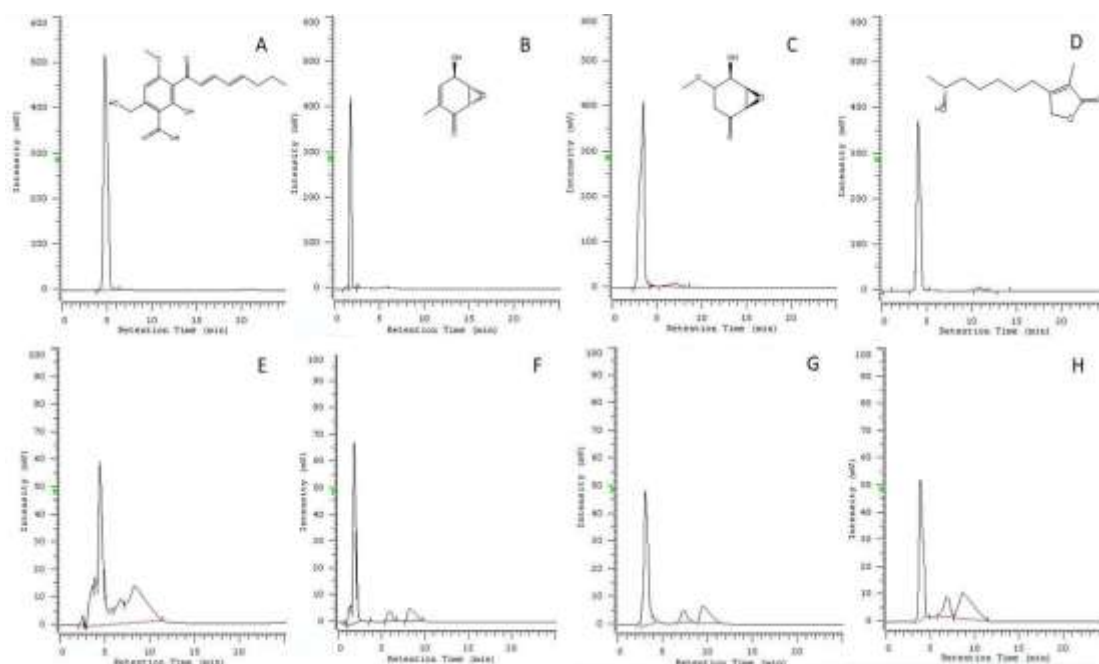


**Figure 2.** Chromatographic profiles of: **A**, standard sample of cavoxin (**1**), 1 mg/mL at 286 nm; **B**, standard sample of *epi*-epoformin (**2**), 1 mg/mL at 237 nm; **C**, standard sample of sphaeropsidone (**3**), 1 mg/mL at 257 nm; **D**, standard sample of seiridin (**4**), 1 mg/mL at 215 nm; **E**, culture medium (BBM) 72 h after the addition of cavoxin (**1**), 0.1 mg/mL at 286 nm; **F**, culture medium (BBM) 72 h after the addition of *epi*-epoformin (**2**), 0.1 mg/mL at 237 nm; **G**, culture medium (BBM) 72 h after the addition of sphaeropsidone (**3**), 0.1 mg/mL at 257 nm; **H**, culture medium (BBM) 72 h after the addition of seiridin (**4**), 0.1 mg/mL at 215 nm.

between -8% (12.5 mg/L) and 84% (50 mg/L). Indeed, the EC50 of cavoxin was 35.98(22.77- 56.67) mg/L (Table 3). For *epi*-epoformin, a significant difference in the concentration-response curves can be observed in Figure 3 (B). The maximum detected effect was 94% at 12.5 mg/L. *epi*-epoformin EC50 was 35.98 (22.77- 56.67) mg/L. For Seiridin, effects ranged between 6% (12.5 mg/L) and 21% (100 mg/L) (Figure 3 C) and for these low effects the EC50 after 72 h of exposure was not determined in exposure scenarios. About *R. subcapitata* exposure to sphaeropsidone, the effects varied between 21% (at 3.125 mg/L) and 90% (at 50 mg/L) (Figure 3D). The EC50 values of sphaeropsidone was 12.78 (8.95-18.64) mg/L (Table 3). In Figure 4, the results about the LI (%) of *A. fischeri* were reported for Cavoxin (Figure 4 A), *epi*-epoformin (Figure 4 B), Seiridin (Figure 4 C), and Sphaeropsidone (Figure 4 D). As a general overview of the obtained results, the LI always evidenced inhibitory effects at the two highest tested concentrations for all the investigated compounds.

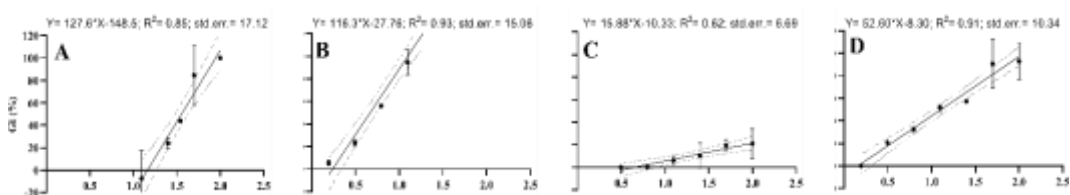


**Figure 3.** Concentration-response relationship of Cavoxin (A), *epi*-Epoformin (B), Seiridin (C) and Sphaeropsidone (D) exposed to *R. subcapitata*; concentrations in the x-axis are expressed as mg/L: GI = growth inhibition.

Considering the exposure of *A. fischeri* to Cavoxin (Figure 4 A), from 12.5 mg/L to 100 mg/L concentrations the luminescence was reduced upper 67%. At the two lowest concentrations the inhibitory effects were considered not harmful (< 40% effect). The EC50 values of Cavoxin was 8.57 (5.24-14.42) mg/L (Table 3).

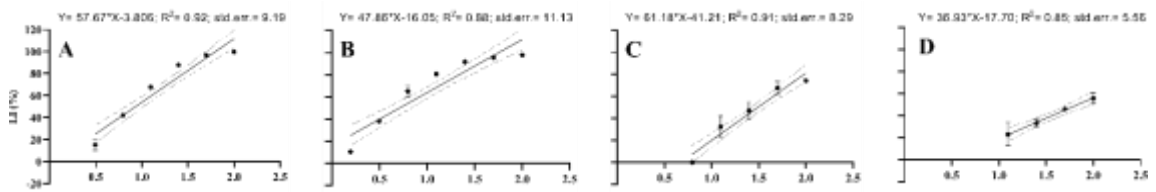


**Figure 4.** Concentration-response relationship of Cavoxin (A), *epi-epoformin* (B), Seiridin (C) and Sphaeropsidone (D) exposed to *A. fischeri*; concentrations in the x-axis are expressed as mg/L: LI = luminescence inhibition.

The luminescence of *A. fischeri* after *epi-epoformin* exposure significantly ( $p < 0.05$ ) decreased from 6.25 mg/L, up to 100 mg/L (Figure 4 B). Effects of *epi-epoformin* were not significantly different from the control at 3.12 mg/L. The EC50 values of *epi-epoformin* was 5.12 (2.50-11.58) mg/L (Table 3). About the exposure of Seiridin, *A. fischeri* was the only one that showed sensitivity toward this compound. The luminescence was reduced up to 75% in the considered concentration range (Figure 4 C) and the EC50 value calculated was of 30.96 (16.02-59.84) mg/L. The Sphaeropsidone the highest concentrations (100 mg/L and 50 mg/L) showed slight adverse effects ranging between 46% and 55%, while the two lowest treatments presented no effect (Figure 4 D). The EC50 value estimated for Sphaeropsidone was 68.14 (54.43-85.29) mg/L.

In Figure 5, the results of the I (%) of *D. magna* were reported for Cavoxin (Figure 5 A), *epi-epoformin* (Figure 5 B), Seiridin (Figure 5 C), and Sphaeropsidone (Figure 5 D). A linear regression model was considered to fit data concentration-response relationships and the equations allowed the determination of EC50, EC20, EC10, and EC5 that were

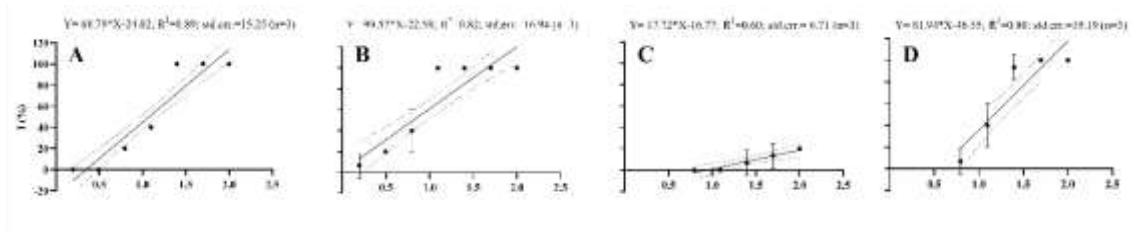


**Figure 5.** Concentration-response relationship of Cavoxin (A), *epi*-epoformin (B), Seiridin (C) and Sphaeropsidone (D) exposed to *D. magna*; concentrations in the x-axis are expressed as mg/L; I = immobility.

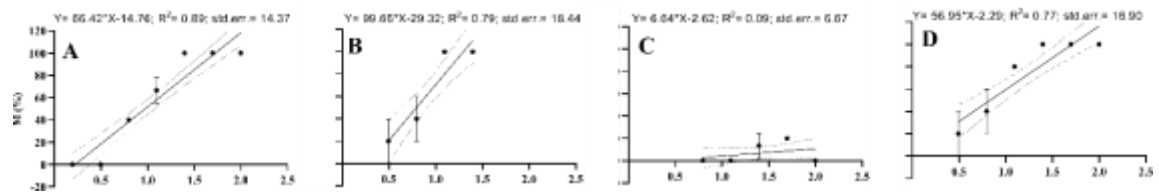


**Figure 6.** Concentration-response relationship of Cavoxin (A), *epi*-Epoformin (B), Seiridin (C) and Sphaeropsidone (D) exposed to *C. elegans*; concentrations in the x-axis are expressed as mg/L; M = mortality.

summarized in Table 3. No significant effects were detected at the first lowest exposure concentrations for Cavoxin, *epi*-epoformin and Sphaeropsidone, and also the other concentrations for Seiridin. Results with *D. magna* showed that the relative toxicity order was Cavoxin > *epi*-epoformin > Sphaeropsidone > Seiridin. For daphnids exposed to Cavoxin, all exposure concentrations evidenced a concentration-response significant toxic effect up to 40% at 12.5 mg/L. Indeed, the EC50 of cavoxin was estimated as 1.91 mg/L. The exposure to *epi*-epoformin showed effects ranged between 6.7% (1.25 mg/L) and 100% (12.5 mg/L). About *D. magna* exposure to Sphaeropsidone, the effects varied between 6.7% and 100%. The EC50 values of *epi*-epoformin and sphaeropsidone, measured with the same organisms, are of 5.36 and 15.07 mg/L. For Seiridin, no significant differences ( $p < 0.001$ ) between concentration were highlighted. The EC5, EC10, EC20 and

EC50 values in the investigated concentration range cannot be detected. In Figure 6, the results about the M (%) of *C. elegans* were reported for Cavoxin (Figure 6 A), *epi*-epoformin (Figure 6 B), Seiridin (Figure 6 C), and Sphaeropsidone (Figure 6 D). The EC50, EC10, and EC5 values were summarized in Table 3. No significant effects were detected at all exposure concentrations for Seiridin. The mortality of nematodes showed a similar toxicity trend for Cavoxin and Sphaeropsidone, but with higher toxicity level (80%) at 12.5 mg/L (Sphaeropsidone). Indeed, the nematode EC50 values were of 9.44 (4.73- 20.52) mg/L, 3.12 (1.70- 6.19) mg/L and 6.88 (2.97- 19.69) mg/L for Cavoxin, *epi*-epoformin, Seiridin and Sphaeropsidone respectively (Table 3).

**Table 3.** EC5, EC10, EC20 and EC50 values for cavoxin, *epi*-epoformin, seiridin and sphaeropsidone after exposure of *R. subcapitata*, *A. fischeri*, *D. magna* and *C. elegans*; values are in mg/L; n.d. = not determined; EC = effective concentration; average EC values are provided  $\pm$ 95% confidence limit values in brackets (n = 3).

Organism	Compound	EC5	EC10	EC20	EC50
<i>Raphi docelis subcap itata</i>	Cavoxin	15.97 (10.11- 25.13)	17.48 (11.07- 27.51)	20.93 (13.25- 32.96)	35.98 (22.77- 56.67)
	<i>epi</i> -epoformin	1.91 (1.28- 2.99)	2.11 (1.41- 3.33)	2.58 (1.70- 4.10)	4.67 (2.98- 7.70)
	Seiridin	n.d.	n.d.	n.d.	n.d.
	Sphaeropsidone	1.78 (1.32- 2.45)	2.22 (1.63- 3.07)	3.43 (2.49- 4.82)	12.78 (8.95- 18.64)
<i>Aliivibrio fischeri</i>	Cavoxin	1.42 (0.93- 2.24)	1.74 (1.13- 2.75)	2.59 (1.66- 4.16)	8.57 (5.24- 14.42)
	<i>epi</i> -epoformin	0.59 (0.33- 1.15)	0.75 (0.41- 1.48)	1.20 (0.64- 2.48)	5.12 (2.50- 11.58)
	Seiridin	5.69 (2.95- 11.00)	6.87 (3.56- 13.28)	10.01 (5.18- 19.35)	30.96 (16.02- 59.84)
	Sphaeropsidone	4.12 (3.29- 5.15)	5.62 (4.49- 7.04)	10.49 (8.38- 13.14)	68.14 (54.43- 85.29)
<i>Daphnia magna</i>	Cavoxin	2.64 (0.22- 1.37)	3.12 (0.26- 1.60)	4.36 (0.38- 2.20)	1.91 (1.11- 5.66)
	<i>epi</i> -epoformin	1.89 (1.13- 3.36)	2.12 (1.26- 3.79)	2.68 (1.57- 4.84)	5.36 (3.03- 10.04)
	Seiridin	n.d.	n.d.	n.d.	n.d.
	Sphaeropsidone	4.26 (1.20- 5.06)	4.90 (1.38- 7.33)	6.49 (1.83- 12.96)	15.07 (4.26- 16.34)
<i>Caenorhabditis elegans</i>	Cavoxin	1.98 (1.08- 3.91)	2.36 (1.28- 4.70)	3.34 (1.77- 6.80)	9.44 (4.73- 20.52)
	<i>epi</i> -epoformin	1.10 (0.63- 2.05)	1.24 (0.71- 2.32)	1.56 (0.88- 2.97)	3.12 (1.70- 6.19)
	Seiridin	n.d.	n.d.	n.d.	n.d.
	Sphaeropsidone	1.12 (0.58- 2.54)	1.37 (0.69- 3.19)	2.05 (1.00- 5.02)	6.88 (2.97- 19.69)

## **Conclusions**

The aim of this work was to evaluate the possible exploitability of fungal metabolites as novel conservation products against the biological colonisation of cultural heritage surfaces.

Since commercial and traditional biocides are known to be hazardous both to human health and the environment, the toxicological profiles together with chemical stability of four fungal metabolites previously described were tested for its application in the Cultural Heritage field. The use of this simple and not expensive method may be very useful in conservation and restoration fields to evaluate the efficiency of control methods against biodeteriogenic microorganisms. Early results have demonstrated the effectiveness ability of the method in controlling against microorganisms.

The identification of chemical-stable and long-lasting compounds confirms the possible implication of fungal metabolites in the development of conservation products capable of preventing biological colonisation in the medium/long-term. However, the results obtained so far must be considered as the first promising step of a novel research field, which disclose new opportunities and stimulate further investigations. In this perspective, more assays need to be performed to evaluate the inhibition activity and eco-compatibility of the identified compounds. Afterwards, experimental studies must be carried out for the purpose of evaluating the possible interaction between the biocide compounds and cultural heritage materials.

## References

1. Hueck HJ (1965) The biodeterioration of materials as a part of hylobiology. *Materi und Org* 1:5–34
2. Caneva G, Nugari MP, Salvadori O (2008) *Plant biology for cultural heritage: biodeterioration and conservation*. Getty Conservation Institute, Los Angeles
3. Pawlik Ł, Phillips JD, Šamonil P (2016) Roots, rock, and regolith: Biomechanical and biochemical weathering by trees and its impact on hillslopes—a critical literature review. *Earth Sci Rev* 159:142–159
4. Ricci S, Altieri A. (2008). Il ruolo delle briofite nel deterioramento dei Beni Culturali. In: Alef M (ed) *Biologia ed ecologia delle Briofite*. Antonio Delfino, Roma, pp. 417–434
5. Gadd GM (2017) Fungi, rocks, and minerals. *Elements* 13:171–176
6. Albertano P (2012) Cyanobacterial biofilms in monuments and caves. In: Whitton BA (ed) *Ecology of cyanobacteria II*. Springer, Dordrecht, pp 317–343
7. Mapelli F, Marasco R, Balloi A, Rolli E, Cappitelli F, Dafonchio D, Borin S (2012) Mineral–microbe interactions: biotechnological potential of bioweathering. *J Biotechnol* 157:473–481
8. Salvadori O, Casanova-Municchia A. (2016). The role of fungi and lichens in the biodeterioration of stone monuments. *Open Conf Proc J*, 7 (suppl. 1: M4), 39–54
9. Convention Concerning the Protection of the World Cultural and Natural Heritage, 1972. [https://whc.unesco.org/en/convention text/](https://whc.unesco.org/en/convention_text/). Accessed 02 April 2020
10. Bartoli F., Municchia A.C., Futagami Y., Kashiwadani H., Moon K.H., Caneva G. (2014). Biological colonisation patterns on the ruins of Angkor temples (Cambodia) in the biodeterioration vs bioprotection debate, *Int. Biodeter. Biodegr.* 157–165, <http://dx.doi.org/10.1016/j.ibiod.2014.09.015>.
11. C. Urzì, F. De Leo, L. Bruno, L. Krakova, D. Pangallo, P. Albertano, How to control biodeterioration of cultural heritage: An integrated methodological approach for the diagnosis and treatment of affected monuments,

Thessaloniki, Greece, Proceedings of the Symposium on Works of Art and Conservation  
Science Today (2010),  
<http://dx.doi.org/10.13140/2.1.2443.0888>.

12. Sanmartín P, Villa F, Cappitelli F, Balboa S, Carballeira R (2020b) Characterization of a biofilm and the pattern outlined by its growth on a granite-built cloister in the Monastery of San Martiño Pinario (Santiago de Compostela, NW Spain). *Int Biodeter Biodegrad* 147:104871
13. Tonon C, Favero-Longo SE, Matteucci E, Piervittori R, Croveri P, Appolonia L, Meirano V, Serina M, Elia D (2019) Microenvironmental features drive the distribution of lichens in the House of the Ancient Hunt, Pompeii, Italy. *Int Biodeterior Biodegrad* 136:71–81
14. Caneva G, Bartoli F, Savo V, Futagami Y, Strona G (2016) Combining statistical tools and ecological assessments in the study of biodeterioration patterns of stone temples in Angkor (Cambodia). *Sci Rep* 6:32601
15. Schumacher J, Gorbushina A (2020) Light sensing in plant-and rock associated black fungi. *Fungal Biol* 124:407–417
16. Salvadori O, Charola AE. (2011). Methods to prevent biocolonisation and recolonisation: an overview of current research for architectural and archaeological heritage. In: Charola AE, McNamara C, Koestler RJ (eds) *Biocolonisation of stone: Control and preventive methods. Proceedings from the MCI Workshop Series. Smithsonian Contributions to Museum Conservation (Vol 2)*. Smithsonian Inst. Press, Washington, pp. 37–50
17. X. Liu, H. Meng, Y. Wang, Y. Katayama, J.-D. Gu, Water is a critical factor in evaluating and assessing microbial colonisation and destruction of Angkor sandstone monuments, *Int. Biodeter. Biodegr.* 133 (2018) 9–16, <http://dx.doi.org/10.1016/j.ibiod.2018.05.011>.
18. X. Liu, H. Meng, Y. Wang, Y. Katayama, J.-D. Gu, Water is a critical factor in evaluating and assessing microbial colonisation and destruction of Angkor sandstone monuments, *Int. Biodeter. Biodegr.* 133 (2018) 9–16, <http://dx.doi.org/10.1016/j.ibiod.2018.05.011>.
18. L. Traversetti, F. Bartoli, G. Caneva, Wind-driven rain as a bioclimatic factor affecting the biological colonisation at the archaeological site of Pompeii,

- Italy, *Int. Biodeter. Biodegr.* 134 (2018) 31–38, <http://dx.doi.org/10.1016/j.ibiod.2018.07.016>.
19. Pinna D (2017) *Coping with biological growth on stone heritage objects: methods, products, applications, and perspectives*. Apple Academic Press, Oakville
  20. Fidanza MR, Caneva G (2019) Natural biocides for the conservation of stone cultural heritage: a review. *J Cult Herit* 38:271–286
  21. Masi, M., Petraratti, M., De Natale, A., Pollio, A., & Evidente, A. (2021a). Fungal metabolites with antagonistic activity against fungi of lithic substrata. *Biomolecules*, 11(2), 295.
  22. Evidente, A.; Randazzo, G.; Iacobellis, N.S.; Bottalico, A. Structure of cavoxin, a new phytotoxin from *Phoma cava* and cavoxone, its related chroman-4-one. *J. Nat. Prod.* **1985**, 48, 916-923.
  23. Cala, A., Masi, M., Cimmino, A., Molinillo, J. M., Macias, F. A., & Evidente, A. (2018). (+)-*epi*-Epoformin, a phytotoxic fungal cyclohexenepoxide: Structure activity relationships. *Molecules*, 23(7), 1529.
  24. Evidente, A., Randazzo, G., & Ballio, A. (1986). Structure determination of seiridin and isoseiridin, phytotoxic butenolides from culture filtrate of *Seiridium cardinale*. *Journal of natural products*, 49(4), 593-601.
  25. Evidente, A., Maddau, L., Scanu, B., Andolfi, A., Masi, M., Motta, A., & Tuzi, A. (2011). Sphaeropsidones, phytotoxic dimedone methyl ethers produced by *Diplodia cupressi*: A structure– activity relationship study. *Journal of natural products*, 74(4), 757-763.
  26. Andolfi, A., Maddau, L., Basso, S., Linaldeddu, B. T., Cimmino, A., Scanu, B., & Evidente, A. (2014). Diplopimarane, a 20-*nor-ent*-pimarane produced by the oak pathogen *Diplodia quercivora*. *Journal of natural products*, 77(11), 2352-2360.
  27. Evidente, A., Sparapano, L., Fierro, O., Bruno, G., Giordano, F., & Motta, A. (1998). Sphaeropsidone and episphaeropsidone, phytotoxic dimedone methylethers produced by *Sphaeropsis sapinea* f. sp. *cupressi* grown in liquid culture. *Phytochemistry*, 48(7), 1139-1143.

28. Masi, M., Meyer, S., Clement, S., Cimmino, A., & Evidente, A. (2021b). Effect of cultural conditions on the production of radicinin, a specific fungalphytotoxin for buffelgrass (*Cenchrus ciliaris*) biocontrol, by different *Cochlioboulus australiensis* strains. *Natural product research*, 35(1), 99- 107.
29. ISO. Water Quality–Fresh Water Algal Growth Inhibition Test with Unicellular Green Algae; ISO 8692; ISO: Geneva, Switzerland, 2012.
30. ISO. Water Quality–Determination of the Inhibitory Effect of Water Samples on the Light Emission of *Aliivibrio fischeri* (Luminescent BacteriaTest)–Part 3: Method Using Freeze-Dried Bacteria; 30ISO 11348-3; ISO: Geneva, Switzerland, 2007.
31. ISO 6341:2012. Water Quality-Determination of the Inhibition of the Mobility of *Daphnia Magna* Straus (Cladocera, Crustacea)–Acute Toxicity Test; International Organisation for Standardisation: Geneva, Switzerland, 2012. Available online: <https://www.iso.org/standard/54614.html> (accessed on 21 April 2021).

**CHAPTER 8**  
**GENERAL CONCLUSIONS**

Historical buildings, archaeological sites, stone monuments, wall paintings and frescoes support microbial life. Microalgae, bacteria, cyanobacteria, fungi and lichens are able to colonize the external surfaces of buildings and monuments giving the surface a dirty, neglected and unsightly appearance. Many factors affect the colonisation of cultural heritage by microorganisms: light exposure, moisture, pH, temperature, nutrients, materials. The study of subaerial biofilms is a key field for all that concerns microecology, conservation science and development of anti-fouling systems. Cyanobacteria and microalgae are often the pioneers in colonisation of stone surfaces where they develop phototrophic biofilms. However, there is strong evidence that heterotrophic eukaryotes such as fungi can act as first colonizer, thus enhancing the formation of mixed consortia.

A huge step in this direction has been provided by *in vitro* colonisation experiments, which made possible to selectively investigate the ability of microorganisms to attach and colonize as well as the refractoriness of the surface subjected to colonisation. In *in vitro* colonisation experiments here presented, the pioneer attitude together with structural strategies of three main groups of microorganisms (microalgae- cyanobacteria and fungi) was tested and monitored in the short-term. The selected microorganisms, *Fusarium oxysporum*, *Nostoc commune* and *Bracteacoccus minor* were previously sampled in a campaign carried out in UNESCO archeological sites in the bay of Naples, Italy. Using metallurgical and confocal laser scanning microscopy coupled with digital image analysis it has been possible to establish the fine structure and architecture of the studied microorganisms and hypothesize about their ecological interactions. These findings are useful for treatment design and restoration strategies of deteriorated monuments, where these and other related organisms are likely to occur. In accordance with the great interest of recent research to counteract the growth of deteriogenic microorganisms on stone cultural heritage the present study represents also a first step in the use of fungal metabolites to allow a better preservation of artwork and to guarantee the conditions suitable for their conservation. The toxicological profiles of the tested compounds in the present work were also tested. Taken together, the findings reported in the present work represent an encouraging advance in the characterization of subaerial biofilms both in terms of the

microbiome's structure and ecological interaction. Moreover, the setting of reproducible *in vitro* colonisation experiments coupled with the use of image analysis, defining a greatly support for monitoring microbial growth on stone substrata. To our knowledge, this study represents the first attempt to characterize the ecology of microbial biofilm growing on cultural heritage using metrics normally applied in ecology or in landscape ecology, and usually referred to large geographical areas. Understanding the extent of cooperation and coordination and the evolution of biofilm communities, is essential for any predictive model of biofilm formation and for the design of strategies to remove biofilm infections.

## BIBLIOGRAPHY

AA.VV. Regulation (EU) No 528/2012 of the European Parliament and of the Council of 22 May 2012 Concerning the Making Available on the Market and Use of Biocidal Products. 2012. Available online: <http://data.europa.eu/eli/reg/2012/528/2019-11-20> (accessed on 18 September 2020).

Adamiak, J.; Bonifay, V.; Otlewska, A.; Sunner, J.A.; Beech, I.B.; Stryzewska, T.; Kanka, S.; Oracz, J.; Zyzelewicz, D.; Gutarowska, B. Untargeted metabolomics approach in halophiles: Understanding the biodeterioration process of building materials. *Front. Microbiol.* 2017, 8.

Allsopp, C.; Allsopp, D. An updated survey of commercial products used to protect materials against biodeterioration. *Int. Biodeterior. Biodegrad.* 1983, 19, 99–146

Arino X., Hernandez-Marine M., Saiz-Jimenez C. - Colonisation of Roman tombs by calcifying cyanobacteria. (1997). *Phycologia* 36, 366-373.

Baglioni, P., Chelazzi, D., & Giorgi, R. Nanotechnologies in the conservation of cultural heritage: a compendium of materials and techniques (pp. 1-56). (2015). Amsterdam, The Netherlands:: Springer.

Baquedano Estévez, C.; Moreno Merino, L.; de la Losa Román, A.; Durán Valsero, J.J. The lampenflora in show caves and its treatment: An emerging ecological problem. *Int. J. Speleol.* 2019, 48, 249–277.

Barberousse H, Ruot B, Yéprémian C, Boulon G (2007) An assessment of façade coatings against colonisation by aerial algae and cyanobacteria. *Building and Environment* 42(7):2555-2561

Barranguet C., Veuger B., van Beusekom S.A.M., Marvan, P., Sinke, J.J., Admiraal, W., 2005. Divergent composition of algal bacterial biofilms developing under various external factors. *Eur J Phycol* 40: 1-8.

Barker W.W., Banfield J.F. - Biologically versus inorganically mediated weathering reactions: relationships between minerals and extracellular microbial polymers in lithobiotic communities. (1996). *Chem Geol* 132, 55-69.

Bertuzzi, S.; Candotto Carniel, F.; Pipan, G.; Tretiach, M. Devitalization of poikilohydric lithobionts of open-air monuments by heat shock treatments: A new case study centred on bryophytes, *Int. Biodeter. Biodegr.* 2013, 84, 44–53.

Brehm U., Gorbushina A., Mottershead D. - The role of microorganisms and biofilms in the breakdown and dissolution of quartz and glass. (2005). *Palaeogeography Palaeoclimatology Palaeoecology* 219, 117-129.

Cámara, Beatriz, et al. "Biodeterioration of marble in an underwater environment." *Science of the Total Environment* 609 (2017): 109-122.

Caneva G., De Marco G., Dinelli A., Vinci M. - The wall vegetation of the roman archaeological areas. (1992). *Science and Technology for Cultural Heritage* 1, 217-226.

Caneva, G.; Nugari, M.P.; Salvadori, O. *Plant Biology for Cultural Heritage: Biodeterioration and Conservation*; Getty Publications: Los Angeles, CA, USA, 2008, ISBN 978-0-89236-939-3.

Caneva, G., Pieroni, A., & Guarrera, P. (Eds.). (2013). *Etnobotanica: conservazione di un patrimonio culturale come risorsa per uno sviluppo sostenibile*. Edipuglia.

Cendrine M., Vandenkoornhuyse P., Bohannan B. J.M., Peay K., and Leibold M. A.. "A landscape of opportunities for microbial ecology research." *Frontiers in Microbiology* 11 (2020): 2964.

Cockell C.S., Herrera A. - Why are some microorganisms boring? (2008). *Trends Microbiol* 16, 101-106.

Crispim C.A., Gaylarde C.C. - Cyanobacteria and biodeterioration of cultural heritage: a review. (2005). *Microb Ecol* 49(1), 1-9.

Cutler N.A., Viles H.A., Ahmad S., McCabe S., Smith, B.J. - Algal 'greening' and the conservation of stone heritage structures. (2013). *Science of the Total Environment* 442, 152-164.

Cuzman O.A., Ventura S., Sili C., Mascalchi C., Turchetti T., D'Acqui L.P., Tiano P. - Biodiversity of phototrophic biofilms dwelling on monumental fountains. (2010). *Microb Ecol* 60(1), 81-95.

Danin A., Caneva G. - Deterioration of limestone walls in Jerusalem and marble monuments in Rome. (1990). *Int Biodet* 26, 397-417.

Davies D. - Understanding biofilm resistance to antibacterial agents. (2003). *Nat Rev Drug Discov* 2(2), 114-22

Del Mondo, A.; Pinto, G.; De Natale, A.; Pollio, A. In vitro colonisation experiments for the assessment of mycelial growth on a tuff substratum by a *Fusarium solani* strain isolated from the Oplonti (Naples, Italy) archaeological site. *Int. J. Cons. Sci.* 2017, 8, 651–662.

Decho A.W., 2000. Microbial biofilm in intertidal systems an overview. *Cont Shelf Res* 20: 1257-1273.

Di Martino, Patrick, and Patrick Martino. "Biodeterioration of Stone Monuments." *The Open Conference Proceedings Journal*. Vol. 7. No. Suppl 1: M1. 2016.

Dyda, M.; Pyzik, A.; Wilkojc, E.; Kwiatkowska-Kopka, B.; Sklodowska, A. Bacterial and fungal diversity inside the medieval building constructed with sandstone plates and lime mortar as an example of the microbial colonisation of a nutrient-limited extreme environment (Wawel royal castle, Krakow, Poland).

Microorganisms 2019, 7, 416.

Escadeillas G., Bertron A., Blanc G., Dubosc A. - Accelerated testing of biological stain growth on external concrete walls. Part 1: Development of the growth tests. (2007). *Mater Struct* 40, 1061-1071.

Favero-Longo S.E., Castelli D., Fubini B., Piervittori R. - Lichens on asbestos cement roofs: bioweathering and biocovering effects. (2009). *Journal of Hazardous Materials* 162, 1300-1308.

Fernandes, P. - Applied microbiology and biotechnology in the conservation of stone 99 cultural heritage materials. (2006). *Appl Microbiol Biotechnol* 73, 291-296.

Fuentes, Elsa, and Beatriz Prieto. "A laboratory approach on the combined effects of granite bioreceptivity and parameters modified by climate change on the development of subaerial biofilms on cultural heritage." *International Biodeterioration & Biodegradation* 164 (2021): 105295.

Gadd, Geoffrey Michael, et al. "Oxalate production by fungi: significance in geomycology, biodeterioration and bioremediation." *Fungal Biology Reviews* 28.2-3 (2014): 36-55.

Giannantonio D.J., Kurth J.C., Kurtis K.E., Sobecky P.A. - Effects of concrete properties and nutrients on fungal colonisation and fouling. (2009). *International Biodeterioration & Biodegradation* 63, 252-259.

Gioventù E., Lorenzi P.F., Villa F., Sorlini C., Rizzi M., Cagnini A., Griffò A., Cappitelli F., (2011), "Comparing the bioremoval of black crusts on colored artistic lithotypes of the Cathedral of Florence with chemical and laser treatment", *International Biodeterioration & Biodegradation*, 65(6), 832-839.

Griffin P.S., Indictor N., Koestler R.J. - The Biodeterioration of stone: a review of deterioration mechanisms, conservation case histories, and treatment. (1991). *International Biodeterioration & Biodegradation* 28, 187-207.

Gorbushina A.A. - Life on the rocks. (2007). *Environ Microbiol* 9(7), 1613-1631.

Gorbushina A.A., Broughton W.J. - Microbiology of atmosphere-rock interface: how biological interactions and physical stresses modulate a sophisticated microbial ecosystem. (2009). *Annual Review of Microbiology* 63, 431-550.

Grbić L., Vukojević M., Simić S.J., Krizmanić G., Stupar J.M. - Biofilmforming cyanobacteria, algae and fungi on two historic monuments in Belgrade, Serbia. (2010). *Archives of Biological Science* 62, 625-631.

Grottoli, A.; Beccaccioli, M.; Zoppis, E.; Fratini, S.; Schifano, E.; Santarelli, M.L.; Uccelletti, D.; Reverberi, M. Nanopore Sequencing and Bioinformatics for Rapidly Identifying Cultural Heritage Spoilage Microorganisms. *Front. Mater.* 2020, 7.

Guillitte O., 1995. Bioricceptivity: a new concept for building ecological studies. *Sci total Environ* 167.

Guiamet, Patricia, et al. "Biodeterioration of funeral sculptures in La Recoleta Cemetery, Buenos Aires, Argentina: Pre-and post-intervention studies." *Colloids and Surfaces B: Biointerfaces* 101 (2013): 337-342.

Haubner N., Schumann R., Karsten U. - Aeroterrestrial microalgae growing in biofilms on facades - Response to temperature and water stress. (2006). *Microbial Ecology* 51, 285-293.

Hauer T.J. - Phototrophic biofilms on the interior walls of concrete Iterson-type cooling towers. (2010). *Appl Phycol* 22, 733-736.

Hueck H.J. - The biodeterioration of materials - an appraisal. *Biodeterioration of materials*. (1968). Walters A.H., Elphick, J.S. (Eds.), Elsevier, 6-12.

Hueck H.J. - The biodeterioration of materials as part of hylobiology. (1965). *Mater Org* 1(1), 5-34.

Jacob, Jacqueline P., et al. "Impact of free-range poultry production systems on animal health, human health, productivity, environment, food safety, and animal welfare issues." *Issue Paper-Council for Agricultural Science and Technology* 61 (2018).

Krumbein W. E., 2003. Patina and cultural heritage - a geomicrobiologists perspective. p.39-47 in: R. Kozłowski (ed.): *Proceedings of the 5th European Commission Conference "Cultural Heritage Research: a Pan European Challenge"*, Cracow, 16-18 May 2002.

Li, A.; Xiong, J.; Yao, L.; Gou, L.; Zhang, W. Determination of dust and microorganism accumulation in different designs of AHU system in Shaanxi History Museum. *Build. Environ.* 2016, 104.

Lian B., Chen Y., Zhu, L., Yang R. - Effect of microbial weathering on carbonate rocks. (2008). *Earth Sci Front* 15, 90-99.

Lisci M., Monte M., Pacini E. - Lichens and higher plants on stone: a review. (2003). *International Biodeterioration & Biodegradation* 51, 1-17.

Liu, Z.; Zhang, Y.; Zhang, F.; Hu, C.; Liu, G.; Pan, J. Microbial community analyses of the deteriorated storeroom objects in the Tianjin Museum using culture-independent and culture-dependent approaches. *Front. Microbiol.* 2018, 9.

Louca, S., Polz, M. F., Mazel, F., Albright, M. B. N., Hubere, J. A., O'Connor, M., et al. (2018). Function and functional redundancy in microbial systems. *Nat. Ecol. Evol.* 2, 936–943. doi: 10.1038/s41559-018-0519-1.

Lo Schiavo, S., De Leo, F., & Urzi, C. (2020). Present and future perspectives for biocides and antifouling products for stone-built cultural heritage: Ionic liquids as a challenging alternative. *Applied Sciences*, 10(18), 6568.

Lustrato G., Alfano G., Andreotti A., Colombini M.P., Ranalli G., (2012), “Fast biocleaning of mediaeval frescoes using viable bacterial cells”, *International Biodeterioration & Biodegradation*, 69, 51-61.

Mascalchi, M.; Orsini, C.; Pinna, D.; Salvadori, B.; Siano, S.; Riminesi, C. Assessment of different methods for the removal of biofilms and lichens on gravestones of the English cemetery in Florence. *Int. Biodeter. Biodegr.* 2020, in press.

Masi, M., Petraretti, M., De Natale, A., Pollio, A., & Evidente, A. (2021). Fungal metabolites with antagonistic activity against fungi of lithic substrata. *Biomolecules*, 11(2), 295.

Mazzoni, M., Alisi, C., Tasso, F., Cecchini, A., Marconi, P., & Sprocati, A. R. (2014). Laponite micro-packs for the selective cleaning of multiple coherent deposits on wall paintings: The case study of Casina Farnese on the Palatine Hill (Rome-Italy). *International Biodeterioration & Biodegradation*, 94, 1-11.

Morton L. H. G., Surman, S. B., 1994. Biofilms in biodeterioration a review. *Int Biodeterior Biodegr* 32: 203–221.

Palla F., Barresi G., Giordano A., Schiavone S., Trapani M.R., Rotolo V., Parisi M.G., Cammarata M., (2016), “Cold-active molecules for a sustainable preservation

and restoration of historic-artistic manufacts”, *International Journal of Conservation Science*, 7, 239-246.

Pfendler, S.; Einhorn, O.; Karimi, B.; Bousta, F.; Cailhol, D.; Alaoui- Sosse, L.; Alaoui-Sosse, B.; Aleya, L. UV-C as an efficient means to combat biofilm formation in show caves: Evidence from the La Glacière Cave (France) and laboratory experiments. *Environ. Sci. Pollut. Res.* 2017, 24, 24611–24623.

Pickett, S. T., & Cadenasso, M. Landscape ecology: spatial heterogeneity in ecological systems.(1995). *Science*, 269(5222), 331- 334.

Pinna, Daniela, Barbara Salvadori, and Monica Galeotti. "Monitoring the performance of innovative and traditional biocides mixed with consolidants and water-repellents for the prevention of biological growth on stone." *Science of the Total Environment* 423 (2012): 132- 141.

Pinna, Daniela. "Biofilms and lichens on stone monuments: do they damage or protect?" *Frontiers in microbiology* 5 (2014): 133.

Pinna, D. *Coping with Biological Growth on Stone Heritage Objects. Methods, Products, Applications, and Perspectives*; Apple Academic Press: Oakville, ON, Canada, 2017, ISBN 9781771885324.

Price C.A. - Stone conservation an overview of current research. (1996). In: *Research in conservation*. Santa Monica, CA Getty Conservation.

Ranalli G., Zanardini E., Sorlini, C. - Biodeterioration - Including cultural heritage (2009). In: Schaechter M. (Ed.) *Encyclopedia of Microbiology*, 191-205.

Riminesi, C.; Olmi, R. Localized microwave heating for controlling biodeteriogens on cultural heritage assets. *Int. J. Conserv. Sci.* 2016, 7, 281–294.

Roeselers G, van Loosdrecht MCM, Muyzer G. Heterotrophic pioneers facilitate phototrophic biofilm development. *Microb Ecol.* 2007; 54:578-585.

Roldan M., Calero E., Hernandez Marine M., 2003. Aerophytic biofilms in dim habitats. In: Saiz- Jimenez C. (Ed), *Mol Bio Cult Herit.* A.A. Balkema, Lisse 163-169.

Romani, Mattea, et al. "High bacterial diversity in pioneer biofilms colonizing ceramic roof tiles." *International Biodeterioration & Biodegradation* 144 (2019): 104745.

Rotolo V., Barresi G., Di Carlo E., Giordano A., Lombardo G., Crimi E., Costa E., Bruno M., Palla F., (2016), "Plant extracts as green potential strategies to control the biodeterioration of cultural heritage", *Int. Journal of Conservation Science.*

Saiz-Jimenez C. - Deposition of anthropogenic compounds on monuments and their effect on airborne microorganisms. (1995). *Aerobiologia* 11, 161-175.

Samad L.K., Adhikary S.P. - Diversity of microalgae and cyanobacteria on building facades and monuments in India. (2008). *Algae* 23 91-114.

Sanchez-Silva M., Rosowsky D. - Biodeterioration of construction materials: state of the art and future challenges. (2008). *J Mater Civil Eng* 20, 352-365.

Sanmartín P, Rodríguez A, Aguiar U (2020a) Medium-term field evaluation of several widely used cleaning-restoration techniques applied to algal biofilm formed on a granite-built historical monument. *Int Biodeterior Biodegrad* 147:104.

Schopf J.W. - Cyanobacteria: pioneers of the early earth. (1996). *Nova Hedwigia* 112, 13-32.

Schnabel L. - The treatment of biological growths on stone: A conservator's

viewpoint. (1991). In: Koestler R.J. (Ed.) *International Biodeterioration of Cultural Property*. Elsevier London and New York, 125-131.

Schumacher, J., & Gorbushina, A. A. (2020). Light sensing in plant-and rock-associated black fungi. *Fungal biology*, 124(5), 407-417.

Stupar M., Ljaljević Grbić M., Subakov Simić G., Jelikić A., Vukojević J., Sabovljević M. - A sub-aerials biofilms investigation and new approach in biocide application in cultural heritage conservation: Holly Virgin Church (Gradac Monastery, Serbia). (2012). *Indoor and Built Environment* 25(5), 826-837.

Sutherland I.W. - Biofilm exopolysaccharides: a strong and sticky framework. (2001). *Microbiology* 147, 3-9. 19.

Tiano, P., 1993. Biodegradation of cultural heritage: decay mechanisms and control methods. In: *Conservation of stone and other materials. Vol.2. Prevention and treatment*, Thiel M.J. (ed), Rilem/UNESCO Paris, pp.573-580, ISBN 0419188509, E & FN Spon Press, London.

Tiano A., Carreras, M., Ridao P., Zirilli A. - On the identification of non-linear models of unmanned underwater vehicles. (2002). In: 10<sup>th</sup> Mediterranean Conference on Control and Automation 9-12, Lisbon, Portugal.

Tiano, P. - Biodegradation of cultural heritage: decay mechanisms and control methods. (2002, b). In *Seminar article, New University of Lisbon, Department of Conservation and Restoration* (pp. 7-12).

Tolker-Nielsen T., Molin S. - Spatial organization of microbial biofilm communities. (2000). *Microb Ecol* 40, 75-84.

Tomaselli L., Lamenti G., Bosco M., Tiano P. - Biodiversity of photosynthetic microorganisms dwelling on stone monuments. (2000). *International*

Biodeterioration & Biodegradation 46(3), 251-258.

Tonon, C., Favero-Longo, S. E., Matteucci, E., Piervittori, R., Croveri, P., Appolonia, L., ... & Elia, D. (2019). Microenvironmental features drive the distribution of lichens in the House of the Ancient Hunt, Pompeii, Italy. *International Biodeterioration & Biodegradation*, 136, 71-81.

Tretiach, M.; Bertuzzi, S.; Candotto Carniel, F. Heat shock treatments: A new safe approach against lichen growth on outdoor stone surfaces. *Environ. Sci. Technol.* 2012, 46, 6851–6859.

Trovão, João, et al. "A contribution to understand the Portuguese emblematic Ançã limestone bioreceptivity to fungal colonisation and biodeterioration." *Journal of Cultural Heritage* (2021).

Turick C.E., Berry C.J. - Review of concrete biodeterioration in relation to nuclear waste. (2016). *J Environ Radioact* 151, 12-21.

Urzi C. - Microbial deterioration of rocks and marble monuments of the Mediterranean basin: a review. (2004) *Corrosion Reviews*, 22(5–6), pp.441–458.

Urzi C., De Leo F. - Evaluation of the efficiency of a water repellent and biocide compounds against microbial colonisation of mortars. (2007). *International Biodeterioration & Biodegradation* 60, 25-34.

Urzi C., Realini M. - Colour changes of Noto's Calcareous Sandstone as related with its colonisation by microorganisms. (1998). *International Biodeterioration & Biodegradation* 42, 45-54.

Viles H.A., Cutler N.A. - Global environmental change and the biology of heritage structures. (2012). *Global Change Biology* 18, 2406-2418.

Villa F., Pitts B., Lauchnor E., Cappitelli F., Stewart P.S. - Development of a laboratory model of a phototroph-heterotroph mixed-species biofilm at the stone/air interface. (2015). *Front Microbiol* 6, 1251.

Wakefield R.D., Jones M.S. - An introduction to stone colonizing micro-organisms and biodeterioration of building stone. (1998). *Quarterly Journal of Engineering Geology and Hydrogeology* 31, 301- 313.

Warscheid, T.; Braams, J. Biodeterioration of stone: A review. *Int. Biodeterior. Biodegrad.* 2000, 46, 343–368.

Zakharova, Kristina, et al. "Microcolonial fungi on rocks: a life in constant drought?." *Mycopathologia* 175.5-6 (2013): 537-547.

Zhou, L. Research on Landscape Architecture Design Based on Ecological Restoration and Sustainable Utilization. (2021). In *IOP Conference Series: Earth and Environmental Science* (Vol. 692, No. 4,p. 042085). IOP Publishing.

## AKNOWLEDGEMENTS

Firstly, I would like to express my most sincere gratitude to both Prof. Antonino Pollio and Prof. Antonino De Natale for the continuous support of my Ph.D. study and related research: their guidance helped me in all the time of research and writing of this thesis. Moreover, their far-beyond-the-average human value has been only even with their incredible patience, motivation, and immense knowledge. Besides my advisors, I would like to thank Dr. Angelo Del Mondo, for his insightful comments and encouragement, but also for inciting me to widen my research from various perspectives. I would also like to thank Prof. Sergio Esposito who supported me and offered deep insight into the study. I thank all my fellow colleagues and students for all the fun we have had and for all the science we made in the last three years: you all made me feel like in a wonderful team, and I wish you all the best in career. Also, I thank all of my friends and colleagues in the Department of Biology: in particular, I wish to thank Emanuela Di Iorio, Gianluca Fasciolo, Eduardo Penna, Antonietta Siciliano, Teresa Barra, Luigi Marra and Giorgia Santini for their supportive friendship and for helping in all the tricky situations. Last but not the least, I would like to thank my boyfriend, Mario who carried out this study and life path with me, sustaining and encouraging me when I was discouraged, sharing all my difficulties and satisfactions. I love you, unconditionally. My special appreciation and heartiest thanks go to my parents, for being an extraordinary example and support in what really matters... without you, all of this would have not been possible. Mom and Dad, I love you so much! I would like to thank my brother, Emmanuel to whom I dedicate my PhD thesis for supporting me spiritually throughout writing this thesis and my life in general, with unchanged love and understanding.